CHARACTERIZING THE BERTHING LOAD ENVIRONMENT OF THE SEATTLE FERRY TERMINAL, BREMERTON SLIP

By

Jason E. Kwiatkowski

RECOMMENDED:

Timothy H Boggs

Advisory Committee Chair

Chair, Department of Civil Engineering

APPROVED:

Dean, College of Engineering and Mines

Dean of the Graduate School

2/6/13

Date

CHARACTERIZING THE BERTHING LOAD ENVIRONMENT OF THE SEATTLE FERRY TERMINAL, BREMERTON SLIP

A

THESIS

Presented to the Faculty

of the University of Alaska Fairbanks

in Partial Fulfillment of the Requirements

for the Degree of

MASTER OF SCIENCE

By

Jason E. Kwiatkowski, B.S.

Fairbanks, Alaska

December 2012

Abstract

This manuscript characterizes and presents design recommendations for berthing demands on ferry landing structures. There is a lack of research focused on the berthing load demand imparted by ferry class vessels, therefore the load criteria used for design is often based on a number of assumptions. This study involved a one-year field study of the structural load environment of wingwalls at the Bremerton Slip of the Seattle Ferry Terminal, located in Elliott Bay adjacent to Seattle, Washington. Measurements of marine fender displacement, vessel approach distance with respect to time, and pile strain were used to determine berthing demands. Berthing event parameters were characterized using the Python programming language, compiled, and analyzed statistically. Probability theory was used to provide design value recommendations for berthing energy, force, approach velocity, berthing factor, and berthing coefficient. This study presents a number of engineering design aids intended to quantify the berthing load environment of wingwalls in the Washington State Ferry System.

Table of Contents

Page

Page

List of Appendices

List of Equations

Page

List of Tables

Page

List of Figures

Page

Page

Page

Page

Chapter 1: Introduction

1.1 Background:

The Washington State Ferry (WSF) system is the largest ferry system in the United States, comprising 22 vessels, 9 routes and 22 terminals. In terms of vehicles carried, it is the largest ferry system in the world. Annual ridership for 2011 exceeded 22 million passengers and approached 10 million vehicles. The Washington State Ferry is a critical link between the highly developed economies of eastern Puget Sound and the growing communities on the Kitsap and Olympic Peninsulas as well as the San Juan Islands. The Seattle Terminal serves as the departure point for ferries bound for Bremerton and Bainbridge Island (Transportation 2012).

This study investigates the loading conditions present at Slip 1 of the Seattle Terminal, which provides service to the community of Bremerton, and is responsible for approximately 10.6% of the ferry system's total traffic. The Bremerton Slip is serviced primarily by 'Super' and 'Issaquah' Class Vessels; the displacements of these vessels ranges between 2947 and 3251 long tons when fully laden (including passengers, cargo, fuel, etc.). There are 15 departures and arrivals per day at the terminal. This research was conducted principally on the wingwalls at Slip 1. Wingwalls are pile-supported structures that serve to arrest a vessel's forward progress by absorbing its kinetic energy through compression of marine fenders and deflection of the pile backing support system.

Although standard structural design procedures apply to port related marine structures, these structures tend to be unique in terms of location, loading conditions, constructability, and configuration (Tsinker 2004). As a result of the challenges associated with developing marine infrastructure, the design of these facilities has, to date, defied standardization. Engineers have typically applied basic concepts and lessons learned from similar structures, to best achieve the objectives

of a project. This approach often results in facilities that are one of a kind. The design process for berthing structures typically begins with a determination of the maximum design-berthing load. The design load for a wingwall can be determined by utilizing several methods, including; the kinetic energy-method, statistical method, and analytical method. There is little information available for ferry class vessels that serve to validate any of these methods directly. The statistical approach involves direct measurements of berthing events and provides information specific to the location being studied. However, the downside of this method is cost and it the data obtained may be challenging to apply to other facilities.

Currently the WSF utilizes a version of the Kinetic Energy Method to design wingwalls at terminals, and although it can provide safe and reliable structures, it requires experience to be applied correctly as many assumptions need to be made. The lack of direct information regarding berthing parameters can result in design assumptions that may not accurately reflect the operating environment of the facility. The WSF operates 22 terminals, all which have similar berthing configurations, and therefore serves as a good candidate for application of the statistical approach as a means to improve understanding of vessel loading conditions. This increased knowledge will serve to reduce uncertainty when updating terminal infrastructure and lead to more cost effective and reliable designs.

1.2 Objective:

When a vessel approaches a berthing facility, it will have some momentum and associated kinetic energy. The berthing facility must be designed to safely absorb the kinetic energy while protecting the boat, cargo, and berthing structure. The goal of this study is to characterize the load environment experienced at the Bremerton Slip, and to provide several design aids that will inform the planning of future Washington State Ferry Terminals.

1.3 Field Campaign:

Over the course of 11 months, measurements from approximately 6,950 impact events were recorded and analyzed. Impact events refer to discrete vessel – structure interactions at each wingwall, each ferry-berthing event will contain two impact events. An integrated and automated system consisting of distance sensors, linear motion transducers, strain gauges, and tidal gauges was used to capture berthing events. Both the north and south wingwalls at the Bremerton slip were instrumented. Each wingwalls instrumentation consisted of: a distance sensor to activate the recording of the event and also measure the approaching vessel's position as a function of time, six linear motion transducers to measure the deflection at each of the marine fenders, and two full bridge strain gauges on each support pile (for a total of 18 gauges per wing wall). This system was then connected via instrumentation wire to a datalogger that recorded the events to a memory card. The datalogger was connected to a cellular modem controlled by a laptop computer in Fairbanks, Alaska.

Two-minute time histories were recorded for each berthing event. The vessel's approach velocity was calculated using a sonic distance sensor that recorded the ferry position every 0.2 seconds. Berthing forces and energies were estimated using deflection data provided by linear motion transducers that were mounted adjacent to the marine fenders of the system. Tidal data was recorded using an ultrasonic distance sensor that allowed estimation of the elevation-of-impact to be determined. Strain gauges were installed on all piles to measure axial strain in the support structure.

1.4 Data Processing:

To evaluate this large data set, a suite of interactive software was developed in order to expedite the data compilation and analysis. Utilizing the Python computing language, several programs were designed to automate the bulk of the event characterization. Raw data from the data logger was first split into berthing event files. Next, berthing events were presented graphically in order to ensure they represented actual vessel berthing events, and to enable the selection of the data points that characterize berthing events. The key data points used to inform the analysis were point of maximum vessel impact, the point just prior to vessel impact (in order to have baseline information concerning the initial state of the system), and a point one second prior to impact (used to calculate the approach velocity). After the event file was appended with the information that characterized the primary vessel impact, all subsequent calculations were performed using this information. The approach velocity perpendicular to the wing wall, berthing force, energy, and tidal data were all written to a summary file that accumulated the statistics from each event. The stiffness of the system was estimated separately using SAP2000, a structural analysis software package.

1.5 Presentation of Results:

The results for the experiment will be displayed in a multiple formats intended to provide as much information to practicing engineers as possible. Recorded and estimated parameter values are presented in tables, histograms, probability distribution fits, cumulative distribution fits, and probability plots. A reliability based design approach is presented as a foundation for rationally determining the value of design parameters. The reliability based data is presented in tables as a function of reliability level, as service and ultimate values, as well as in plots that are based upon the number of vessel berthing-events a structure is expected to receive during its service life.

Chapter 2: Literature Review

2.1 Overview

The load environment of vessel berthing structures has been primarily studied with regards to vessels of relatively large displacements such as tankers and cargo ships. Ferry class vessels have seen little direct study with a few exceptions noted in the following sections.

Understanding the loading environment of a marine fender system is of critical importance to berthing facility design, and leaves much to the engineer's judgment. A summary of berthing energy, applicable research, and current methods to assess berthing energy is presented in this section.

2.2 Berthing Energy

In order for a vessel to unload its contents, it must come to a stop in a manner that safely dissipates its kinetic energy. Some portion of the vessel's energy can be dissipated by the use of its propeller, thrusters, or tugboats. However, most berthing procedures will require that the dock structure absorb the remainder of the energy applied by the vessel as it comes to rest. The interface between the approaching vessel and the dock is where energy absorbing marine fenders are utilized to protect shore side infrastructure from approaching vessels(Gaythwaite 2004; Tsinker 2004).

Designing a marine fender system must begin with an assessment of the kinetic energy of vessels that will be landing at the site. There are four accepted methods to calculate this energy; the kinetic energy method, the statistical method, the empirical approach, and mathematical modeling. Berthing energy is a function of vessel size, approach velocity, configuration of the structure, environmental conditions, and hydrodynamic effects. In practice it is assumed that all berthing

energy will be absorbed by the fender system, though in theory some of the energy will be absorbed by the structure supporting the fender system. Fenders mounted on flexible structures are an exception, these configurations absorb 10% to 25% of the total energy to be absorbed. The common procedure is to develop an approximation of the incoming vessel's kinetic energy and then evaluate how the berthing facility will respond (deflect) based upon load-deflection characteristics of the structure and fender system (Gaythwaite 2004).

2.3 Kinetic Energy Method

The most widely used method for marine facilities is the kinetic energy method. This is the method prescribed by PIANC - the World Association for Waterborne Transport Infrastructure (PIANC 2002), the Unified Facilities Criteria (DOD 2005), the British Standard for Maritime Structures (BSI 1994) and others. The kinetic energy method (Equation 2.1) assumes the displacement tonnage is known, and that the energy to be absorbed by the fender system, is the product of the vessels apparent kinetic energy and a number of coefficients that describe various aspects of the system. These coefficients are collectively referred to as berthing coefficients, and describe aspects such as the eccentricity of the vessel approach, geometric configuration of the ship at point of impact, deformation characteristics of the ship's hull, the configuration of the berthing structure, and the effective mass of the vessel (DOD 2005).

$$E_w = \frac{W}{2g} v^2 C_m C_g C_d C_c C_e \qquad \text{Equation 2.1}$$

$$C_b = C_m C_g C_d C_c C_e \qquad \text{Equation 2.2}$$

Where:

E_w = Berthing Energy to be absorbed by wingwall system.

C_b = Berthing coefficient, a product of coefficients

W = Weight of vessel in pounds

g = Acceleration of gravity

v = Berthing velocity normal to the berth

C_m = Effective mass or virtual mass coefficient, accounts for added mass due to entrained water (water that moves with the vessel). Model and prototype experiments were used to develop the following Equation. This equation is referenced in (Costa 1964) , (DOD 2005), and (Gaythwaite 2004).

$$C_m = 1 + \frac{2D}{B} \qquad \text{Equation 2.3}$$

Where:

D = Maximum draft of ship

B = Beam width of ship

C_g = Geometry coefficient; dependent on geometric configuration of ship at point of impact

C_d = Deformation coefficient, this accounts for the energy reduction effects due to deformation of the ship's hull and deflection of the ship along its longitudinal axis.

C_c = Configuration coefficient; this accounts for the difference between an open and solid pier or wharf, and the 'cushioning' effect of water when berthing occurs at solid structure when it has been shown that the water cushion absorbs significant portions of the berthing energy

C_e = Eccentricity coefficient; this accounts for the vessels rotation dependent on angle of approach and point of contact with berthing structure, see Equation 2.4 (DOD 2005) and Figure 2.1 below;

$$C_e = \frac{k^2}{(a^2 + k^2)} \qquad \text{Equation 2.4}$$

Where:

k = Radius of longitudinal gyration of the ship, feet.

a = Distance between ship's center of gravity and the point of contact on the ship's side, projected onto the ship's longitudinal axis.

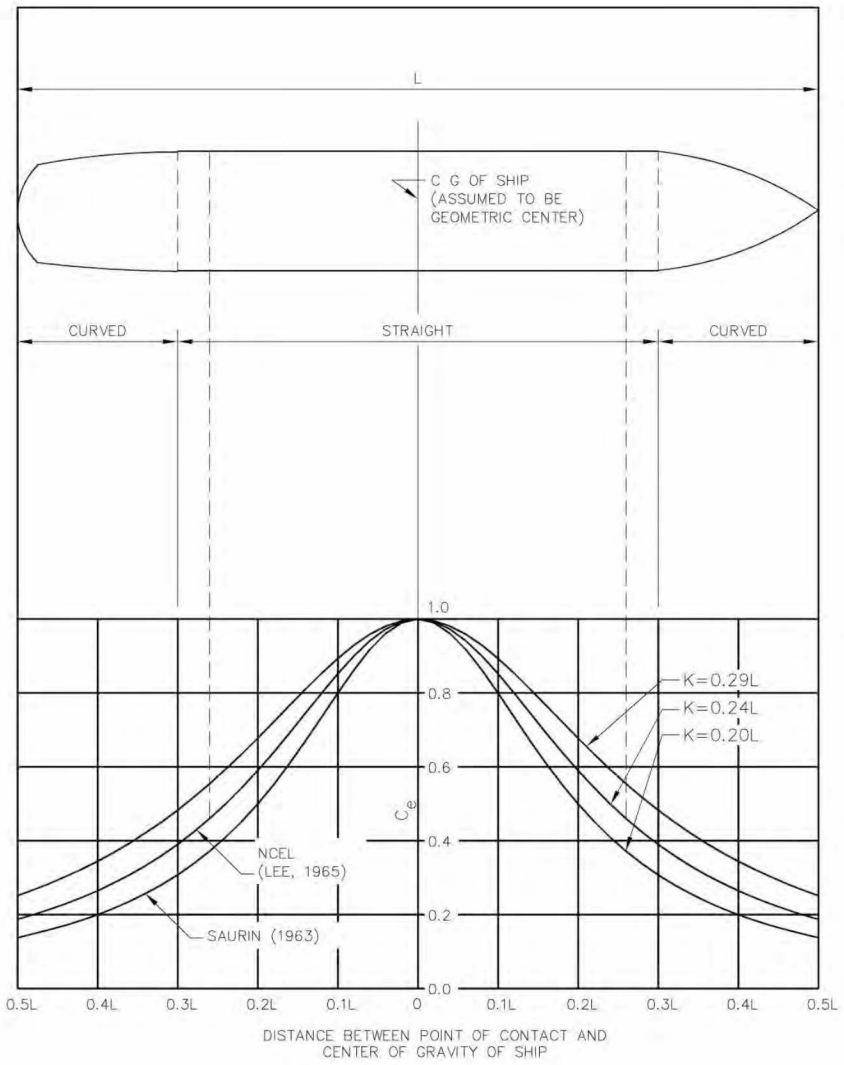

Figure 2.1: Eccentricity Coefficient, C_e (DOD 2005)

The kinetic energy method utilizes the vessel's approach velocity, and choosing a suitable value can be a challenge for ferry designers, since berthing conditions can vary widely from amongst facilities in terms of approach conditions, vessel size, and exposure. The published data regarding approach velocities is primarily focused on tankers and cargo ships utilizing the assistance of tugs during berthing maneuvers. Also, and much of this information is provided by fender manufacturing companies (Gaythwaite 2004).

Research performed in the early 1990's in Washington State (Jahren and Jones 1993) is particularly useful as it involves measurements at the Kingston Terminal and provides the basis for much of WSF terminal design standards. Using video analysis techniques, 568 berthing events at the Bremerton Terminal were recorded and analyzed to describe the distribution of approach velocities of WSF vessels between 2095 and 3335 long tons. The mean perpendicular velocity found in this study was 0.44 feet per second and a methodology for defining a design approach velocity was introduced in Equation 2.5 (Jahren and Jones 1993).

$$v_{design} = FS_v * v_n \qquad \text{Equation 2.5}$$

Where:

v_{design} = Design approach velocity, feet per second

FS_v = Factor of safety for approach velocity, based upon a review of safety factors for various materials; suggested to be 2.0

v_n = Approach velocity that exceeds n percent of observations in empirical approach velocity distribution; n is chosen as 95% in both (Jahren and Jones 1996) and (Jahren and Jones 1993)

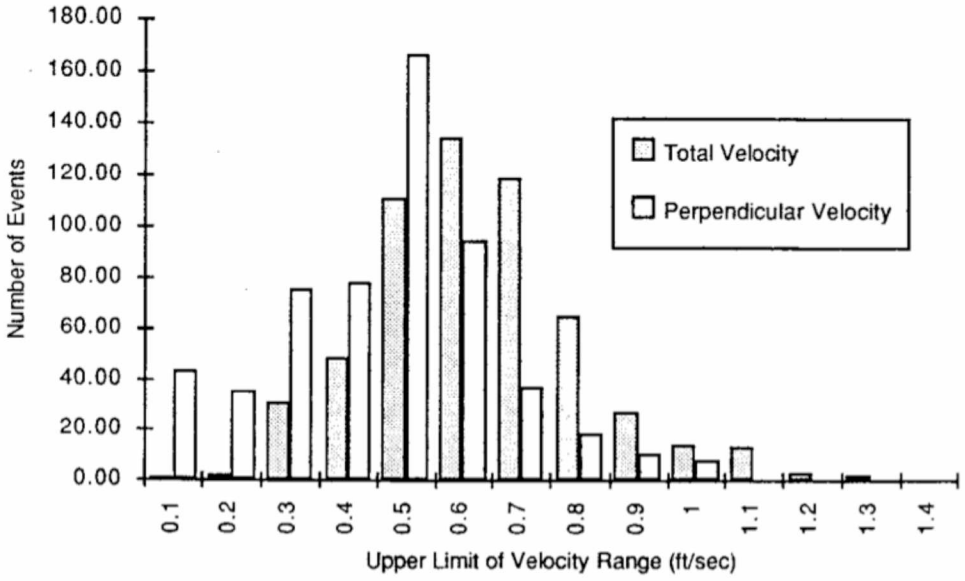

Figure 2.2: Velocity Histogram (Jahren and Jones 1993)

Depending on the berthing maneuvers, several design approach velocities are recommended, the largest value of which could be considered the design approach velocity for a 'Super' class vessel of 2.0 feet per second in the surge direction, and 1.6 feet per second in the direction normal to the wingwalls. This is in agreement with the British Standard (BSI 1994) and information found in (Gaythwaite 2004), which prescribe approach velocities for ferry and 'roll on roll off' (RORO) vessels to be 1.6 to 3.3 feet per second. Both of the previously mentioned sources cite Brolsma's approach velocity curves (Figure 2.3) as a starting point for selection of vessel approach velocity values. Brolsma utilized probability distributions to derive vessel approach velocity curves (Brolsma 1977). However a recent report by (Beckett-Rankine 2010) has investigated the development of these velocity curves and has found them to have serious statistical deficiencies, and also found that historical revision of the velocity standards has been accomplished without supporting explanation. The report recommends an update to reflect more modern berthing procedures and more maneuverable vessels (Beckett-Rankine

2010). The Beckett-Rankine report provides some insight into the discrepancy between recorded data at WSF terminals and the literature.

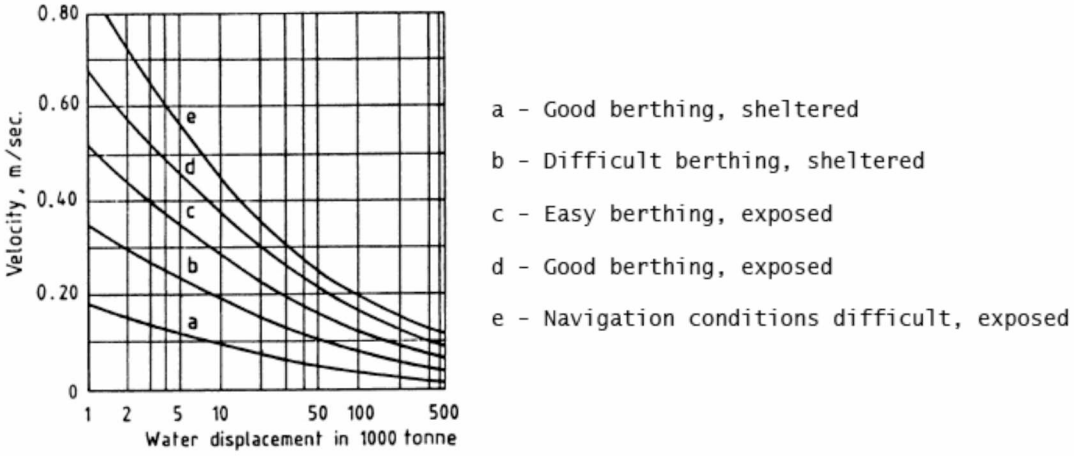

Figure 2.3: Brolsma Approach Velocity Curves, (BSI 1994)

The Kinetic Energy method is used widely in practice, despite the challenges associated with selecting suitable berthing coefficients and approach velocities. Without data collected from a berthing facility site, the accuracy of the design assumptions is subjective in nature, and can lead to designs grossly over or under-designed (Gaythwaite 2004).

One of the goals of this study is to provide information regarding a berthing coefficient that can be utilized in WSF design procedures, as well as providing approach velocities to improve the accuracy and efficiency of future wingwall designs. The current state of practice for the Washington state structural engineers working on marine projects is to use the kinetic energy method (Equation 2.1). The approach velocity currently utilized for design of WSF terminals is 2.53 feet per second (WSF 2012). Berthing coefficients currently employed are an amalgamation of empirical evidence and published information from published literature.

2.3 Analytical Approach

Highly developed analysis techniques are becoming more common as software and computational techniques have evolved to handle the complex interaction of wind, wave, vessel, and mooring systems. These techniques are particularly useful for unique scenarios where it is desired to test several possible configurations when no site information is readily available (Gaythwaite 2004).

Mathematical simulation of ship berthing has traditionally been accomplished by using frequency domain analysis or time domain analysis. The frequency domain has been widely used due to its relative simplicity compared with the time-domain analysis. Frequency domain analysis is based in mechanical vibration theory, and involves a separate equation for each degree of freedom of a vessel's motion, and several coefficients to utilize (Gaythwaite 2004).

$$\big(M + a(\omega)\big)\ddot{x} + b(\omega)\dot{x} + cx = F(t) \qquad \text{Equation 2.6}$$

Where:

M = Vessel mass

ω = Vessel motion frequency

$a(\omega)$ = Added mass coefficient

x = Vessel displacement

$\dot{x}$ = Vessel velocity, at vessel's center of mass

$\ddot{x}$ = Vessel acceleration, at vessel's center of mass

$b(\omega)$ = Damping coefficient

c = Linear spring constant

$F(t)$ = Time varying forcing function

The frequency domain technique has some fundamental shortcomings that can provide misleading results, and it has given way to time domain analysis (Gaythwaite 2004). Time domain arose in the 1960's and involves the convolution integral over the past history of the exciting force with the impulse response function (Cummins 1962).

$$(M + m')\ddot{x} + \int_{-\infty}^{t} K(t-\tau)\dot{x}d\tau + cx = F(t) \qquad \text{Equation 2.7}$$

Where:

M = Vessel mass

m' = Constant inertial coefficient

x = Vessel displacement

$\dot{x}$ = Vessel velocity

$\ddot{x}$ = Vessel acceleration

$K(t-\tau)$= Impulse response function, τ represents variable integration time of earlier vessel position

c = Hydrostatic restoring force coefficient

$F(t)$ = Arbitrary varying forcing function

From this methodology, a time history of vessel motion in response to an arbitrary force (or system of forces) is derived. Values for the constant inertial coefficient and the impulse response coefficient cannot be determined directly and are derived from frequency dependent hydrodynamic coefficients (Gaythwaite 2004).

This procedure is further elaborated upon in (Fontijn 1980) and describes the behavior of a ship berthing to a jetty. There are assumptions made to facilitate solving that include the ship being idealized as a rigid prismatic body, only sway and yaw are considered, the water is calm, the fluid exists unbounded in the horizontal direction, and the bottom is flat. Experimental results gave satisfactory agreements with predictions made from the time domain analysis with hydrodynamic coefficients adapted from a three dimensional situation.

The Naval Facilities Engineering Service Center (NFESC) utilizes a model that employs a computational fluid mechanics approach. The model combines a Renyolds-Averaged Navier Stokes (RANS) numerical method with a six-degree of freedom motion program for time domain simulation of ship and fender reactions. The model has been verified with small scale models and full size model tests (DOD 2005).

2.3.1 Software packages

There are currently at least three software packages that have the capability to do time domain simulation of the dynamic behavior of mooring vessels; TERMSIM, BeAn, and AQWA. The use of these software packages requires highly trained individuals who have a background in the analytical techniques utilized by the software programs. These programs allow for a more rigorous analysis of berthing facility alternatives than the kinetic energy method. The use of advanced software packages is most common when designers are faced with unique and/or complicated vessel-structure interactions that are not easily addressed by the kinetic energy method.

TERMSIM is produced by the Maritime Research Institute Netherlands (MARIN) and is targeted at the export tanker industry. Model tests are carried out in a wave and current basin to assist in calibration of the model, and the software contains extensive databases relating to ship berthing in the marine environment (MARIN 2012).

BeAn, is a software package for berthing analysis that employs a simplified, mathematical model that calculates time histories of fender forces, deflections, and vessel motions. Though, not as advanced as other software packages, it has the benefits of being more suitable for production work (DOD 2005). The software makes use of impulse response techniques of a linearized system (Rizos and Stehmeyer 2004). The mathematical background for BeAn is based upon analytical models and solution techniques first published by H. L. Fontijin in (Fontijn 1988).

AQWA is a product offered by ANSYS®, a multinational simulation software company, and was developed to model fluid-structure interaction. AQWA is a software suite that has extensible capabilities for most marine environment simulations, and it has the ability to integrate with other ANSYS multi-physics simulation software packages, including the ability to work with structural mechanics finite element models (ANSYS 2012).

The Naval Facilities Engineering Command (NAVFAC) worked with the University of Alaska Fairbanks to calibrate analysis and design methods by using ANSYS AQWA to dynamic ferry berthing-events, (Seelig and Lang 2010). The U.S. Navy applied lessons learned in previous work to the specific Alaska modeling done for this study. The AQWA numerical model in this study is built from ferry, float, and pile system components. Using these components, dynamic simulations of ferry berthing were conducted. Calculations were performed in the time domain to describe berthing events. Key parameters were systematically varied to obtain peak load predictions for each simulation. This research focused on berthing in the surge direction (end berthing), and therefore relates well to situations in Washington State. The Alaska ferry vessel berthing-events analyzed using AQWA showed little influence of added mass, and the energy required to be dissipated was due to the vessel alone. Calculated added mass coefficients (C_m) in the end-berthing configuration from the AQWA analysis ranged from 1.038 to 1.121. Large under keel clearance is one reason cited for minimal added mass effect in the end berthing vessels. The study also determined that vessel size is not relevant for peak berthing loads in terms of kinetic energy. The recommendation is that simulations need to be focused on the facility, and that vessel size is not important as long as an adequate range of kinetic energies is considered (Seelig and Lang 2010).

2.4 Statistical Method

The berthing of a ship is a complex maneuver that is dependent on the pilot's experience level as well as environmental and hydrodynamic effects. Each berthing event is a unique combination of these factors, and is a complex phenomenon to analytically model analytically. Terminal design based upon the kinetic energy method requires the engineer to decipher uncertainties associated with approach velocity, the mass of the vessel, and the mechanics of energy dissipation within a fluid, berthing structure and vessel.

The statistical method employs direct measurement of physical berthing parameters coupled with statistical techniques. Proper use of the statistical method provides a direct approach to the value of most interest in design, the berthing energy (Ueda, Hirano et al. 2002). There are various methodologies for measuring berthing parameters such as deflection and approach velocity, and using these measured parameters, berthing energies can be deduced, and described statistically.

Relationships between berthing energy and frequency of occurrence can be developed using statistics and probability theory. This relationship can be used to extrapolate probabilities associated with design energy parameters having a likelihood of occurring or being exceeded. The designer selects a design energy value with an acceptably low probability of the value being exceeded within a given operational period. Uncertainties associated with approach velocity, mass, hydrodynamic effects, etc. are undefined, but are captured with the statistical sample, therefore releasing the engineer from the subjective judgments of berthing parameters (Ueda, Umemura et al. 2001; Gaythwaite 2004).

The Washington State Ferry system has benefitted from direct measurements and statistical analysis since at least the early 1990's. (Jahren and Margaroni 1993) utilized three different methods in order to track approach path and velocity of ferry vessels operating between Edmonds and Kingston, Washington. Through the use of video recording of vessel landings; video logging of the vessel's

radar screen inside the pilothouse; and global positioning system (GPS), the study quantified approach velocity patterns as ships approached the ferry terminal. The authors recommend the use of GPS techniques for vessel velocity measurements due to improved accuracy and decreased labor requirements (Jahren and Margaroni 1993).

Jahren and Jones looked into design criteria for Fenders at ferry landings at the Edmonds terminal, just North of Seattle, Washington. Using video analysis techniques, a data set of 568 berthing events at the Edmonds Ferry Terminal were analyzed in order to describe the distribution of approach velocities (both perpendicular and parallel to the wingwall), of vessels with published displacements between 2095 long tons and 3335 long tons. Utilizing closed circuit video cameras aimed at each wingwall, approach velocity was estimated by scaling video images that contained calibration markings on the ferry deck, to the timestamp of the recording. Multiple viewers were required for this estimation procedure, as observations contained significant variation; the reported accuracy of this study was stated to be ± 0.2 feet per second for the vessel approach velocity estimations. A similar video analysis technique was utilized to investigate berthing energy. During the study, the wingwall was deflected with a barge mounted winch in order calibrate movements in the video image of the wingwall timbers. Experienced observers then estimated the deflection of the wingwall from the video recording in order to estimate the amount of energy absorbed by the wingwall. From this information an estimated berthing coefficient was estimated from 18 events to be $C_b = 0.6$ (Jahren and Jones 1996).

A study concerned with sizing fenders given traditional ship berthing energy methods and applying statistical methods was done by (Ueda, Umemura et al. 2001). The authors focus on a probabilistic method that considers values of ship size, ship mass, approach velocity, virtual mass coefficient, eccentricity factor, and absorption energy of fenders as variables instead of deterministic values. The use of these variables is then utilized to develop a probability of exceedance using a

monte-carlo simulation to investigate when berthing energy may exceed the energy absorption of the fender. The study was focused on ships between 10,000 DWT and 35,000 DWT, and concludes that many ships in this size range exceed their registered size and therefore should be considered when determining berthing energy. Consideration of all aforementioned parameters with statistical characteristics was then utilized in a monte-carlo simulation to calculate the probability a ships berthing energy would exceed the design energy absorption of the fender system (Ueda, Umemura et al. 2001).

This research is continued in (Ueda, Hirano et al. 2002) where the authors present guidelines for the reliability design of fenders by presenting the statistical characteristics of design factors and safety factors. Given sufficiently large number of observations, it was stated that all cumulative frequency distributions could be approximated by lognormal distributions. However, it should be noted that the authors did not directly assess berthing energy and observe it to be fitting a log-normal distribution. They calculated berthing energy using experimentally determined values of mass, approach velocity, and berthing coefficients. All berthing energy calculations were developed using random numbers that fit a lognormal distribution. Further treatment is given to the capacity side of the facility, as described by 'Z', a "factor of energy absorption of fender", the ratio of actual energy absorption to the manufacturers published value of energy absorption of the fender (Figure 2.4).

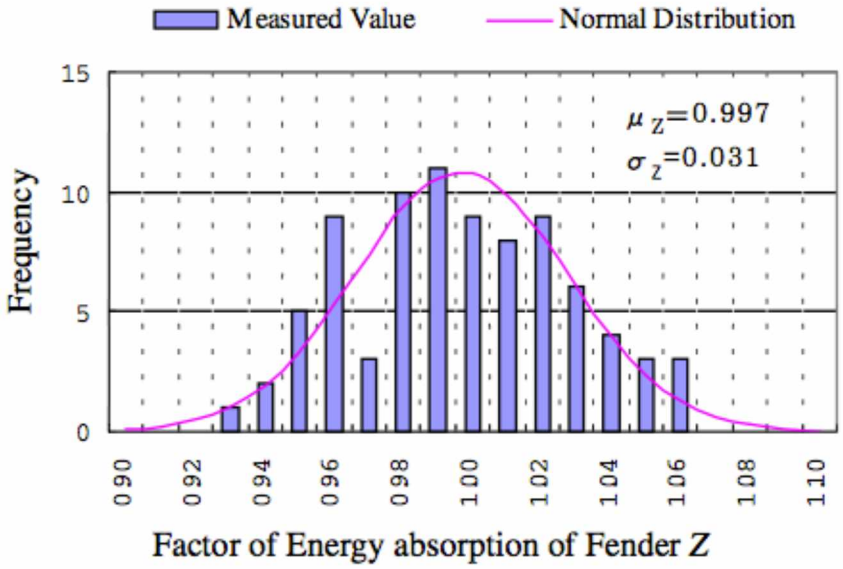

Figure 2.4: Factor of Energy Absorption, (Ueda, Hirano et al. 2002)

(Dickenson 2007) discusses the current state of facility monitoring with regard to port facilities. He states the application of sensors and instrumentation systems at port facilities has lagged behind other sectors of civil infrastructure due to multiple reasons including; installation difficulties, longevity and maintenance concerns in the marine environment, lack of funding sources, amongst other issues. Unlike highway transportation systems, buildings, dams, and power facilities, ports have not typically been included into long-term instrumentation programs. He states that the use of instrumentation systems would help to validate the increasingly heavy reliance on numerical methods to simulate performance of waterfront structures. Most of these issues have been surmounted by other sectors of civil infrastructure, where application of instrumentation systems combined with data processing and analysis has provided direct benefits to engineering evaluation of system performance, maintenance, and life cycle cost evaluation (Dickenson 2007).

Though statistical methods are currently used, a consensus for measurement techniques and application of statistical techniques has not been reached. Unfortunately, due to cost and the individuality of berthing locations, there is not much applicable berthing energy information to draw from in most cases. In situations where a facility operator has incentive to implement a direct measurement system, the information can be a benefit to long-term facility planning and lifecycle costs.

2.5 Empirical Approach

Another method that takes advantage of measured data is the empirical approach. Relationships or formulas can be developed by some combination of measured data and past experience. This methodology is suited to sites that have fairly constant vessel size, and berthing frequency, and berthing conditions (Gaythwaite 2004). The design energy has been proposed by (Girgrah 1977) as based on vessel displacement and a constant that can be varied to a designer's experience:

$$E_f = \frac{\Delta}{120+\sqrt{\Delta}} \qquad \text{Equation 2.8}$$

Where:

Δ = Vessel displacement in long tons

E_f = Design fender energy in long-ton meters

2.6 Reliability Engineering

Traditionally, the approach to engineering marine structures has focused on embedding a high factor of safety into a design. This is a deterministic method in which a multiplier, know as a factor of safety, is applied to the expected load, or stress, a system would expect to experience in order to come up with a robust design. Utilizing the concept of reliability represents a shift in the way failures are treated. The reliability point of view treats system and component failures as random probabilistic occurrences. Given a large enough sample, this random failure process may be described by a probability distribution; and the systems' likelihood of failure (or non-failure) can be predicted statistically (Ebeling 1997).

Reliability is defined to be the probability that a system or component will perform its intended function for a specified period of time under prescribed

operating conditions (Ebeling 1997). Given that all failure modes cannot be eliminated for a given design, reliability engineering is also concerned with identifying the most likely failure modes, and actively working towards mitigating the effects of those failures. The goal is to meet a specified probability of success at a given statistical confidence level. If a system does not perform it's intended function, it is seen to be unreliable even if no failure has occurred (Ebeling 1997).

Determining reliability in an operational sense requires specific description of several factors. An unambiguous and observable description of failure must be explicitly defined. These failures need be defined relative to the function performed by the system or component in question. A specified interval must be chosen, such as a unit of time, or number of cycles. And the system should be observable in its normal state, including design loads, environment, and other operational conditions. Reliability theory is also based on specified operating conditions, no system can be considered reliable given unlimited operational conditions (Ebeling 1997). As a system's reliability increases, so do initial costs associated with the system design; the challenge is to select an appropriate reliability level that balances the initial costs and maintenance/failure costs over the lifecycle of the system.

Strict application of reliability theory for complex systems, such as wingwalls can be difficult to implement due to the challenges associated with combining the reliabilities of the various components in the overall structural assembly. This study will focus on the application of reliability concepts to the demand placed on the structure, not on the capacity of the individual components or composite structural assembly.

2.7 Load Resistance Factor Design

From a basis in reliability theory, load resistance factor design (LRFD) is rapidly becoming the standard methodology for designing buildings and bridges in the United States and abroad. Load resistance factor design considers capacity (strength of materials or components in an assembly) to be a statistical quantity, which assumes strength is merely a probability that it will not be less than a specified value. LRFD also treats demand in this same way; a probability that the load will not be greater than a specified value. Typically materials will have a coefficient that is less than one to factor the capacity downward in order to accommodate uncertainties associated with fabrication and materials. Demand placed on a structure utilizes factors greater than one in order to account for uncertainties in the loads' application (Gaylord, Gaylord et al. 1992). The goal of applying LRFD is to ensure a safe and functioning structure by designing with a rational approach based on the quantified uncertainties of applied loads and material properties.

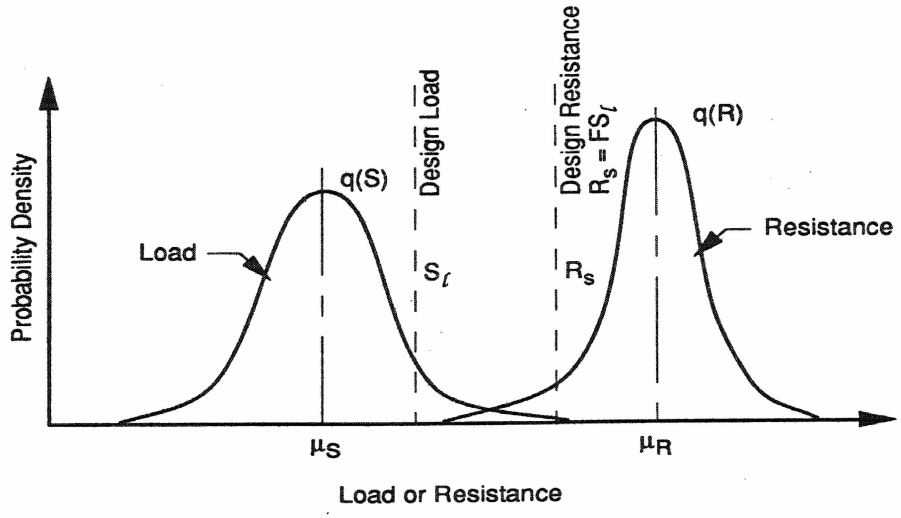

Figure 2.5: LRFD Figure, (Jahren and Jones 1993)

The LRFD methodology takes into account the following factors (Gaylord, Gaylord et al. 1992):

- Variability of a material's mechanical properties
- Uncertainty of loading conditions
- Possibility of deterioration of structural health over time
- Quality of fabrication
- Risks associated with structural failure with regard to injury, loss of life, and damages

Figure 2.5 displays graphically an application of the LRFD principles, the probability density for load is *q(S)* located on the left, and the probability density for resistance is located on the right *q(L).* A structure would then be designed for a load that is some factor greater than the mean load, and also designed so that the capacity of the structure is designed for a factor well below the mean capacity. Following this procedure, a failure will only occur when an unusually high demand is placed on an unusually weak structure (Jahren and Jones 1993).

Chapter 3: Means and Methods

3.1 Overview

The load environment of vessels with displacements between 1,000 and 10,000 long tons is not well understood. Yet vessels of this size, which include passenger and vehicle ferries, can put a high demand on their berthing structures resulting from a large amount of landings over the service life of the facility. The loading information for passenger ferries is an area without much data, and as such, has led to the development of structures with known capacity, but no real corroborating evidence regarding demand. This has led to berthing structures designs that are based on empirical observations and experience that has been developed over time. The designs of the structures are largely a result of improvements made over previous generations after a number of operational cycles and failures.

It is the intent of this study to improve the knowledge base regarding the load environment of the Washington State Ferry System. Through monitoring of the Bremerton slip at the Seattle Terminal over approximately one year, the goal of the study is:

- Present the operational characteristics of the Bremerton Slip at the Seattle Terminal
- Formulate probability-based design criteria consistent with reliability based engineering methods
- Provide a number of design aids that can be utilized by Washington State Ferries' engineers

Findings are based on over 6950 berthing events observed, recorded, and analyzed at the Bremerton terminal. The instrumentation was designed to provide for a comprehensive time history of the vessel-structure interaction before, during, and after impact. The following measurements were recorded with respect to time:

- Vessel position
- Fender displacements
- Strain in pilings
- Tide level

3.2 Site Description

The Seattle Ferry terminal is located in Elliott Bay, within Puget Sound, and adjacent to downtown Seattle, Washington. The terminal features three end berths: Slip 1 services the community of Bremerton, located on the Olympic peninsula, Slip 2 is used as an alternate berth, and Slip 3 services the ferry route to Bainbridge Island. The instrumentation was deployed on the Bremerton terminal – Slip 1.

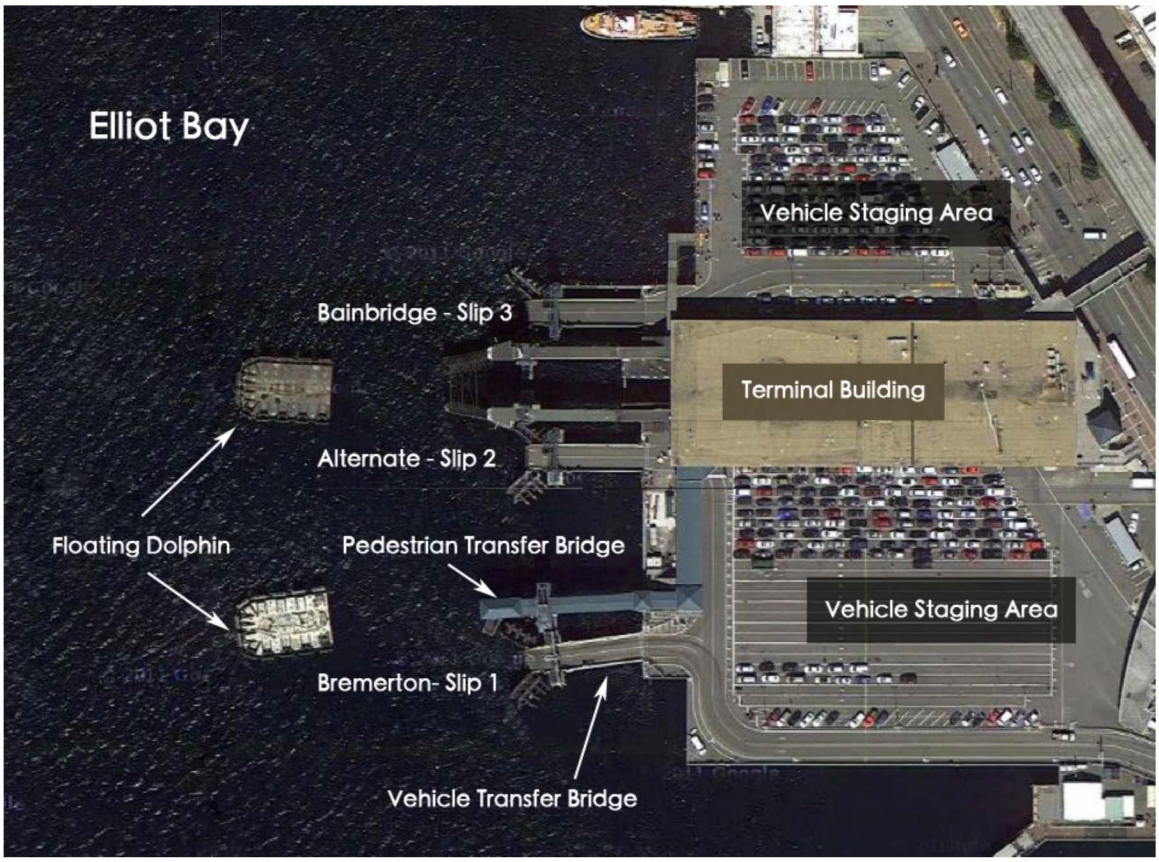

Figure 3.1: Seattle Ferry Terminal aerial view; courtesy Google Maps

3.3 Berthing Structure Description

The Bremerton slip consists of two wingwalls and a vehicle transfer bridge connected to a pile supported wharf that serves as the access point for the ferries, and includes a terminal building that consists of ticketing, concessions, and additional operational facilities. Each wingwall is oriented at 40 degrees relative to the vehicle transfer bridge, and consists of vertical and angled pipe piles, steel framing elements, an impact face, and marine fenders.

The most seaward pile line serves the purpose of being a vessel impact structure, and consists of an impact/wearing face comprised of timbers and replacement wide flange beams covered in ultra-high-molecular-weight polyethylene (UHMW) plastic that are attached to steel wide flange walers, which are welded to three 24" steel pipe piles. This outer pile line is embedded into the sea floor to a depth of 20'.

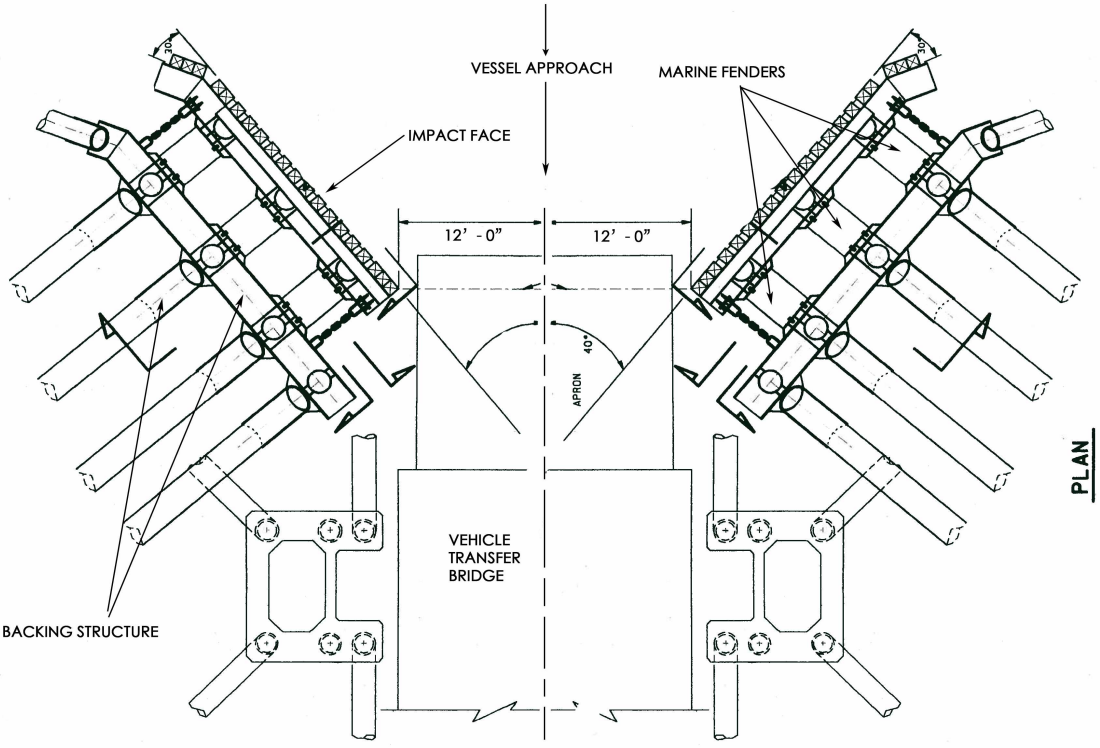

Figure 3.2: Bremerton slip As Built Drawing Plan View, courtesy WSF

The impact wall is connected to the backing structure by elastomeric buckling column fenders, which serve to absorb the impact of the ferry, and also with chains that prevent excessive lateral displacement of the wall. Three sets of fenders are located between the wearing fender and backing structure. The backing structure consists of a space frame that includes four 24" diameter vertical steel piles filled with concrete, four 30" diameter steel 'batter' piles filled with concrete, and one 24" steel 'endo' pile filled with concrete. The structure contains considerable amounts of steel framing to connect the piles, and consists of wide flange beams and 16" steel piles. See Figure 3.2, 3.3, and Figure 3.4 for details.

Figure 3.3: Photos of wingwall structure

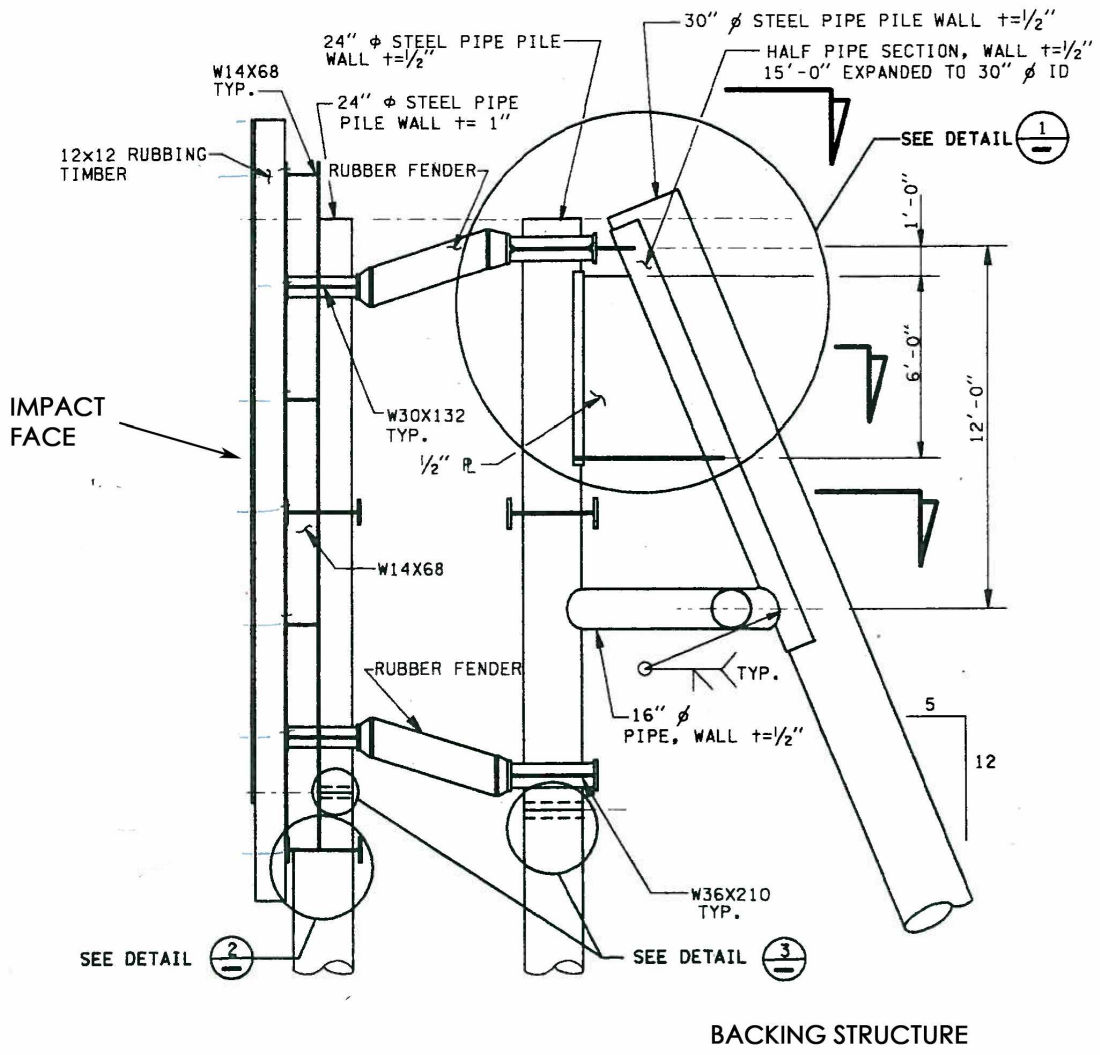

Figure 3.4: Wingwall As Built, elevation view; courtesy WSF

3.4 Vessel Description

The Bremerton terminal is primarily sevices the M/V Kitsap and M/V Kaleetan, double ender vehicle and passenger ferry vessels. Vessels landing at the Bremerton slip during the study have published displacements between 2475 and 2704 long tons, respectively. Fully laden vessels with passengers, vehicles, and fuel increases the displacement range to between 2947 and 3251 long tons, Table 3.1 contains additional information. A picture of the M/V Kitsap is shown in Figure 3. 5.

Figure 3.5: M/V Kitsap

Table 3.1: Vessel Information

Vessel	Gross Tonnage (long tons)	Length (ft)	Beam (ft)	Draft (ft)	Passengers	Vehicles	Horsepower
Kitsap	2475 published, 2947 operational	328’	78’ 8”	16’ 6”	1200	124	5250
Kaleetan	2704 published, 3251 operational	382’	73’ 2”	18’ 6”	2000	144	8000

All vessels in the Washington State Ferry system have diesel electric propulsion on both ends. Illustrations of the vessels are represented in Figures 3.6 and 3.7.

Figure 3.6: Illustration of the Kaleetan, vessel class: Super; courtesy WSF

Figure 3.7: Illustration of Kitsap, vessel class: Issaquah; courtesy WSF

3.5 General Berthing Procedure Description

The general ferry berthing procedure consists of decelerating from the crossing velocity, and slowly maneuvering into the berth. The incoming ferry utilizes two wingwall structures oriented at approximately 40 degrees to the vehicle transfer-bridge when berthing and unloading passengers and vehicles. The opposing wingwalls form a pocket shaped berth that is used to attenuate the impact energy of berthing events (Playter 1994). Depending on weather conditions, the vessel may use one or both wingwalls to arrest its forward progress before coming to rest between both walls in order to proceed with the off-loading procedure. After coming to a stop, the vessel is tied-off to the transfer bridge and remains under power using the wing walls and a large floating dolphin on the north side of the vessel to maintain a stable position for loading/unloading.

3.6 Instrumentation Description

In order to measure the berthing parameters, an instrumentation system based on the principles used in the 2010-2011 Auke Bay Load Environment study was designed and implemented at the Bremerton slip at the downtown Seattle Ferry Terminal. In order to capture the complete berthing event, the instrumentation was installed on both the north and south wingwalls. See Figure 3.8 and 3.9 for further details regarding instrumentation layout.

The instrumentation scheme at the Bremerton Slip of the Seattle ferry terminal consisted of :

- Two Campbell Scientific® CR5000 Data Loggers housed in Environmental protection boxes
- Three Senix TSPC ultrasonic distance sensors
- Six Celesco Aluminum Linear Motion Transducers (LMTs)
- Six Celesco Stainless Steel Pressure Tested Linear Motion Transducers
- Thirty-six 90 degree chevron strain gauges (two ¼ bridges per gauge)
- One Toughbook field laptop running Campbell Scientific's RTDAQ and LoggerNet software
- Two Sierra Wireless™ Airlink Raven XT cellular digital modems and associated hardware
- Beldin 5 strand shielded instrumentation wire

The system was designed to monitor berthing parameters relevant to engineering design of berthing structures at the Bremerton slip subjected to vessel impacts. Each instrumentation system was wired into a datalogger, which was designated as North or South, corresponding to the wingwall position relative to the transfer bridge. The dataloggers were programmed using the CRBasic language, using the CRBasic Editor from Campbell Scientific®. CRBasic is a computer language optimized to control Campbell Scientific dataloggers by offering functionality that supports and simplifies scientific measurements and data collection.

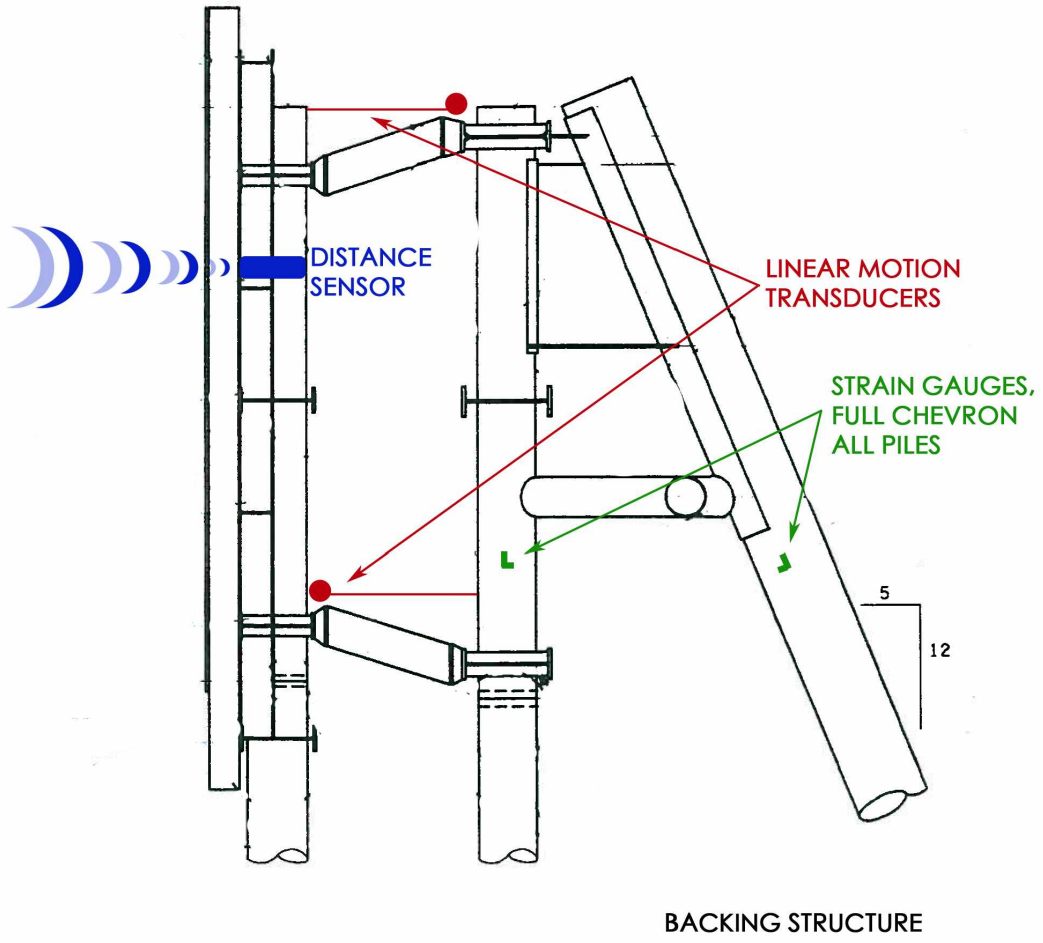

Figure 3.8: Instrumentation of wingwall, elevation

In order to accurately capture the parameters of a berthing event, the system operated at 5Hz continuously. When a ship crossed a threshold distance of 20 feet from the face of the wingwall, the dataloggers initiated a new event table, and recorded the states of all system sensors onto an internal flash memory card. Once the vessel initiated the recording sequence, data was recorded for several minutes. After observing numerous landings, it was determined that two minutes was an

adequate amount of time to capture the response of the wingwall prior to, during, and after berthing procedures. See Figures 3.10, 3.11, and 3.12 for photographs of the installed instrumentation.

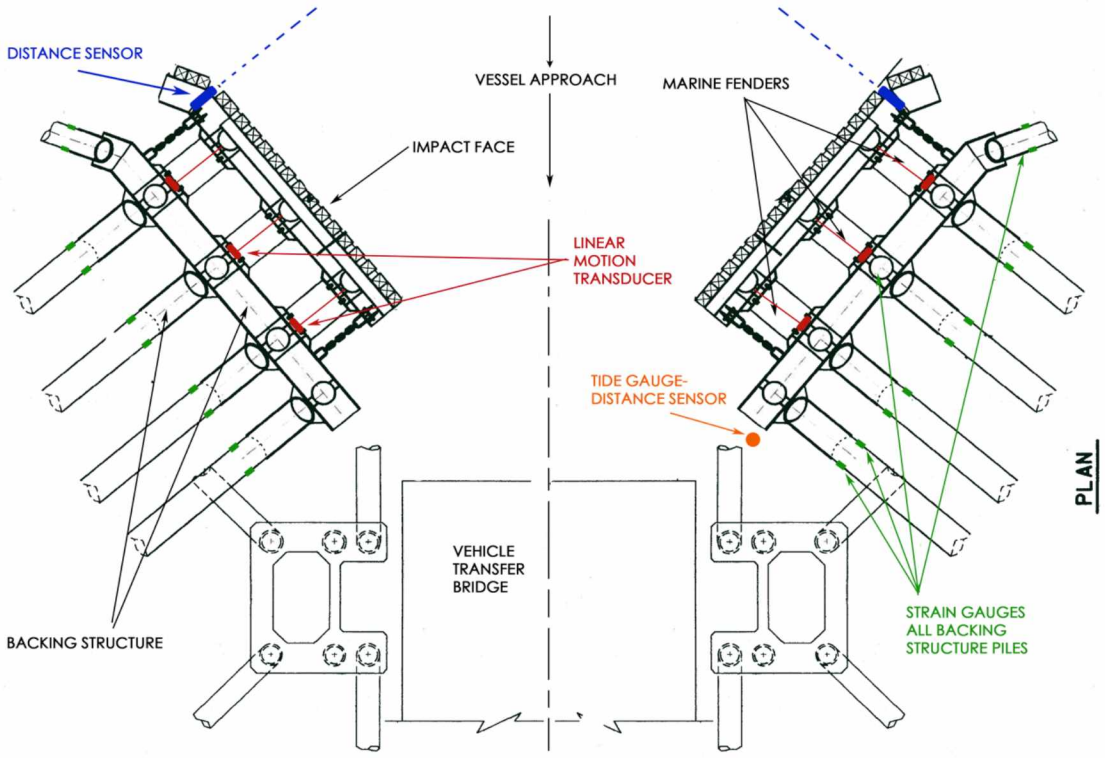

Figure 3.9: Instrumentation of wing walls, plan view

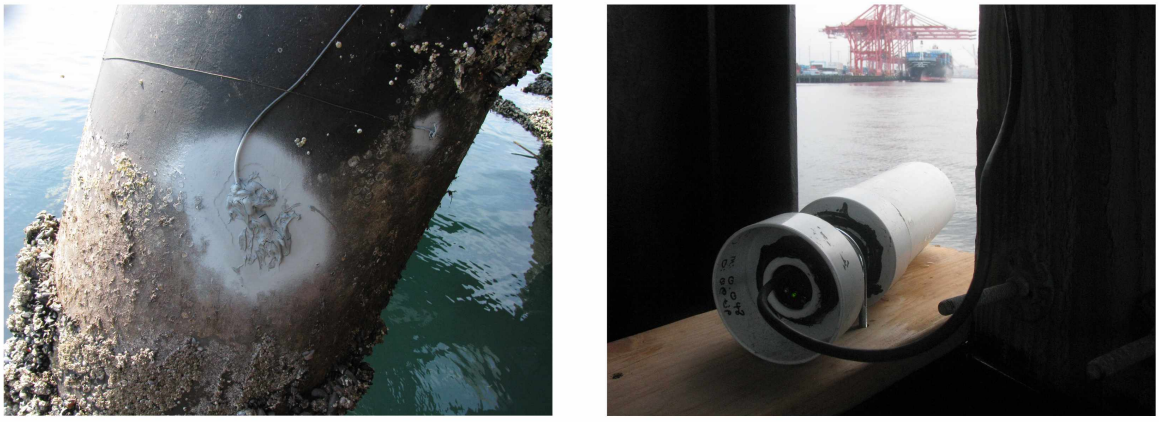

Figure 3.10: Strain gauge (left) and distance sensor (right) installation; strain gauge installation, covered in silicone and zinc-rich paint to protect against the corrosive effects of saltwater. Right; distance sensor used to record vessel position measurements.

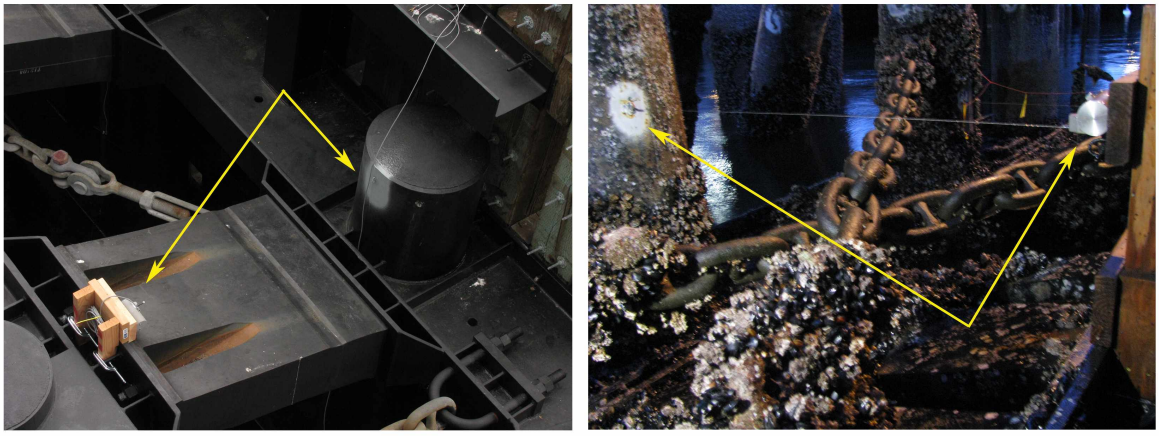

Figure 3.11: Linear Motion Transducer photos; Upper Linear Motion Transducer (left) with cable affixed to vertical pile. Lower LMT (right) in the intertidal zone above the marine fender and above the chains.

Figure 3.12: Datalogger and Distance Sensor photos; Datalogger (left) wired with wingwall instrumentation; distance sensor (right) measuring the tide elevation.

3.7 Vessel Position Measurements

Monitoring of the incoming vessel position was accomplished using Senix ToughSonic® TSPC ultra-sonic distance sensors. Vessel position information represents one of the most important tasks of the instrumentation installation. This measurement was crucial for two reasons; knowledge of the vessels' position was required to initiate recording of berthing event parameters, and this recorded position, with respect to time, is the basis for the vessel approach velocity calculation. Approach velocity was calculated from vessel position measurements one second before impact. Fender displacements were recorded concurrently with vessel position. Together this information was used to determine the time of impact.

Figure 3.13 displays a typical berthing event at the south wingwall of the Bremerton slip. The sharp valleys in the graphs indicate impact with the wall and align with maximum displacements of the fender system. Though this is a common berthing procedure, many variations were observed.

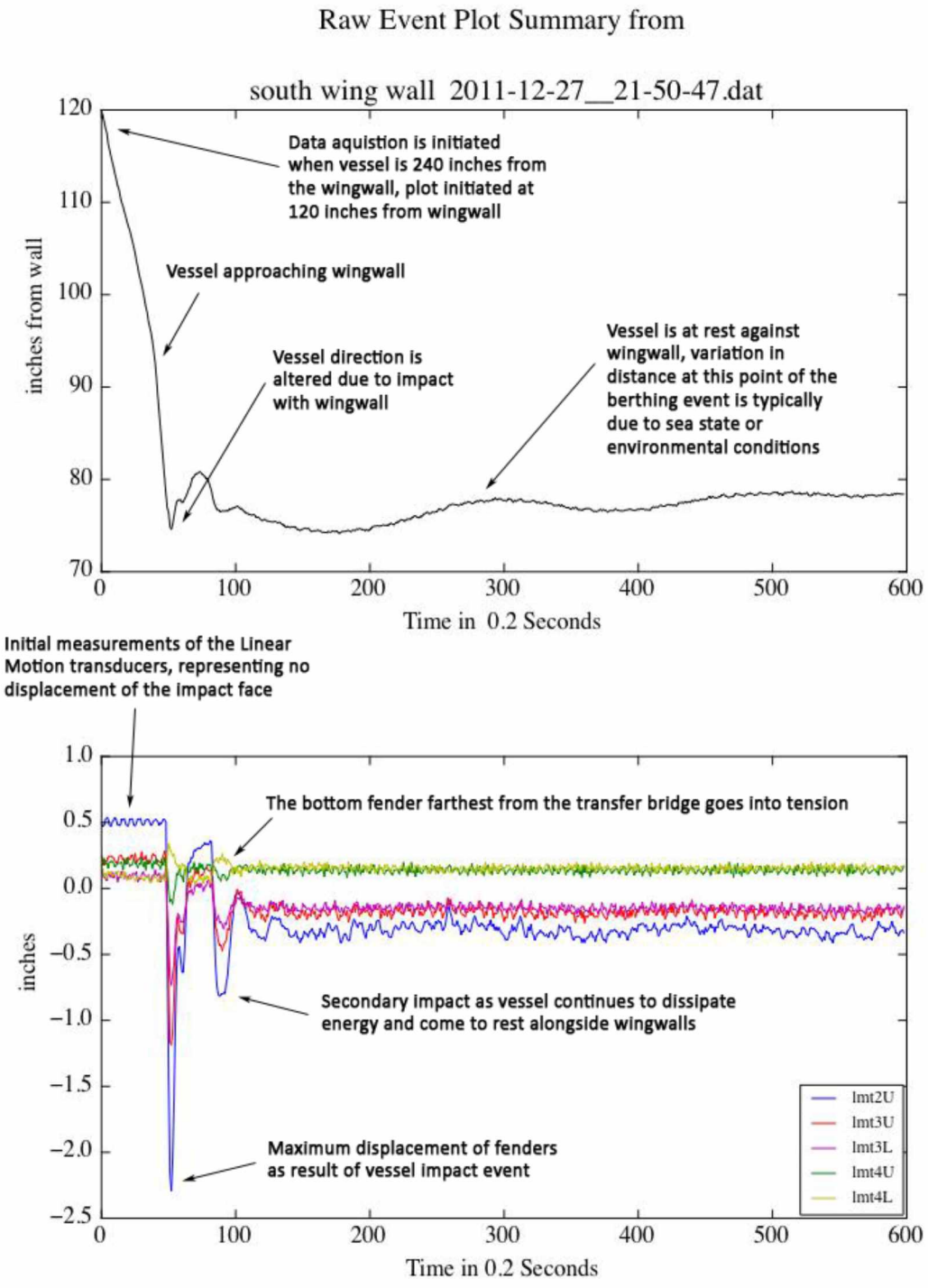

Figure 3.13: Vessel Position and Fender displacement plots with description.

3.8 Data Acquisition

Transferring raw data files from the datalogger in Seattle was accomplished by utilizing a Sierra Wireless™ Airlink Raven XT cellular modem controlled remotely by a laptop computer in Fairbanks. Two pieces of Campbell Scientific® software were employed to control the system remotely, LoggerNet and Real Time Data Acquisition (RTDAQ). LoggerNet was used as an automatic collection protocol, serving primarily to download data from the datalogger at a scheduled time every evening. RTDAQ was used for real time system monitoring of berthing events to observe the functionality of the sensors. Both of these programs allowed for editing and uploading of user developed code to run the instrumentation system. After the information was uploaded to the 'field laptop', it was then backed up and transferred to the post-processing environment. Figure 3.14 illustrates the steps associated with the event capture procedure.

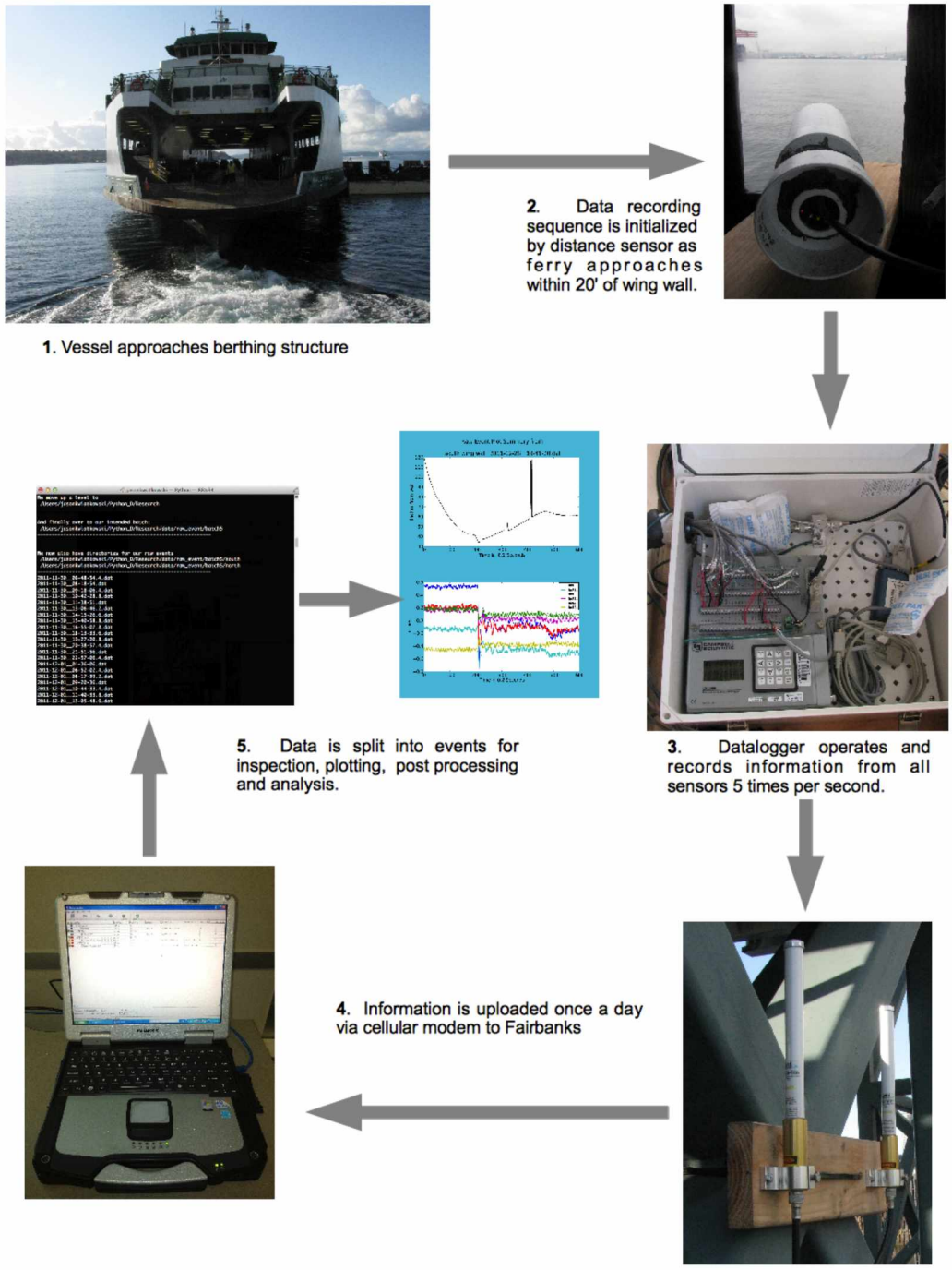

Figure 3.14: Event Data Acquisition Sequence

3.9 Software Description

To evaluate and process this large data set, a suite of interactive software was developed to facilitate the data processing and analysis. Software was developed using Python, an interpreted, interactive, object-oriented, extensible programming language. Several programs were called upon to do the bulk of the event characterization, all were developed using Python version 2.7.4. All programs discussed in this section were developed by the author, see Figure 3.15 for an overview of the process flow,.

The raw data table uploaded from the data logger is a large file that requires refinement for efficient processing; a program named *batch_splitter.py* is used for this first data transformation. The primary purpose of this application is to open the large 'raw' tables from the data logger and filter it into discrete event files representing a single vessel-berthing event. These event files are then organized into batches, each batch contains one month of data at each wing wall.

Following this reorganization of the raw files into discrete berthing events, the next step is to characterize the berthing event by identifying parameters that describe system response. These parameters are then recorded and analyzed later in the process. The first step when characterizing an event is to understand if a berthing event file is valid (Figure 3.16). Often times data is recorded without a vessel landing, for example a bird or passing boat may trigger the system to record, and it is important to eliminate these 'events' from the data set.

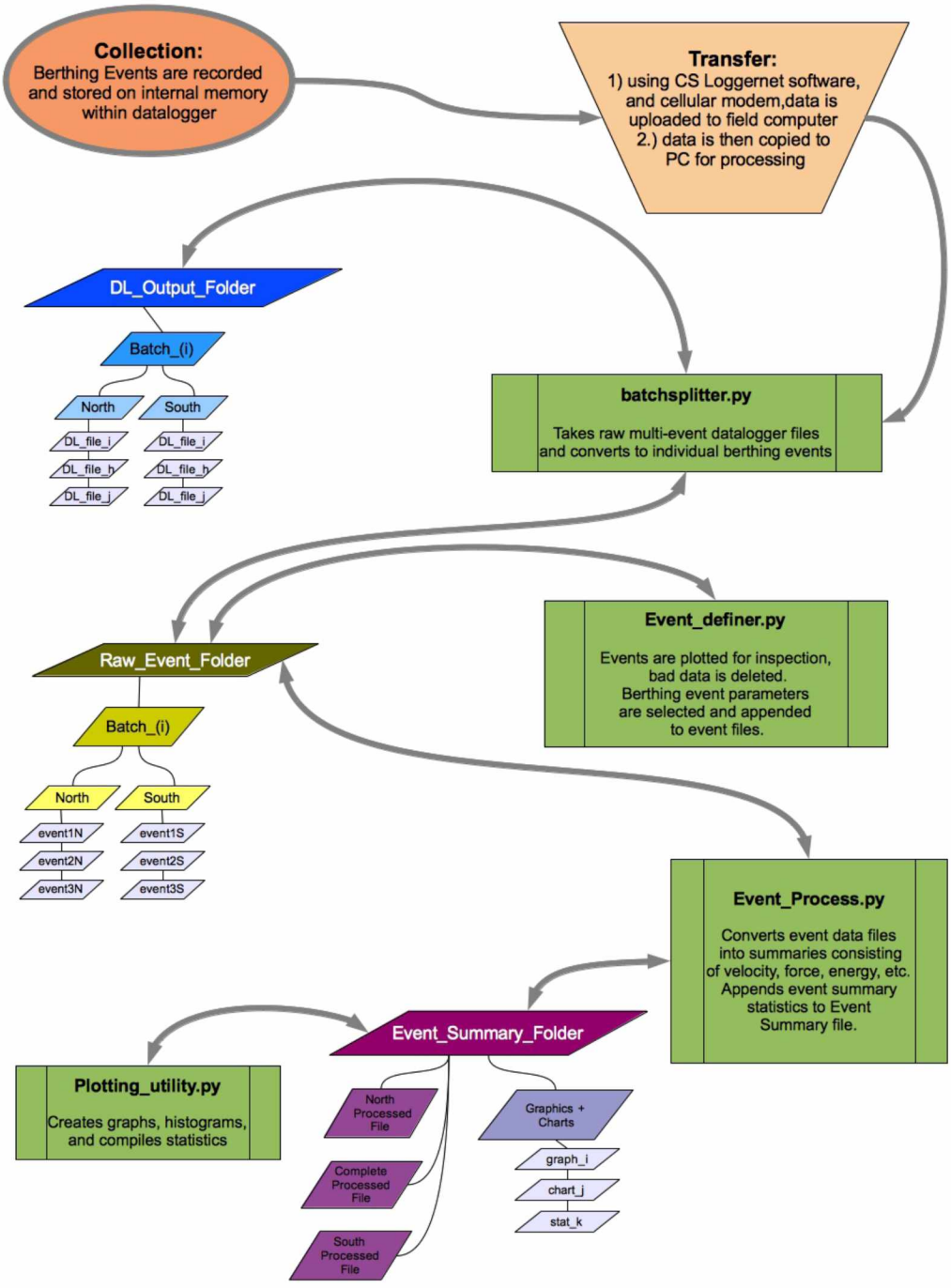

Figure 3.15: Software and Data Interaction Diagram

Characterization of the berthing events is accomplished using the *event-definer.py* application. The goal of *event_definer.py* is to check and interpret an event dataset by visual inspection. This inspection serves to ensure that data recorded and eventually analyzed will in fact represent the system as it behaved, in the context we are interested in. This is accomplished using a graphical user interface (GUI) in conjunction with command line controls. After invoking the program, the user is asked which batch of event files to investigate. Next, an event is plotted in order to ensure it represents an actual berthing event, and to select the key data points that characterize the berthing event. If an event does not represent a ferry landing, it is then deleted.

Once an event is verified, the user is instructed to select (using a mouse or track pad) the point of maximum vessel impact from a plot of the berthing event data. The plot displays two of the linear motion transducer (LMT) displacement measurements, and the position of the ferry (normal to the wingwall) with respect to time. The maximum discrete impact point, as evidenced by displacement of the marine fenders, is selected either automatically or manually depending on characteristics of the berthing event; see Figure 3.16 for more details. The selection of the 'impact point' for this study was selected to be the maximum impact recorded by the LMTs (translating to maximum fender deflections). Maximum deflections associated with a vessel 'power up' against the impact face was not considered to be an impact event and was omitted in the event analysis.

The visual investigation of recorded data enables the filtering of events that do not meet criteria associated with an incoming vessel. Figure 3.16 presents a plot on the right consisting of electronic 'noise', and is devoid of relevant information portrayed by the actual vessel-berthing event on the left.

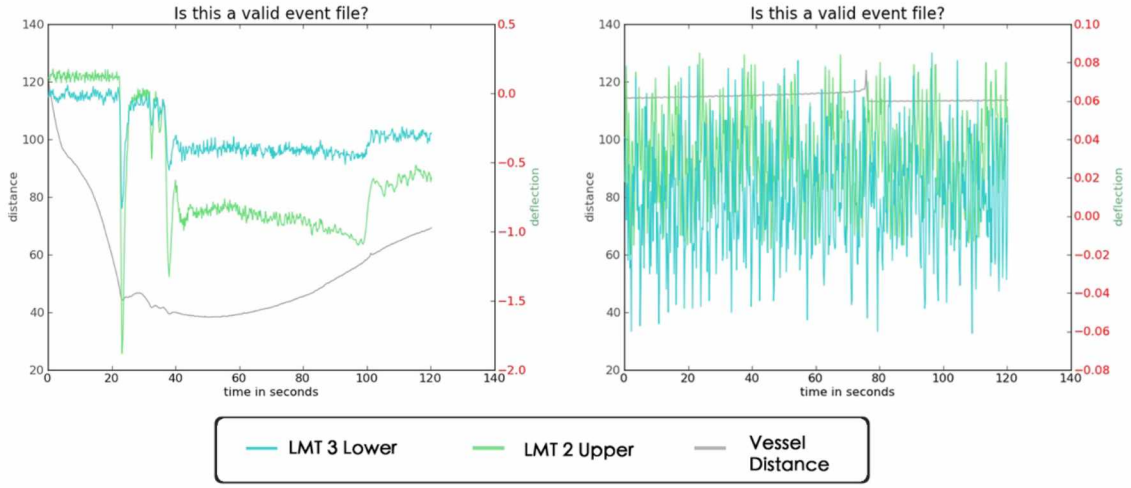

Figure 3.16: Event filtering decision graphic

The *event_definer.py* application allows for manual selection of data points that characterize the berthing event, the point of maximum deflection and the point that represents the initial state of the system are shown in Figure 3.17. Once the maximum displacement is selected, the initial state of the system is then identified and selected using the original graphical selection procedure. The graph is again presented with highlighted points that characterize the berthing event in order to verify that the characterization is accurate. In the event that the points were selected incorrectly, they can be erased and chosen again. Once the accuracy is verified, the indexes (which represent positions within the event file) of the maximum displacement, the initial conditions, and one second prior to the initial impact are appended to the event file as an immutable tuple (a list of data that cannot be altered).

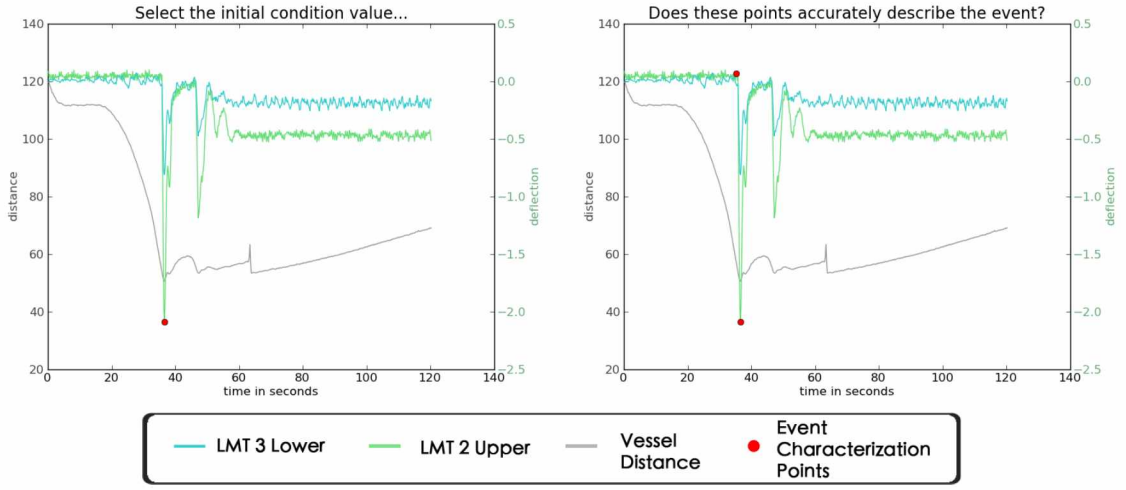

Figure 3.17: Event characterization graphic

After a batch of berthing events has been characterized, the next step is to process the parameters that describe the event (such as initial velocity, force, energy, etc.) and output the data to a summary file using the *event_process.py* application. This program requires a dataset to operate; however, after inputting which dataset to analyze, the processing is completely automated. Once a dataset is specified, the application opens each event file, and uses the output tuple from the previously executed program (*event_definer.py)*, as the basis for all calculations regarding berthing force, energy, and approach velocity. For example: the index values of maximum displacement for each transducer are subtracted from the initial state of the system (resulting in a measurement of fender deflection) and then these values are inputted into polynomials that describe the fender reaction or energy. This is done for all sensors on the wing wall. After all calculations are made, this data is then appended to a summary file that consists of unique berthing events, the raw measurements that make up the event (vessel position, transducer deflection, tide, etc.), and the calculated data that describes the berthing parameters of each

event such as approach velocity, absorption energy per fender, total absorption energy, etc.

In addition to these primary programs a number of other utilities were employed using this framework to facilitate other aspects of the project including plotting, assembling data from the north and south wing walls, checking for duplicate records, amongst others.

3.10 Structural Model

A structural model was created using the software SAP 2000 v15 (produced by Computers & Structures, Inc.) in order to investigate the performance of the entire structural system (Figure 3.18, 3.19). Constructing the model was facilitated by 'as-built' plans and geotechnical information provided by Washington State Ferry personnel. Support characteristics were determined from soil 'PY' curves and idealized as soil springs in the model.

The wingwall system at the Bremerton slip consists of an impact face, marine fenders and a backing structure. The impact face consists of timber, UHMW, and steel-walers attached to three steel vertical pipe piles. As-built information indicates the fender piles were driven 20' below the mud-line. The impact face and piles are connected by 6 buckling column marine fenders to a reaction frame backing structure comprised of vertical and battered concrete filled pipe piles connected by steel wide flange and pipe framing elements. The four vertical piles were driven 50' deep, the four batter piles penetrate 35 ' deep, and the one 'endo' pile (a batter pile driven to resist lateral movement of the wingwall) penetrates 45' below the mud-line (Jahren and Jones 1996).

Figure 3.18: SAP model of wingwall

The primary function of the structural model was to determine the relative stiffness of the structural components. Unit loads were applied to the wingwall model at the experimentally determined center of force (more information regarding the point of impact calculation procedure can be found in Section 3.15). Deflections resulting from the applied loads were recorded vertically halfway

between the fender lines in order to determine impact face and piling stiffness values. The backing structure deflection was determined at the centroid of the four vertical backing structure piles in plan view, and at an elevation between the upper and lower fender mounts on the vertical backing structure piles. The generalized stiffness of the system for this analysis is taken to be the unit load divided by the deflection of the reaction frame backing structure. Information regarding system and component stiffness values can be found in Table 3.2. The wingwall stiffness was calculated to be between 53.95 and 49.47 kips per inch depending on the amount of force applied. A model of the impact face and piles without a backing structure or fenders was utilized to determine stiffness characteristics of the impact face and pilings (see Figure 3.20).

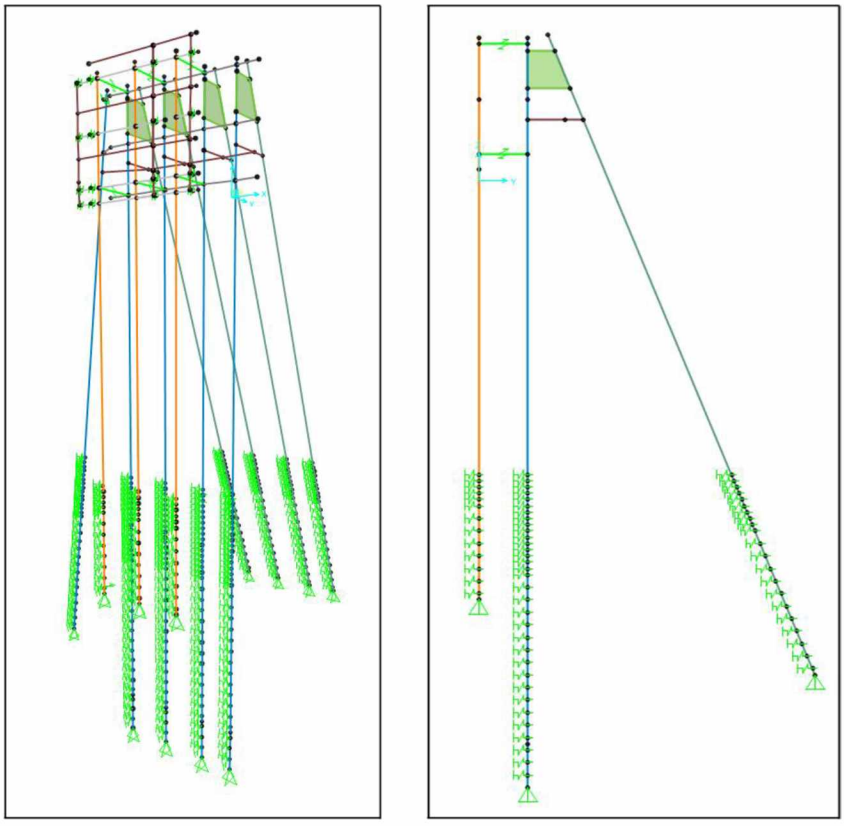

Figure 3.19: SAP wingwall model, isometric and elevation view

Table 3.2: Generalized structural stiffness of assembly and components

Component	**Stiffness**	**Deflection notes**	**Force Application Notes**
Complete Wingwall System	53.95 to 49.47 kips/inch	Deflection measured at center of backing structure, dependent on amount of fender deflection.	Force applied at experimental force centroid
Reaction Frame Support Structure	307.9 kips/inch	Deflection measured at center of backing structure	Forces applied at fender mounts on backing structure
Impact face and piling assembly	2.267 kips/inch	Deflection measured at center of impact face, halfway between upper and lower fender mounts.	Force applied at experimental force centroid
Single Vertical Piling of Impact Face (Impact Face consists of 3 pilings)	0.7554 kips/inch	Halfway between upper and lower fender mounts.	Force applied on pile, halfway between upper and lower fender mounts
Marine Fenders	18.89 to 5.1 kips/inch	Nonlinear stiffness dependent on amount of deflection	Manufacturer's published reactions

The structural model was also used to develop relationships between fender deflection and displacement of the reaction frame support structure. Using the component stiffness values and the fender-reaction frame deflection relationship, energy distribution throughout the wingwall assemblies could be determined. See Table 3.3 and Figure 3.21 for the relative amounts of elastic energy for the structural assemblies.

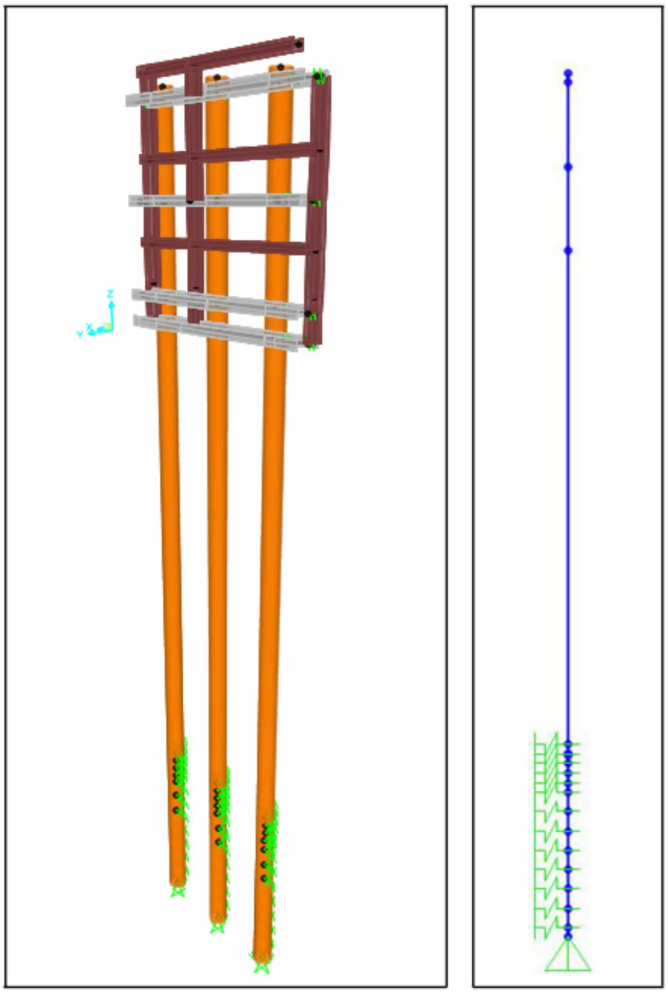

Figure 3.20: SAP Impact Face Model (L); SAP Single Impact Pile Model (R)

Table 3.3: Energy Absorption Characteristics of Structural Components

Force Applied to Structure (kips)	Total deflection of Fenders (inches)	Impact Pile Elastic Energy (kip-feet)	% of total energy	Fender (kip-feet)	% of total energy	Support Structure Elastic Energy (kip-feet)	% of total energy	Total Elastic Energy (kip-feet)
5	0.26	0.000	0.04	0.61	99.48	0.003	0.48	0.62
10	0.50	0.001	0.08	1.18	98.9	0.012	1	1.19
20	0.99	0.004	0.15	2.39	97.9	0.048	1.95	2.44
100	4.96	0.092	0.60	14.03	92.19	1.097	7.21	15.22
250	12.93	0.633	1.09	50.45	87.2	6.770	11.7	57.85
500	27.05	2.742	1.43	160.26	83.63	28.610	14.93	191.61

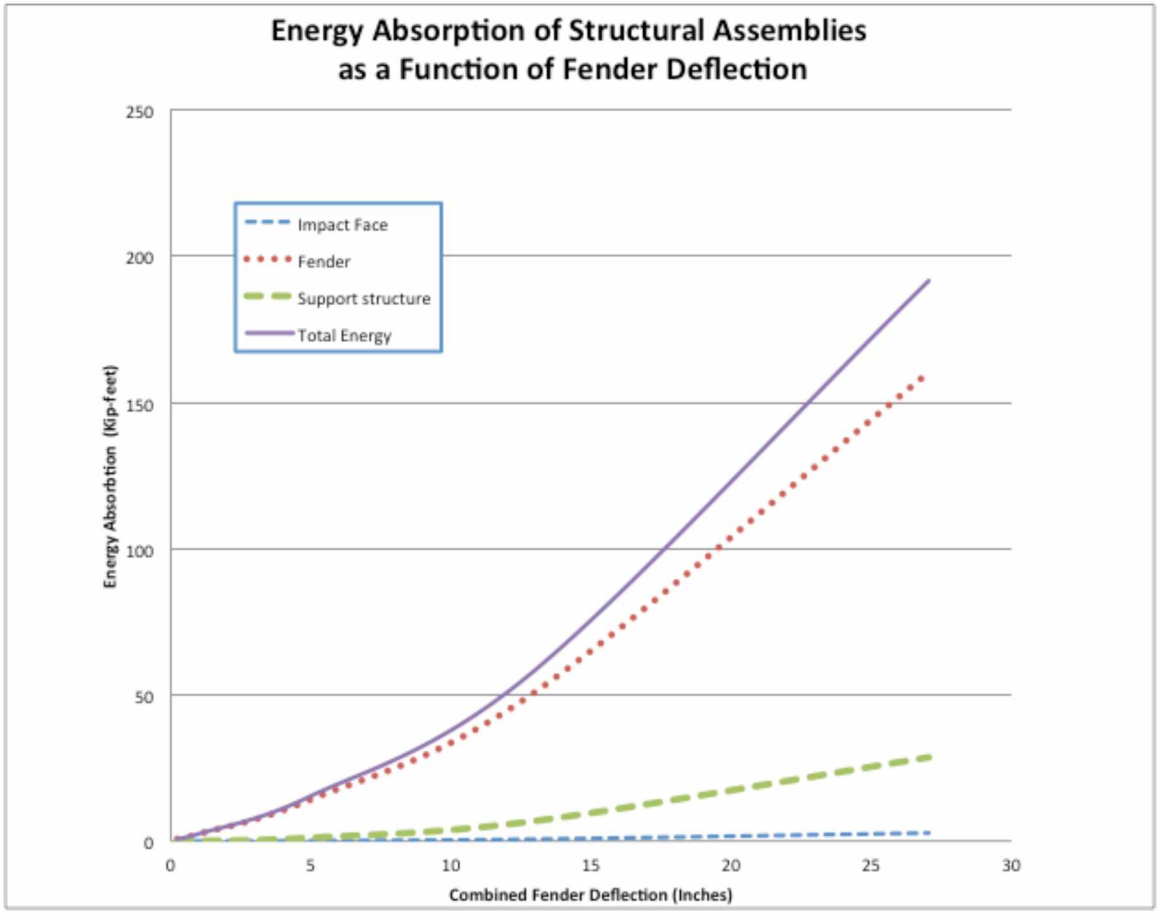

Figure 3.21: Energy Absorption of Structural Assemblies

3.11 Berthing Energy Estimates

Marine structural engineers typically utilize berthing impact energy to design structures for vessel impacts. When a vessel impacts a berthing structure, most of the kinetic energy is transformed to elastic energy of the deformed structure. Marine structural design typically utilizes the conservative assumption that all berthing energy will be absorbed by the marine fender, and the amount of energy transmitted to the backing support structure, and the vessel's hull is minimal (Gaythwaite 2004).

At the Bremerton Terminal, linear motion transducers (LMTs) positioned to record the deflection characteristics of each marine fender with respect to time allowed for berthing energy information to be determined. As a vessel impacts the wingwall, the marine fenders compress as the impact face deflects towards the backing structure. Combining known displacements of the marine fenders, and information regarding the energy-deflection characteristics of the marine fender supplied by the manufacturer (Figure 3.22, Table 3.4, Equation 3.1,), the energy absorbed by a fender can be estimated.

Table 3.4: Trelleborg Fender characteristics

Trelleborg **MV1250 x 1000A**

Nominal Rattings

Energy **283** **Kip Ft**

Reaction **150** **Kips**

Deflection %	mm	inches	inches Squared	Energy %	Energy Kip-Ft	Reaction %	Reaction Kips
-5	-62.5	-2.4606		-2	5.66	-31	-46.5
0	0	0.0000	0.0000	0	0	0	0
5	62.5	2.4606	6.0547	2	5.66	31	46.5
10	125	4.9213	24.2188	7	19.81	58	87
15	187.5	7.3819	54.4923	14	39.62	78	117
20	250	9.8425	96.8752	24	67.92	92	138
28	350	13.7795	189.8754	41	116.03	100	150
35	437.5	17.2244	296.6803	56	158.48	96	144
40	500	19.6850	387.5008	66	186.78	90	135
45	562.5	22.1457	490.4307	76	215.08	85	127.5
50	625	24.6063	605.4700	85	240.55	84	126
57.5	718.75	28.2972	800.7340	100	283	100	150
62.5	781.25	30.7579	946.0468				
100	1250	49.2126					

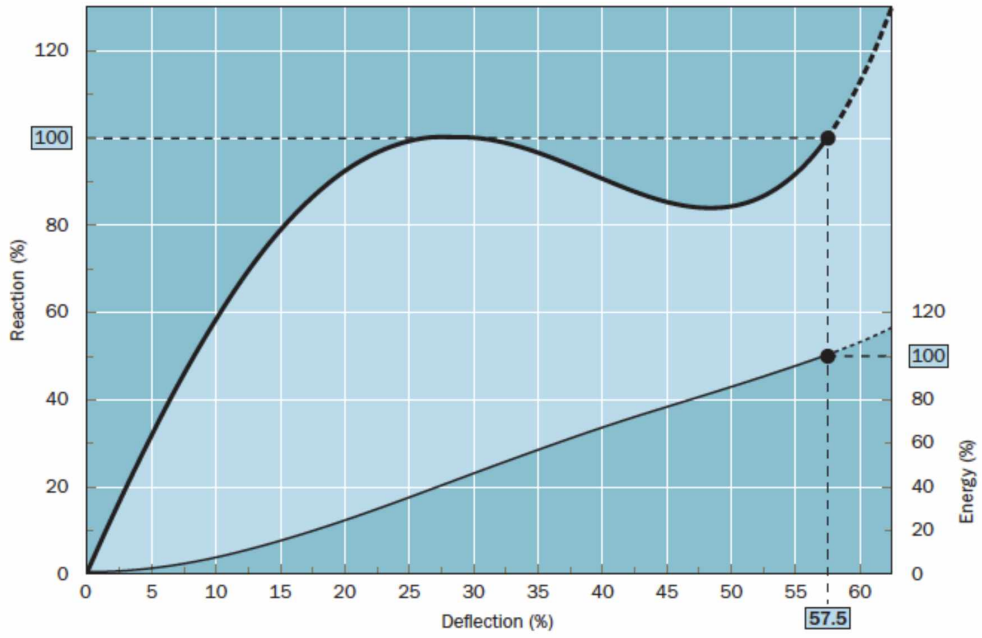

Figure 3.22: Energy absorption of marine fenders, courtesy Trelleborg

$$E_{fender} = 0.00004x^5 - 0.0027x^4 + 0.04x^3 + 0.2856x^2 + 2.1748x$$

Equation 3.1

Where:

E_{fender} = Energy absorbed by marine fender

x = Displacement of fender

The fender system employed on each wingwall at the Bremerton slip in Seattle consists of six buckling column type fenders, mounted in two rows that connect to the pile supported impact face and the space frame backing structure. Each fender employed at the Bremerton slip is rated to absorb 283 kip-feet of energy at maximum displacement.

The energy dissipated by the entire structural system consists not only of energy absorbed by the fenders, but also a portion of the energy is dissipated by the deflection of the impact face and reaction frame backing structure. The energy absorption characteristics are represented as a kinematic model in Figure 3.23.

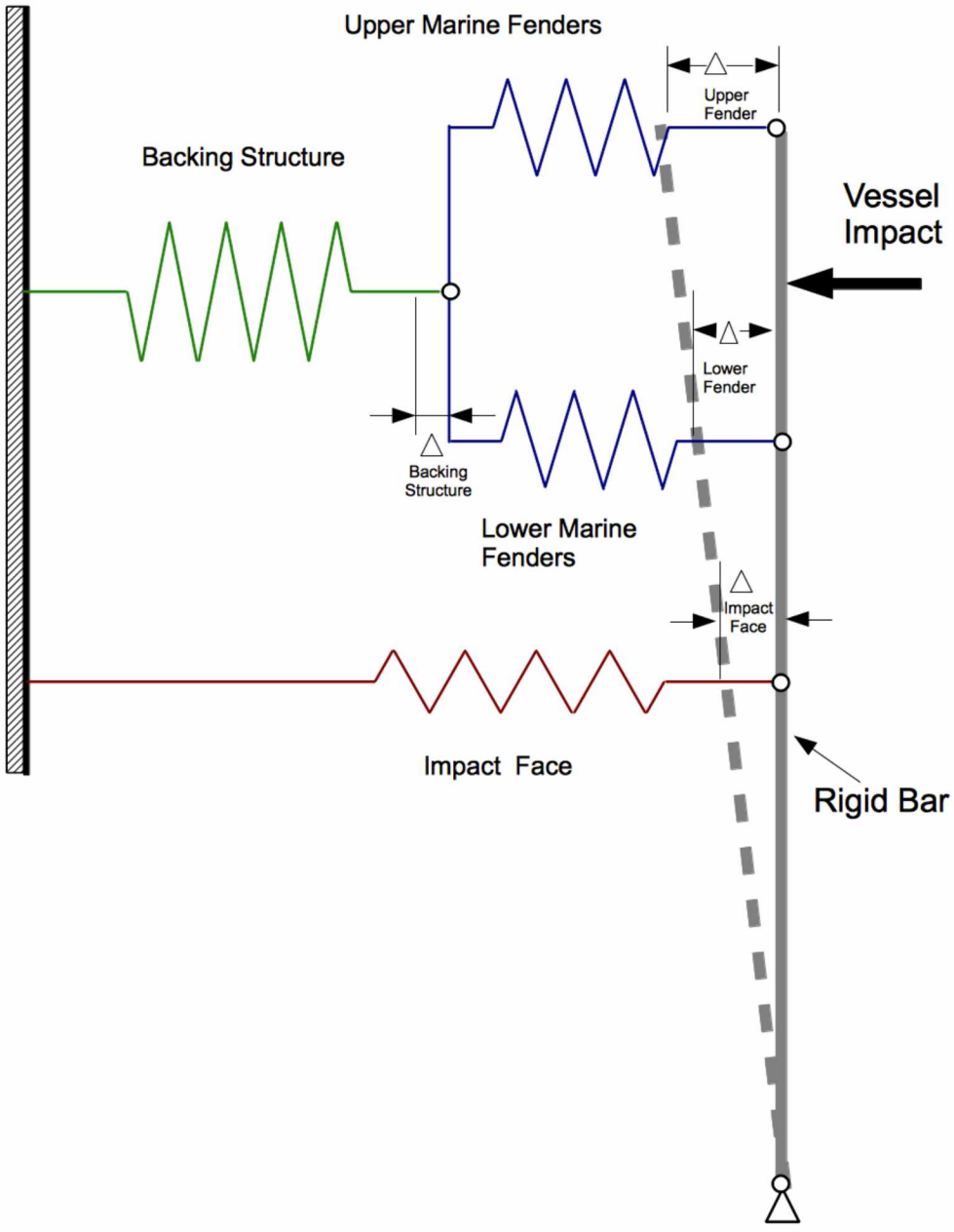

Figure 3.23: Kinematic Model of Wingwall

The equation for the total berthing energy associated with a ferry landing at the Bremerton terminal is described by Equation 3.2.

$$E_{total} = \sum_{i=1}^{6} E_{fender} + \frac{1}{2} K_{frame} \Delta_{frame}{}^{2} + \sum_{j=1}^{3} \left[\frac{1}{2} K_{impact\ pile j} \left(\frac{\Delta_{lmtjL} + \Delta_{lmtjU}}{2} \right)^{2} \right]$$

Equation 3.2

Where:

E_{total} = Total energy absorbed by the complete structural system

E_{fender} = Energy absorbed by marine fender

K_{frame} = Stiffness of reaction frame backing structure

Δ_{frame} = Displacement of backing structure

$K_{impact\ pile}$ = Stiffness of pile supporting the impact face

Δ_{lmtjL} = Displacement of fender *j*L (lower fender, at position '*j*')

Δ_{lmtjU} = Displacement of fender *j*U (upper fender, at position 'j')

Chapter 4: Results

4.1 Overview

At the conclusion of the project, all events were analyzed using the software package described earlier. Following filtering and event characterization, the dataset for the north wingwall was approximately 3448 impact events, the south wingwall dataset contains 3504 impact events, for a total of 6952 vessel impact events.

Results are presented in this section for six parameters; approach velocity, berthing energy, berthing force, berthing factor, berthing coefficient, and vessel point of contact. These parameters are investigated in this section as a collection of individual events at the wingwalls. Results concerning how a particular wingwall experiences berthing parameters is introduced through summary tables in this section and expanded upon with figures and tables in the Appendix A through D. Results in sections 4.2, through 4.8 are displayed through histograms, probability distribution fits, cumulative probability plots, probability of non-exceedance plots, and regression fits.

Section 4.2 and Appendix A provides results of initial approach velocity, Section 4.3 and Appendix B present berthing energy results, Section 4.4 and Appendix C provides berthing force results. Section 4.5 displays berthing coefficient results. Berthing factor results are illustrated in Section 4.6 and Appendix D. Section 4.7 presents reliability design charts. Impact point of contact results are displayed in Section 4.8.

Histograms provide a graphical representation of the frequency distribution of each parameter, such as approach velocity or berthing energy, and their frequency of occurrence. The purpose of the histograms is to display the relative frequencies of each parameter by displaying the number of times magnitudes within a certain range occur over the sample size.

Probability density functions (pdf) are fitted onto the corresponding histograms and attempt to match a well-defined *pdf* to the empirical data. Using probability distributions that correlate with the experimental data, a probability of occurrence can be associated with the experimentally determined results.

Cumulative probability distributions are derived from the cumulative sum of *pdf* curves, and associate measured parameters with the probability of not being exceeded or equaled displayed in percentile form. The purpose of the cumulative probability graph is to display the relative fit between the selected probability distribution and the empirical data.

Percentile plots are another method of visualizing the cumulative probability distributions. The vertical axis of these plots is a percentile value representing a probability that a given parameter value will not occur or be exceeded during a berthing event. This percentile value represents a parameter value of which a given percentage of measurements occurred or were below a parameter value. For example, a percentile value of 0.99 represents a parameter value of which 99% of recorded values were at or below that parameter value, and 1% of recorded values measured above that level. The benefit of the percentile plot is twofold; first they are useful for analyzing the probability of occurrence at extreme values, and secondly they graphically display the 'goodness of fit' of the probability distribution to the experimentally obtained dataset. The angle and degree of linearity illustrates how well the distribution matches the empirical data. The probability distribution is represented as a line, and displays the relationship between the parameter of interest and its probability of not being exceeded in any one berthing event. The distribution line allows for extreme values and corresponding probabilities of occurrence to be estimated, and presents the designer with a methodology for selecting design parameter values – i.e., engineering design criteria.

Parameter values in each section are provided over a range of percentiles matched to the needs of WSF personnel and corresponding design lives of the wingwall structures. The wingwall structures have a design service life of 50 years

which, depending on the terminal, ranges from approximately 200,000 to 730,000 berthing events at current sailing schedules. The Bremerton Terminal 50 year design life is approximately 237,750 berthing events. For instance, a parameter value corresponding to the 99.99th percentile would correspond to a 43.75% probability of not being exceeded over the course of one year at the Bremerton Terminal, which receives approximately 5475 berthing events in a year. A parameter value corresponding to the 99.9999999th percentile would have a 0.005% of not being exceeded in the course of ten years at the Bremerton Terminal, and a 0.02% probability of not being exceeded over the course of 50 years at the Bremerton Terminal. See Section 5.3 for more information concerning reliability and risk level determination.

4.2 Velocity Results

Approach velocity was determined using the sonic distance sensor data with respect to time. The distance sensor recorded the position of the vessel normal to the wingwall and at the seaward side of the wingwall. See Figure 3.8 for the placement of the distance sensor on the wingwall. The position of the distance sensor may have a significant effect on the recorded approach velocity of the berthing vessel; this topic is elaborated upon in section 5.6. See Table 4.1 for a summary of the recorded velocity information. The velocity information in this section represents the combined dataset. Additional velocity data and plots are presented for the North and South Wingwalls separately in Appendix A.

Often, multiple impact events occur during a berthing event. The dataset analyzed for this study has been selected to represent the largest discrete impact event at the wingwall (as determined from the deflection of the marine fenders), which may or may not be the first impact event at the wingwall. Berthing events that contain instances of the vessel 'powering up' against the wingwall in secondary berthing maneuvers are not considered discrete impacts, though they may

represent the maximum deflection of the fenders; in these instances the discrete vessel impact is utilized for parameter determination.

The dataset for velocity information is smaller than the dataset associated with the deflection parameters due to challenges associated with obtaining unambiguous velocity data. The 'end berthing' ferries observed in this study have the common characteristics of a large open "bow" that allows for the transfer bridge to be loaded onto the deck of the ferry to facilitate vehicle loading. This large opening necessitated the distance sensors to be located aft of the open bow, on the seaward side of the wingwalls (see Figure 4.1).

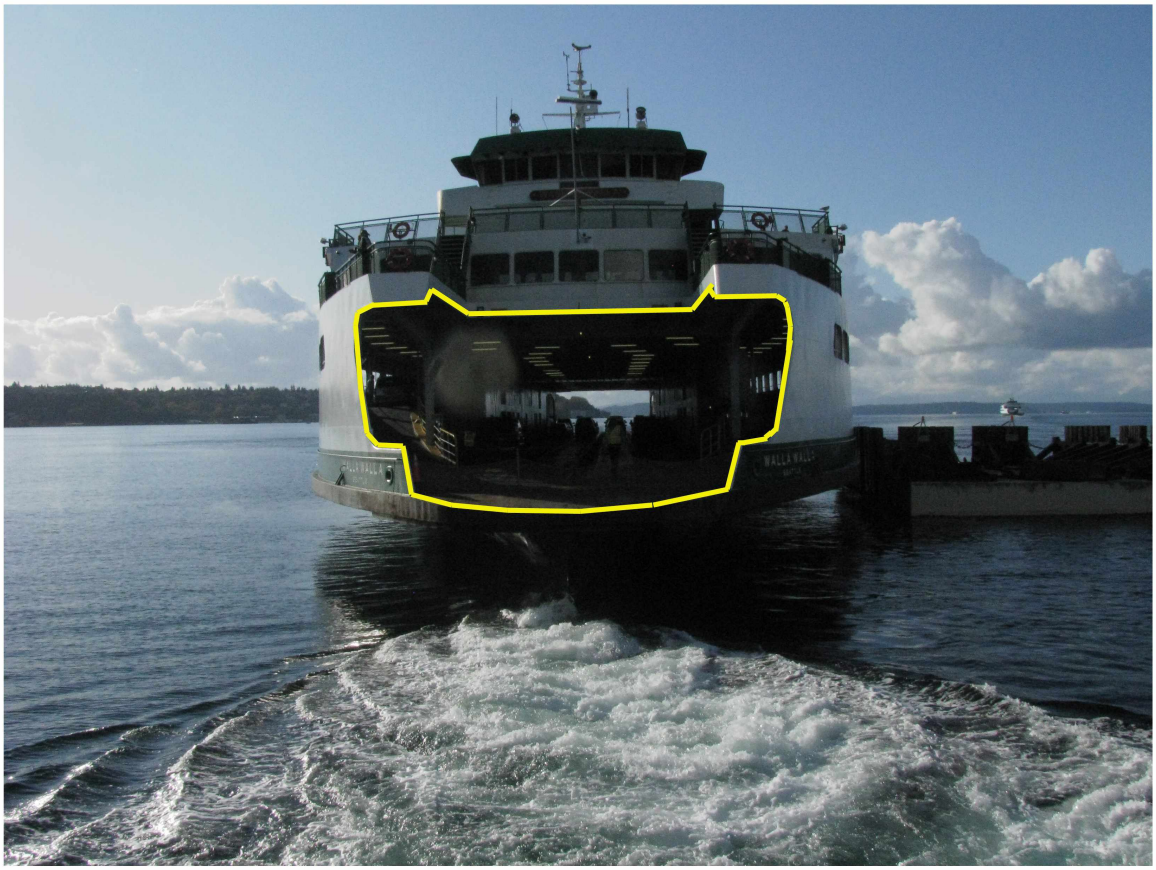

Figure 4.1: Typical Ferry Bow/stern; opening highlighted in yellow

The elevation of distance sensor placement was above the extreme high water of the terminal to keep the equipment from getting wet. This setup provided for generally good position versus time data, however at certain tide levels the distance sensor received data that indicated a return signal that was reflecting off of a curved surface, reflecting off of the vessel's sponson intermittently, or perhaps occasionally passing through an opening in the hull of the vessel. During the event characterization process, any velocity information that was deemed to be suspect at the time of interest was filtered out and removed from the velocity data set; see Figure 4.2. The highest velocities that satisfied the initial characterization went through an additional inspection in order to further scrutinize the validity of the data. The second inspection consisted of re-plotting the vessel position with respect to time, and visually inspecting the berthing event. Velocity information for these outlying events was omitted from the velocity dataset if there was ambiguity regarding the vessels 'actual' position with regards to what the plotted data represented.

The Velocity data was filtered again to remove any values that were less than 0.035 feet per second, (0.42 inches per second). Following event characterization of the entire dataset it was determined that below this rate of speed, the vessel approach velocity approaches zero and did not properly correlate to deflection of the LMTs. Further discussion regarding the characterization of vessel approach velocity can be found in Section 5.6.

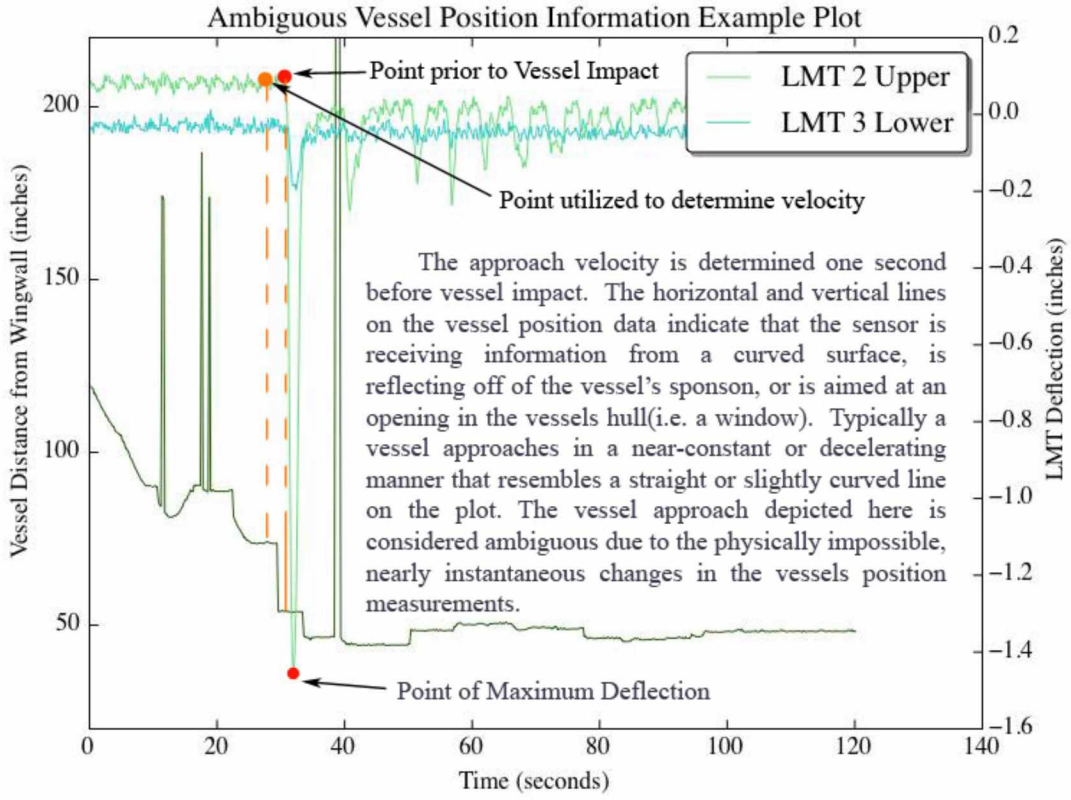

Figure 4.2: Ambiguous vessel position graphic

Table 4.1: Velocity Summary Table

Approach Velocity, feet/second				
Wall	**Mean**	**Standard Deviation**	**Max**	**# of events**
North	0.324196	0.19329	1.6525	2672
South	0.322774	0.20073	1.6358	2455
Combined	0.323515	0.91689	1.6525	5127

After experimenting with several probability distributions, the Weibull Distribution exhibited the closest correlation to the velocity dataset. The Weibull distribution was then applied to the density histogram, the cumulative probability, and probability of non-exceedance plots (probability plots). Matching the empirical data to a probability distribution such as the Weibull allows for the ability to estimate extreme approach velocity values. Using the *percentile* plots illustrates the probability relationship between a given approach velocity and its likelihood of not being exceeded in any one berthing event. The Weibull distribution relates a velocity value to a corresponding probability in order to predict a velocity value that has a given probability (such as 99.999% or 99.9999999%) of not being exceeded in any one berthing event, see Table 4.2.

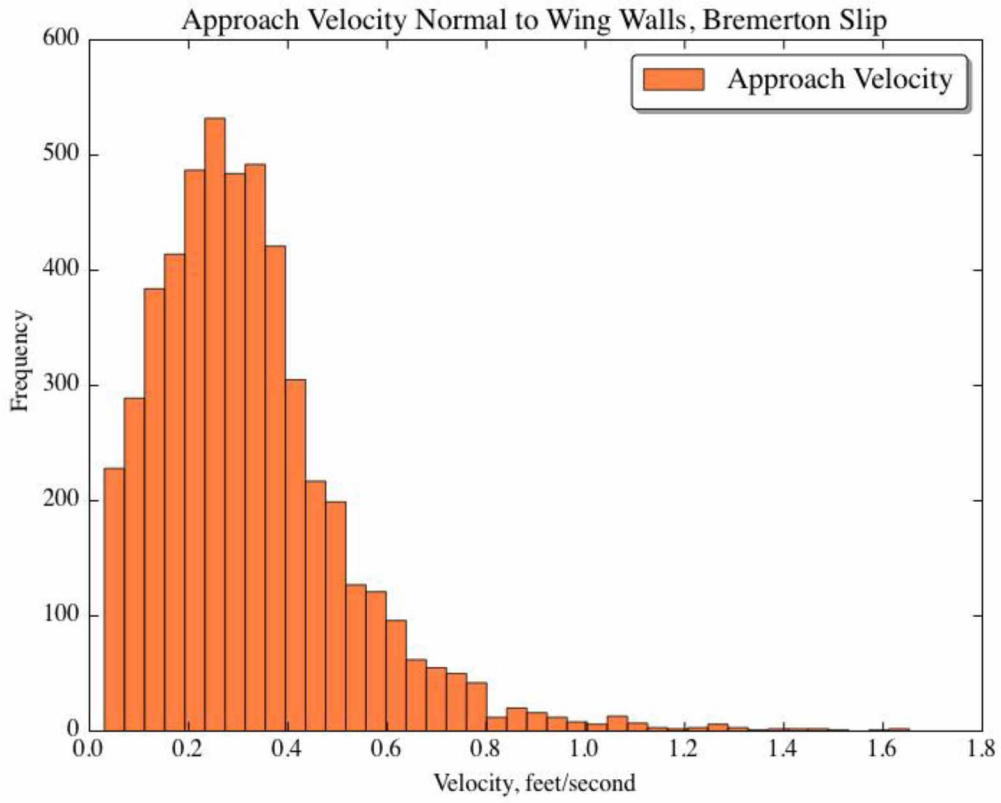

Figure 4.3: Approach Velocity Histogram Normal to Wingwalls

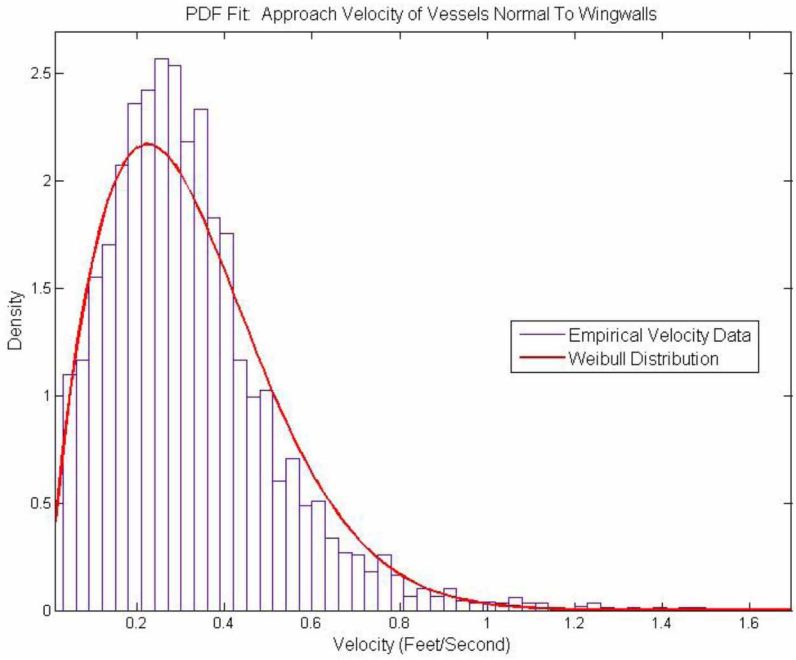

Figure 4.4: Weibull Probability Distribution fit to Approach Velocity Data

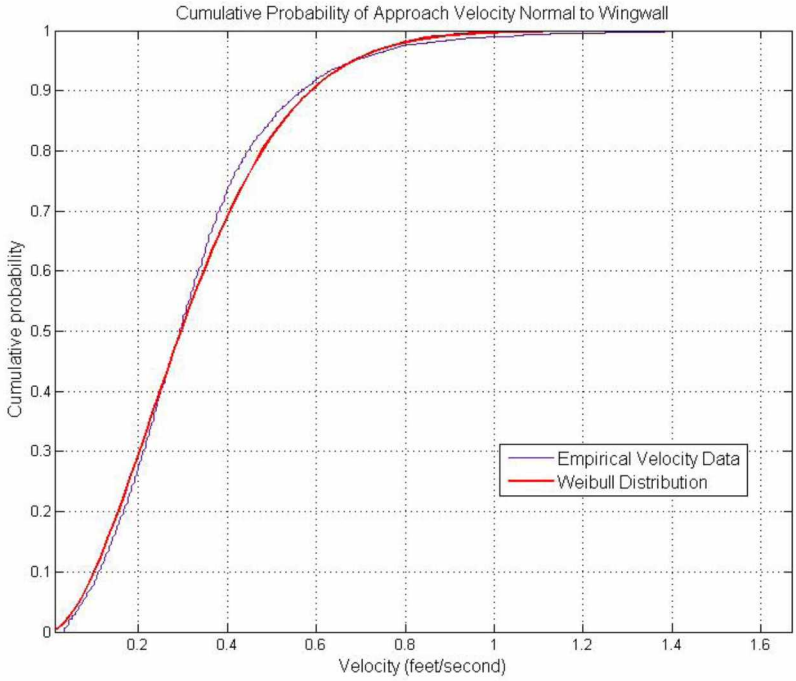

Figure 4.5: Cumulative Probability of Approach Velocity Normal to Wingwall

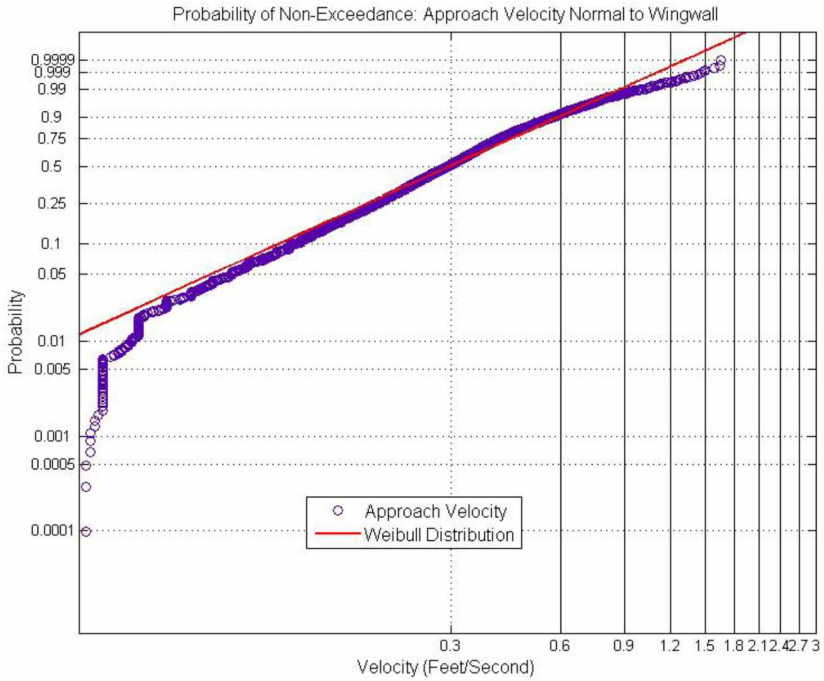

Figure 4.6: Probability of Non-Exceedance: Approach Velocity Normal to Wingwall

Table 4.2: Approach Velocity Probability of Non-Exceedance in any one event

Approach Velocity at Wingwalls			
One Event	Complete Set	North Wingwall	South Wingwall
Probability of Non-Exceedance, %	feet/second	feet/second	feet/second
98	0.79728	0.78845	0.80652
99	0.87558	0.86443	0.88728
99.9	1.1051	1.0866	1.1248
99.99	1.3037	1.278	1.3309
99.999	1.4819	1.4494	1.5165
99.9995	1.5325	1.498	1.5693
99.9999	1.6455	1.6064	1.6872
99.99995	1.6924	1.6513	1.7362
99.99999	1.7978	1.7523	1.8464
99.999999	1.9411	1.8894	1.9965
99.9999999	2.0769	2.0192	2.1389

4.3 Energy Results

Energy Results are presented as histograms, probability distribution fits, cumulative distribution fits and probability curves in Figures 4.6 through 4.9, and expanded further in the Appendix B as Figures B1 through B3.

Berthing Energy is presented for the complete dataset of all berthing events, with each berthing event defined as a vessel impacting either the north or south wingwall. Berthing Energy for these results is the total energy absorbed by the wingwall. Table 4.3 presents a summary of wingwall energy absorption.

Several distributions were fit to the berthing energy data, the lognormal distribution was deemed to be a reasonable fit for the data. Matching the empirical data to the lognormal distribution allows for the ability to estimate extreme energy values the wingwall structure would need to endure. Using the 'percentile' plots, the relationship between a given amount of kinetic energy to be absorbed and its likelihood of not being exceeded in any one berthing event is developed. The lognormal distribution is also used to assign an amount of strain energy to a corresponding probability in order to predict an energy value that has a given probability (such as 99.999% or 99.9999999%) of not being exceeded in any one berthing event, see Table 4.4.

Table 4.3: Summary of Wingwall Energy Absorption

Energy Absorbed by Wingwalls, kip-feet				
Wall	**Mean**	**Standard Deviation**	**Max**	**# of events**
North	12.74	9.095	146.17	3448
South	11.946	8.287	80.476	3484
Combined	12.341	8.707	146.17	6932

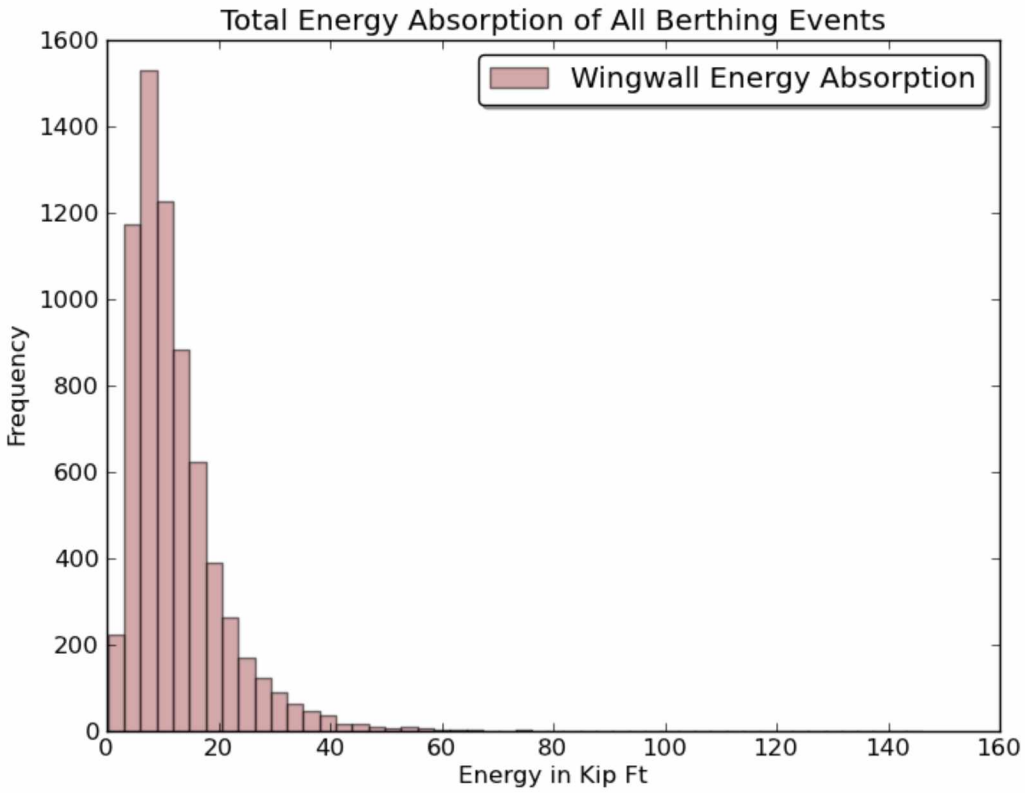

Figure 4.7: Total Energy Absorption of All Berthing Events

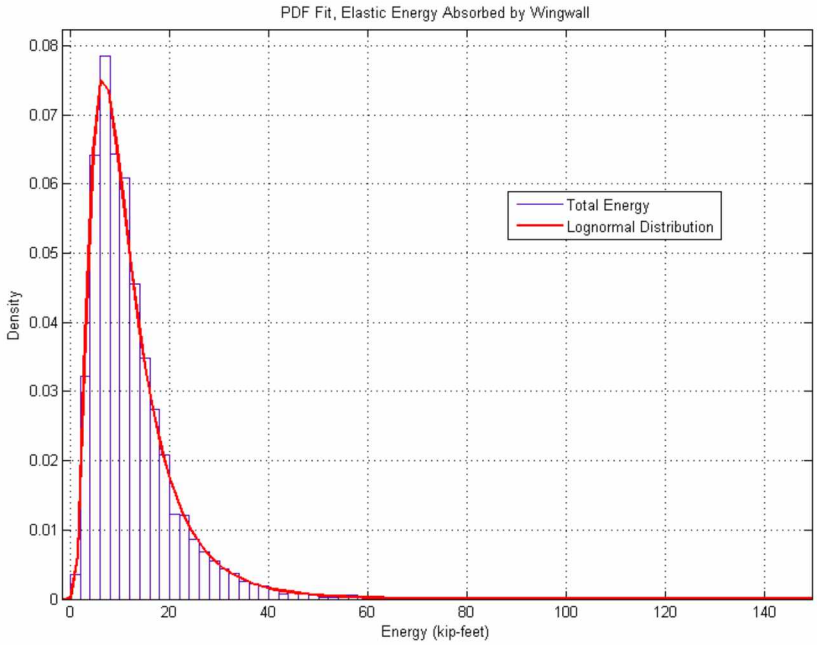

Figure 4.8: PDF Fit: Lognormal Distribution and Energy Absorbed by Wingwall

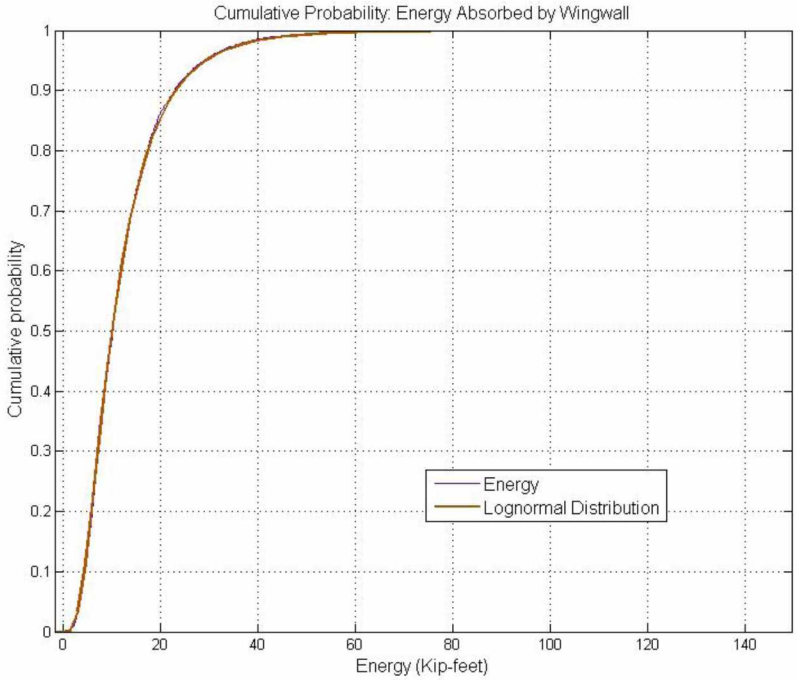

Figure 4.9: Cumulative Probability of Energy Absorbed by Wingwall

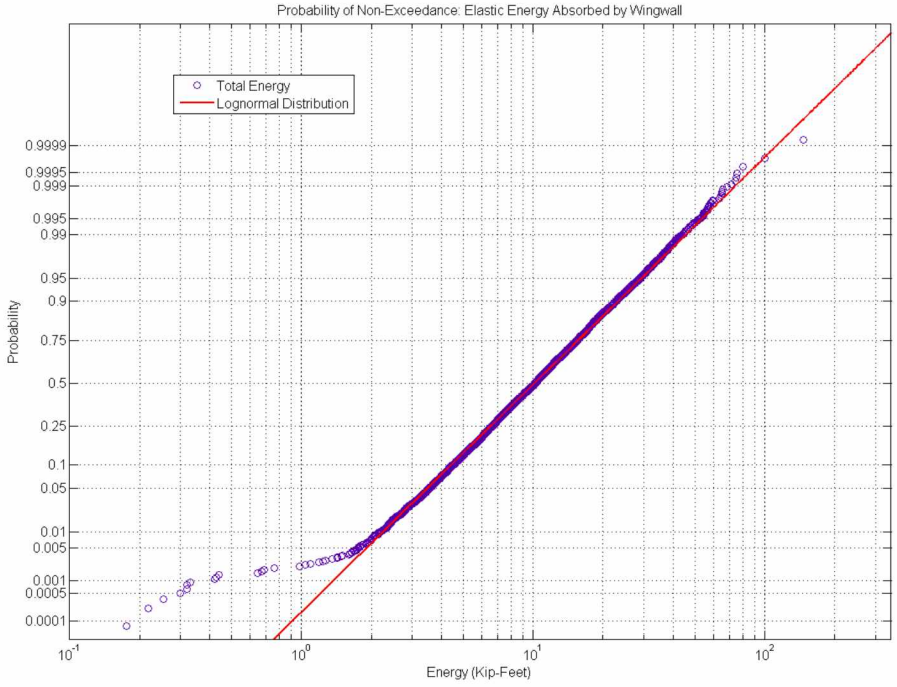

Figure 4.10: Probability of Non-Exceedance: Elastic Energy Absorbed by Wingwall

Table 4.4: Kinetic Energy Probability of Non-Exceedance

Elastic Energy Absorbed by Wingwalls			
One Event	Complete Set	North Wingwall	South Wingwall
Probability of Non-Exceedance, %	kip/feet	kip/feet	kip/feet
98	38.03	38.34	37.57
99	45.37	45.58	44.96
99.9	74.38	73.99	74.32
99.99	111.74	110.24	112.41
99.999	159.09	155.85	161.00
99.9995	175.57	171.65	177.98
99.9999	218.26	212.46	222.06
99.99995	238.68	231.92	243.20
99.99999	291.28	281.89	297.79
99.999999	380.45	366.22	390.71
99.9999999	488.36	467.75	503.65

4.4 Berthing Force

Although designers are most interested in energy imparted to the berthing structure, there are times when utilizing force calculations can be helpful. Designing for force considerations is significantly different than designing for energy, since force is proportional to the stiffness of a system. A stiffer system responds with more force than a soft system if the energy applied to both systems is the same.

$$F_f = K_f(x_f)x_f \qquad \text{Equation 4.1}$$

$$F_f = -0.00005x^5 + 0.002x^4 - 0.0621x^3 - 0.1006x^2 + 19.257x \qquad \text{Equation 4.2}$$

Where:

$F_f =$ Force of fender

$x_f =$ Displacement of fender

$K_f(x_f) =$ Stiffness of fender at displacement x_f

Simple spring mechanics describes the force in a spring as displacement multiplied by stiffness of the spring (Equation 4.1). The fender units installed throughout the WSF systems are buckling column fenders, and the stiffness decreases nonlinearly as the fender is compressed. The manufacturer has provided tools that allow for the development of equations that describe the reaction and energy absorption characteristics of the fender units (Equation 4.2). When a vessel impacts a wingwall, the berthing force is resisted by a combination of the fenders, fender piles and also soil supporting the piling.

Upon berthing, the ferry applies force to the wingwall through the vessel's sponson, a projection from the vessel's hull that is designed for impact forces. To estimate force applied to the wingwall, the measured reaction of the two marine fenders and the calculated stiffness of the impact face and piles are combined to

describe the reaction of the system. The force applied to the wingwall is represented in Equation 4.3.

$$F_{total} = \sum_{i=1}^{6} F_{fender} + \sum_{j=1}^{3} \left[K_{impact\ pile j} \left(\frac{\Delta_{lmtjL} + \Delta_{lmtjU}}{2} \right) \right] \qquad \text{Equation 4.3}$$

Where:

F_{total} = Total force on the wingwall

F_{fender} = Reaction force of marine fender

$K_{impact\ pile}$ = Stiffness of pile supporting the impact face

Δ_{lmtjL} = Displacement of fender jL (lower fender, at position 'j')

Δ_{lmtjU} = Displacement of fender jU (upper fender, at position 'j')

Results concerning the force applied by the vessel are displayed in Figures 4.10 through 4.16 in the form of histograms, distribution fits, and probability plots. Berthing Force is presented for the complete dataset of all berthing events in this section. Information regarding berthing force as applied to the north and south wingwalls, as well as additional tables and figures are displayed in Appendix C. Berthing Force represented here is the combination of the force applied by displacing the marine fender and by displacing the impact face. A summary of berthing force applied to the wingwall is located in Table 4.5.

Several distributions were fit to the berthing energy data. The lognormal distribution and the gamma distribution were found to be the closest matches to our dataset. The lognormal distribution in this instance is quite conservative at the extreme levels, and the gamma distribution may be more realistic at extreme values. Both are presented in this section to illustrate their respective differences. Matching the empirical data to the lognormal and gamma distributions allows for the ability to predict extreme-berthing forces applied to the wingwall structure. Using the *percentile* plots illustrates the probability relationship between a given

amount of kinetic energy that needed to be absorbed and its likelihood of not being exceeded in any one berthing event. The Lognormal and Gamma distributions are also used to assign an amount berthing to a corresponding probability in order to predict an energy value that has a given probability (such as 99.999% or 99.9999999%) of not being exceeded in any one berthing event, see Table 4.6 for the gamma distribution results and Table 4.7 for the lognormal distribution results.

Table 4.5: Berthing Force Summary

Berthing Force at Wingwalls, kips				
Wall	**Mean**	**Standard Deviation**	**Max**	**# of events**
North	74.272	41.7	413.139	3448
South	75.725	40.302	307.286	3484
Combined	75.002	41.01	413.139	6932

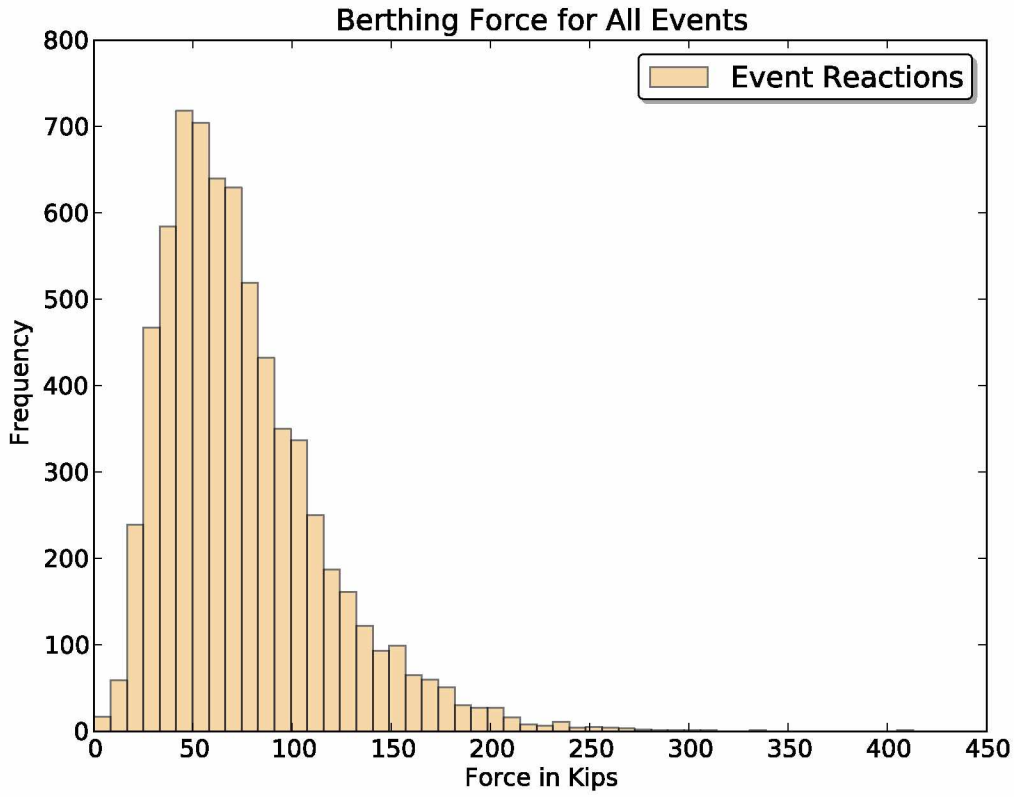

Figure 4.11: Berthing Force Histogram Applied at Wingwalls

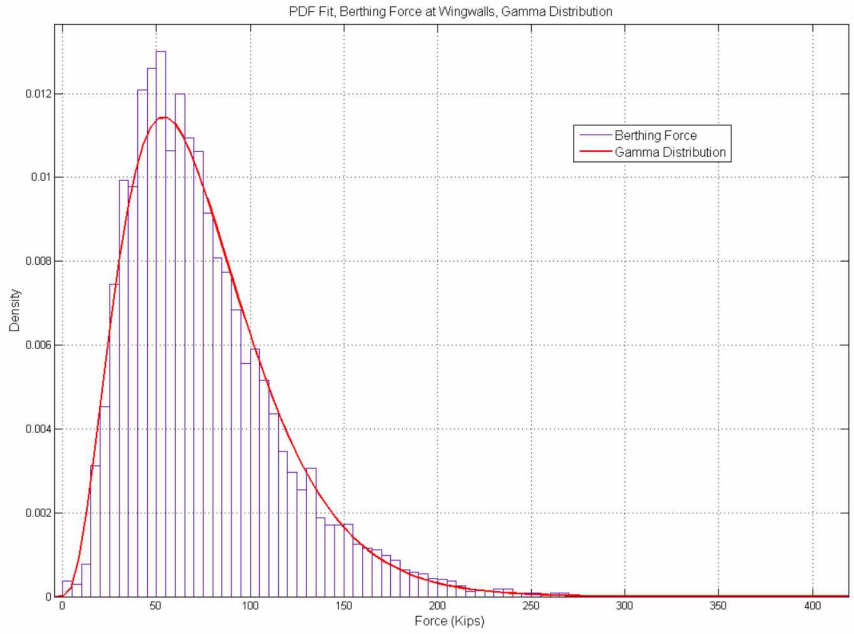

Figure 4.12: PDF Fit: Berthing Force at Wingwall, Gamma Distribution

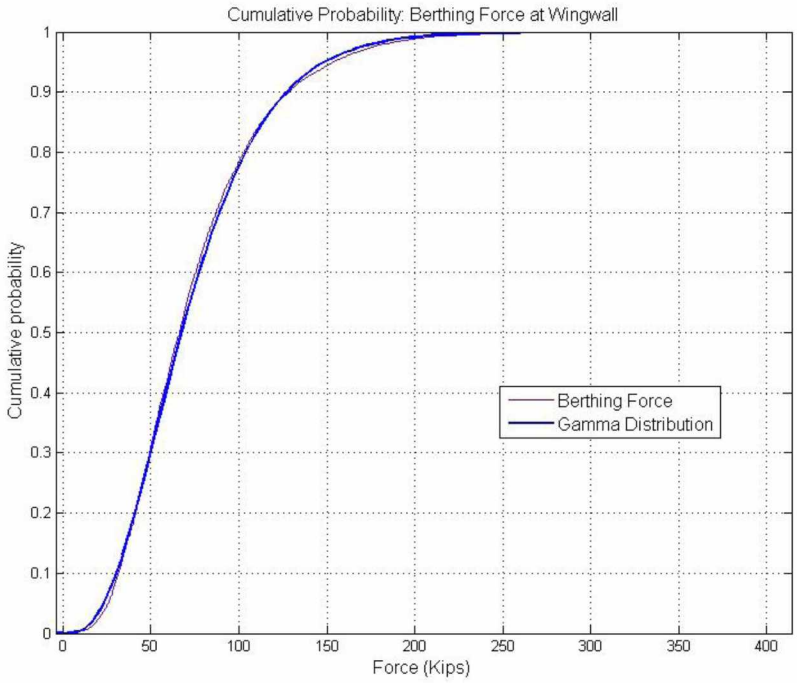

Figure 4.13: Cumulative Probability: Berthing Force Gamma Distribution

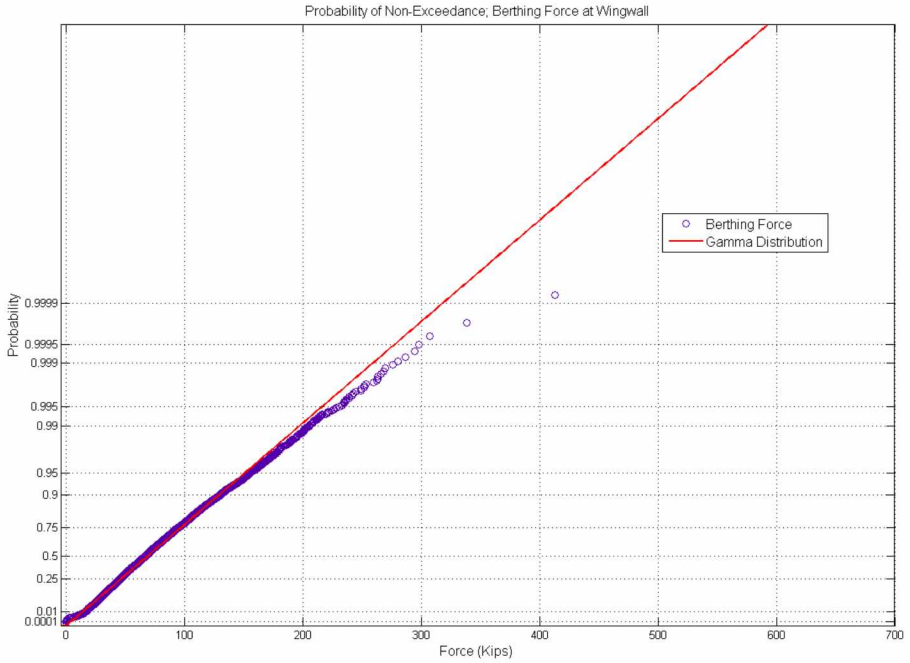

Figure 4.14: Probability of Non-Exceedance: Berthing Force, Gamma Distribution

Table 4.6: Berthing Force Probability of Non-Exceedance, Gamma Distribution

Berthing Force Applied to Wingwalls (Gamma)			
One Event	Complete Set	North Wingwall	South Wingwall
Probability of Non-Exceedance, %	kips	kips	kips
98	177.25	176.44	177.98
99	196.90	196.12	197.59
99.9	258.86	258.21	259.39
99.99	317.71	317.22	318.04
99.999	374.69	374.37	374.80
99.9995	391.58	391.31	391.62
99.9999	430.41	430.27	430.29
99.99995	446.99	446.91	446.80
99.99999	485.21	485.27	484.85
99.999999	539.31	539.58	538.71
99.9999999	592.87	593.34	592.01

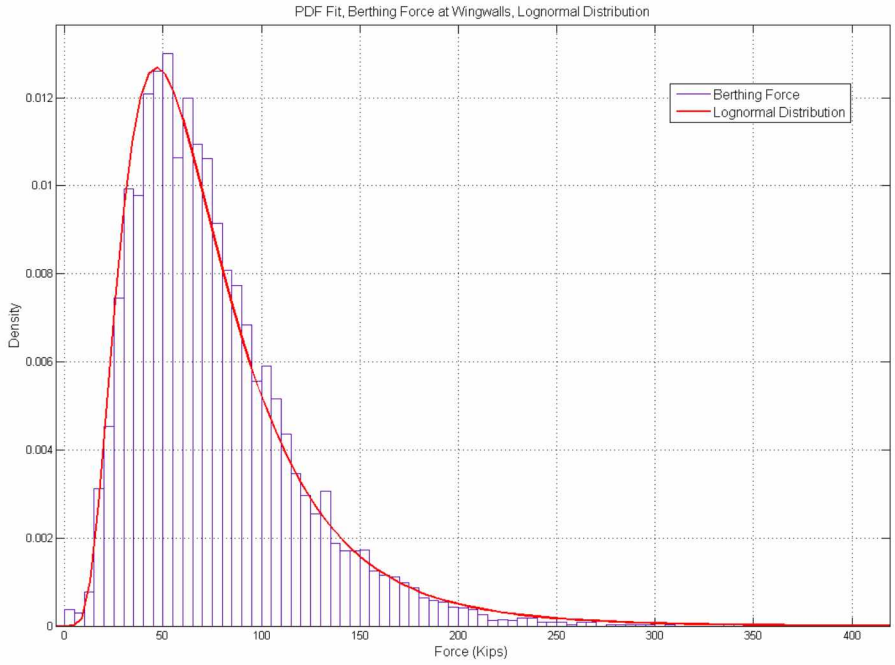

Figure 4.15: PDF Fit: Lognormal Distribution and Berthing Force (Lognormal)

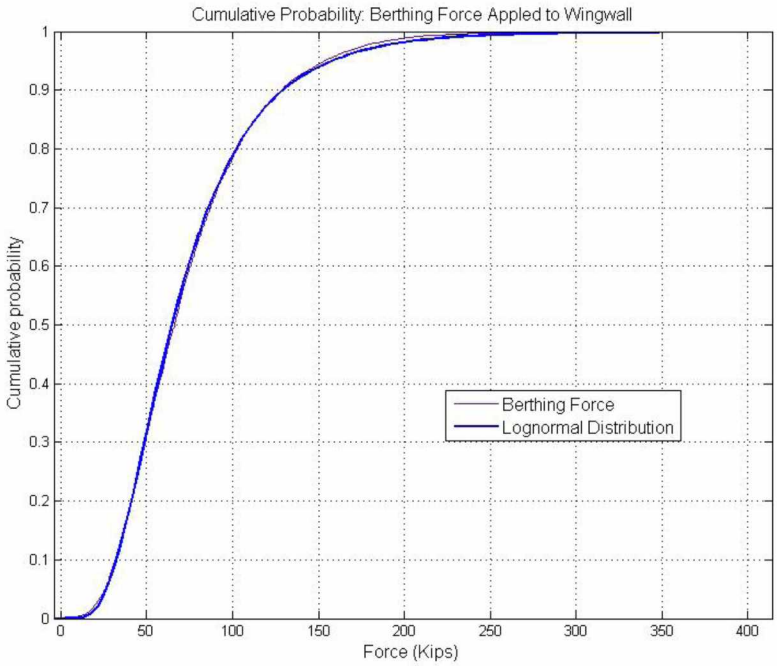

Figure 4.16: Cumulative Probability of Berthing Force (Lognormal)

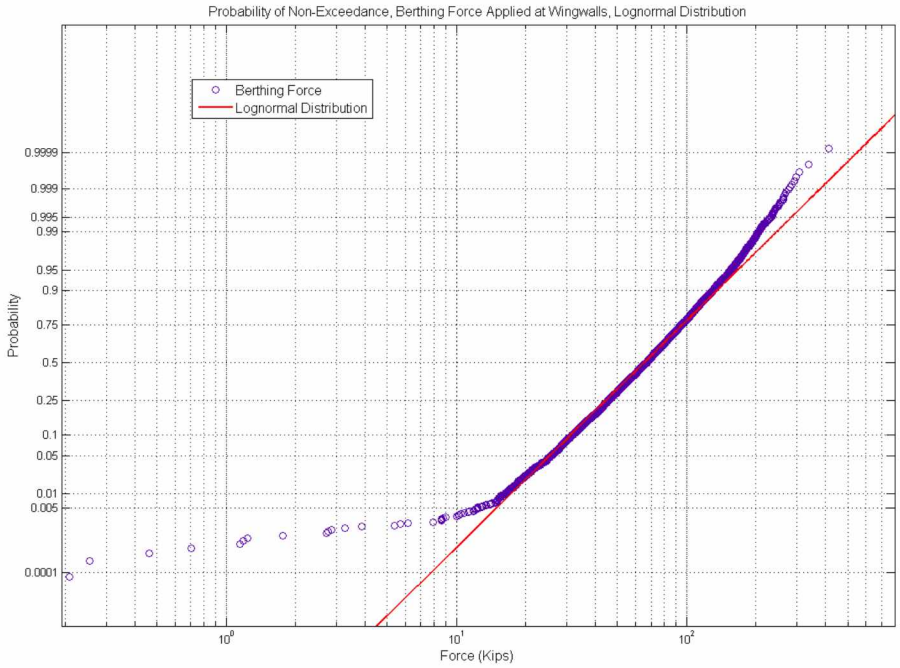

Figure 4.17: Probability of Non-Exceedance: Berthing Force (Lognormal)

Table 4.7: Berthing Force Probability of Non-Exceedance, Lognormal Distribution

Berthing Force Applied to Wingwalls (Lognormal)			
One Event	Complete Set	North Wingwall	South Wingwall
Probability of Non-Exceedance, %	kips	kips	kips
98	209.48	202.66	216.31
99	244.82	236.19	253.47
99.9	378.95	362.75	395.26
99.99	542.94	516.41	569.80
99.999	741.87	701.71	782.73
99.9995	809.38	764.37	855.22
99.9999	980.99	923.27	1039.96
99.99995	1061.68	997.81	1127.01
99.99999	1265.95	1186.06	1347.89
99.999999	1602.92	1495.45	1713.55
99.9999999	1998.64	1857.32	2144.63

4.5 Berthing Coefficient

Describing the amount of energy absorbed by the berthing structure resulting from a vessel impact is complex and often ascertained by estimating a number of coefficients that relate to the interaction of ship and structure. A berthing vessel imparts some amount of energy to the berthing structure that ranges from 40% to over 100% of the vessels' incoming kinetic energy. This is due to a number of factors discussed in Section 2.2 that describe aspects of the ship, the berthing facility, and the berthing maneuvers. Individual evaluation of berthing coefficients is not realistic as they are acting simultaneously when a ship comes to rest. Together, a product of these effects can be described as a berthing coefficient, C_b, (Equation 4.5).

Utilizing direct measurements of berthing events allows for the amount of berthing energy to be quantified, and provides an opportunity to combine the berthing factors (C_m, C_g, C_d, C_c, C_e) into a singular berthing coefficient, C_b. Equation 2.1 then becomes simplified to the format presented in Equation 4.4. The berthing coefficient, Equation 4.5, can be explained as a semi-empirical ratio of energy absorbed by the berthing structure and the vessel's apparent kinetic energy (which is defined to be the kinetic energy based upon the recorded approach velocity, with no berthing coefficients applied).

$$E_T = \frac{W}{2g} v^2 C_b \qquad \text{Equation 4.4}$$

$$C_b = C_m C_g C_d C_c C_e = \frac{E_T}{E_v} \qquad \text{Equation 4.5}$$

Where:

$E_T =$ Total energy absorbed by wingwall, including fender and impact face

$E_v = \frac{W}{2g} v^2 =$ Energy of vessel just prior to impact

Where: W = weight, g= gravity, v = approach velocity

$C_b =$ Berthing Coefficient, consisting of individual coefficients as describe in Section 2.3

The total energy in the above equation E_T, is the energy determined according to procedures in Section 3.11. The vessel energy term, E_v, is measured using the approach velocity recorded for each berthing event, and the published displacement weight for each vessel. Typical values for C_b range from 0.4 to 0.7, however 'direct' end berthing can have a coefficient up to 1.0, and certain situations with low under keel clearance, the berthing coefficient can exceed 1.0 (Gaythwaite 2004).

Berthing coefficient results are displayed in Figures 4.17 to 4.21 in the form of histograms, distribution fits, and probability plots. There are two vessel classes landing with near equal frequency at the Bremerton slip with loaded displacements between 2947 and 3251 long tons. For simplicity, the berthing coefficient calculation utilized the weighted average of these two displacement figures, as the M/V Kaleetan has one more scheduled departure from the Bremerton slip than the M/V Kitsap does. A summary of berthing coefficient results is found in Table 4.8.

Several distributions were fit to the berthing coefficient data, the lognormal distribution was found to be the closest match to our dataset and is also a commonly utilized distribution for lifetime modeling. Matching the empirical data to the lognormal distribution allows for the ability to predict extreme values of the

berthing coefficient. Using the *percentile* plots illustrates the probability relationship between a given berthing coefficient and its likelihood of not being met or exceeded in any one berthing event. The Lognormal distribution is also used to assign a berthing coefficient value to a corresponding probability in order to predict a value that has a given probability (such as 99.999% or 99.9999999%) of not being exceeded in any one berthing event, see Table 4.9.

Table 4.8: Berthing Coefficient Results Summary

Berthing Coefficient, C_b				
Wall	**Mean**	**Standard Deviation**	**Max**	**# of events**
North	3.24	8.948	151.09	2648
South	3.309	9.78	198.68	2417
Combined	3.272	9.36	198.68	5065

The results are not in line with what would be traditionally expected of a berthing coefficient as the mean values exceed limits proposed for 'end berthing' vessels in the literature of approximately 1.1 (Gaythwaite 2004). The mean value of the berthing coefficient represents the wingwall absorbing 3.3 times the energy predicted by a simple application of the kinetic energy method without any berthing coefficients. A discussion of these atypical results follows in Section 5.9, as well as an attempt to utilize the recorded data and devise a useable berthing coefficient in Section 6.4. To summarize those forthcoming sections, a relatively large number of the recorded events had a relatively low velocity at the time of impact. During the berthing maneuvers, vessel controls are used to slow down, steer, and power up the vessel to obtain a stable berthing position for off loading passengers and vehicles. It is believed that the source of additional energy, represented by the empirical berthing coefficient estimations, is a result of vessel control usage during docking. Subsequent sections will elaborate upon this.

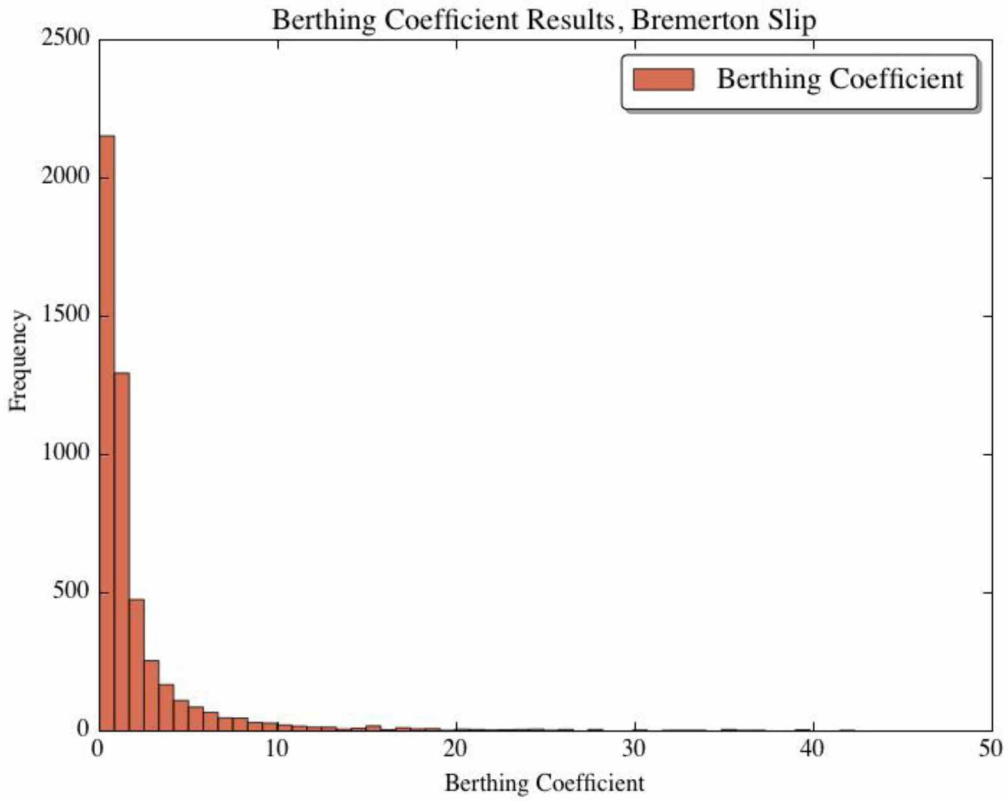

Figure 4.18: Berthing Coefficient Results

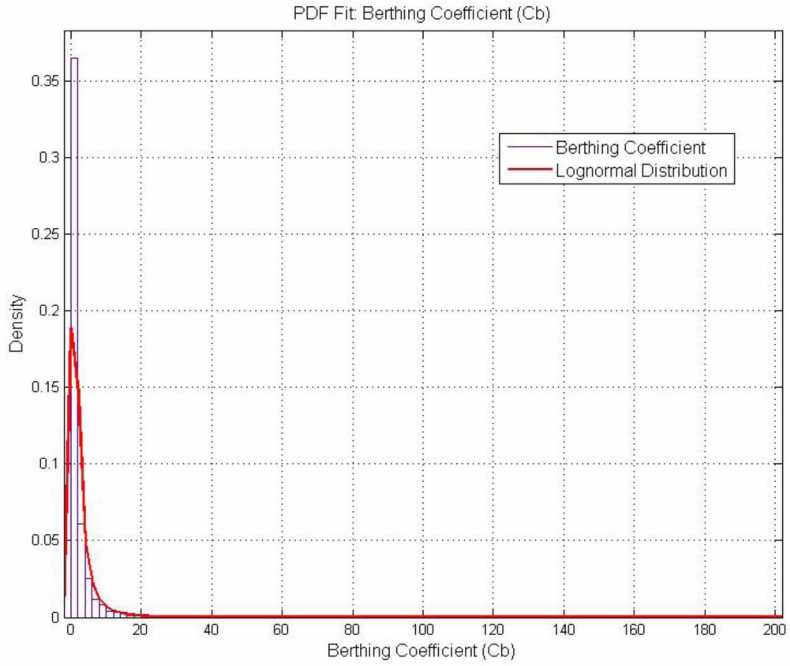

Figure 4.19: PDF Fit: Berthing Coefficient Results and Lognormal Distribution

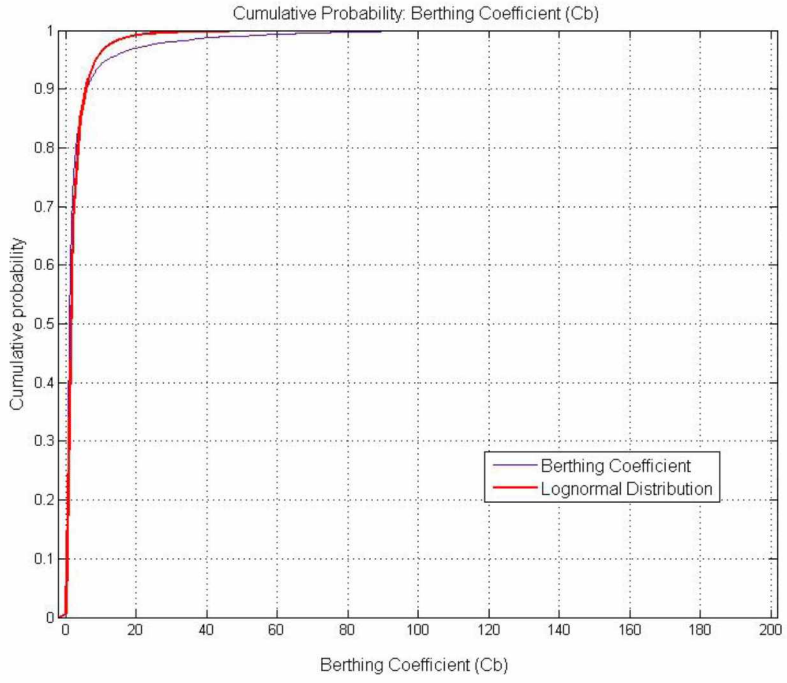

Figure 4.20:Cumulative Probability of Berthing Coefficient Results

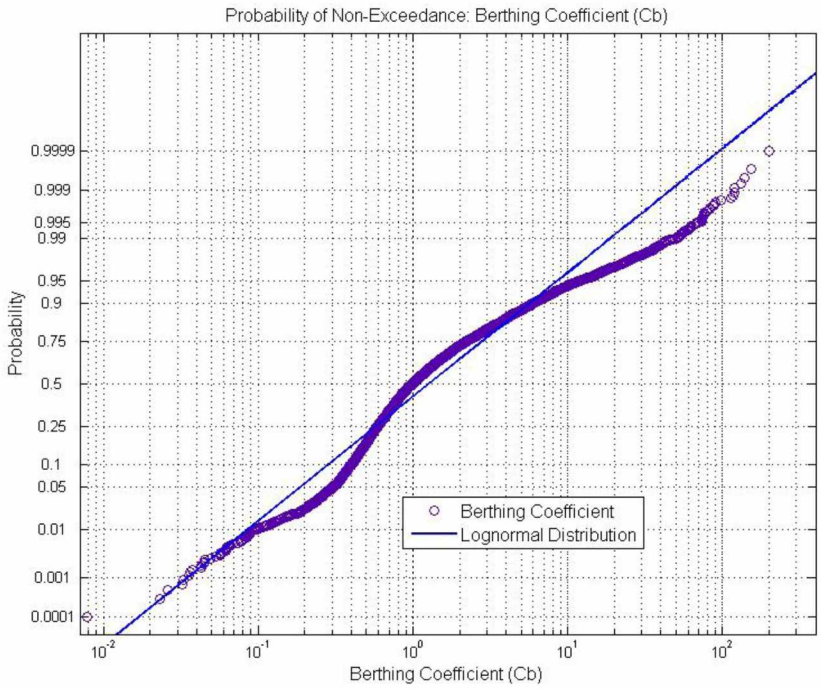

Figure 4.21: Probability of Non-Exceedance: Berthing Coefficient

Table 4.9:Berthing Coefficient Probability of Non Exceedance

Berthing Coefficient, Cb			
One Event	Complete Set	North Wingwall	South Wingwall
Probability of Non-Exceedance, %			
90	5.5445	5.4213	5.6704
95	8.4527	8.1541	8.768
98	13.587	12.909	14.32
99	18.643	17.535	19.86
99.9	45.246	41.366	49.656
99.99	93.872	83.839	105.58
99.999	176.89	154.81	203.23
99.9999	311.86	268.03	365.2
99.99999	523.28	442.34	623.53
99.999999	844.78	703.26	1023

4.6 Berthing Factor

Extending the concept of a berthing coefficient to a scalable tool, the berthing factor, f_b, is introduced. The berthing factor is the energy per unit mass of the vessel. The berthing factor extends the application of the empirically determined berthing energy information to a greater range of vessels displacements. Obtaining the berthing factor is accomplished by dividing the elastic energy of the deformed structure by the mass of the vessel (Equation 4.6). Once the berthing factor has been developed from a sample of berthing events, it can be multiplied by the vessel mass to estimate the amount of energy absorbed by the wingwall (Equation 4.7).

$$f_b = \frac{E_t\, g}{W} \qquad \text{Equation 4.6}$$

$$E_T = \frac{W}{g} f_b \qquad \text{Equation 4.7}$$

Where:

$f_b =$ Berthing factor

$E_T =$ Total energy absorbed by wingwall, fender and impact face

$W =$ Vessel weight

$g =$ Acceleration of gravity

This methodology is further explained in Section 6.3, see examples 6.3.1 and 6.3.2. The primary assumption is that the berthing factor values are directly proportional to the vessel displacements.

Berthing factor results are displayed in Figures 4.22 through 4.25 in the form of histograms, distribution fits, and probability curves. Further plots are located in Appendix D, Figures D1 through D3. The berthing factor is the energy per unit mass of a berthing event. As before, the berthing factor calculation utilized the weighted average of the two vessel displacements. The procedure utilized to estimate the

berthing factor is detailed in Section 3.13, specifically Equation 3.15. A summary of berthing factor results is found in Table 4.10.

Several distributions were fit to the berthing factor data, the lognormal distribution was deemed to be a reasonable fit and is also a commonly utilized distribution for lifetime modeling. Matching the empirical data to the lognormal is a basis for estimating extreme values of the berthing factor. Using the *percentile* plots illustrates the probability relationship between a given berthing factor and its likelihood of not being met or exceeded in any one berthing event. The lognormal distribution is also used to assign a berthing factor to a corresponding probability in order to predict a value that has a given probability (such as 99.999% or 99.9999999%) of not being exceeded in any one berthing event, see Table 4.11.

Table 4.10: Berthing Factor Results Summary

Berthing Factor, f_b				
Wall	**Mean**	**Standard Deviation**	**Max**	**# of events**
North	0.0586	0.0429	0.675	2648
South	0.548	0.0377	0.372	2417
Combined	0.568	0.0405	0.675	5065

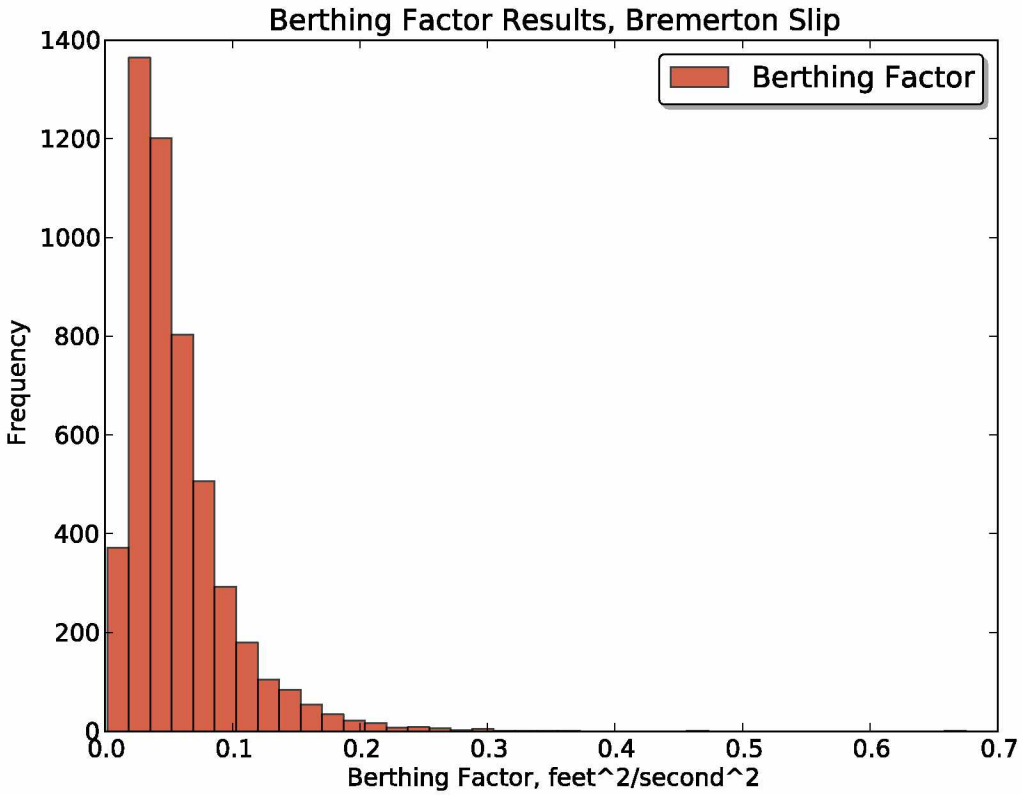

Figure 4.22: Berthing Factor Results, Bremerton Slip

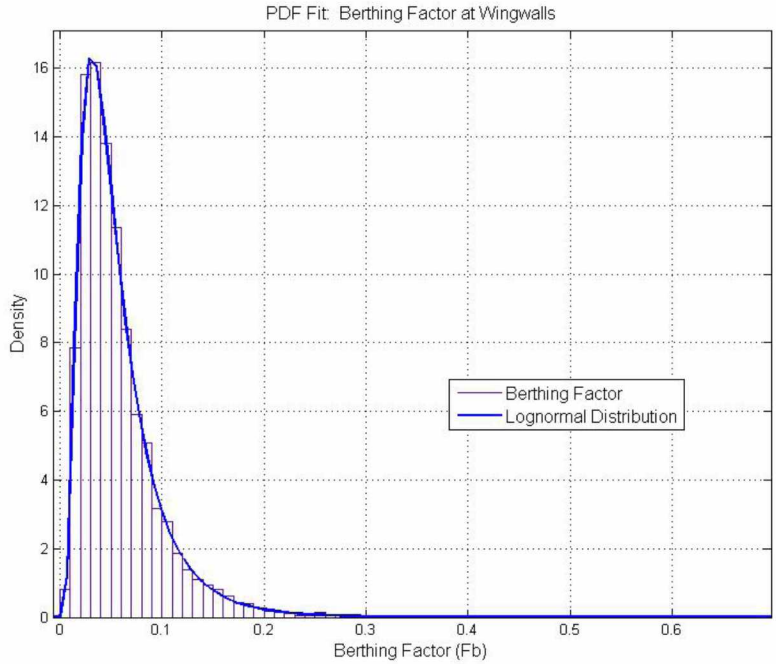

Figure 4.23: PDF Fit: Berthing Factor and Lognormal Distribution

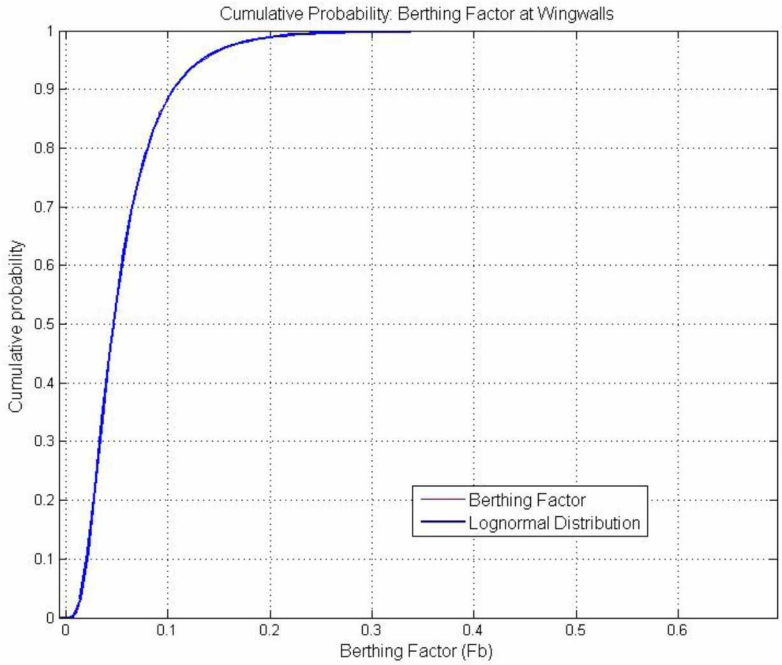

Figure 4.24: Cumulative Probability: Berthing Factor and Lognormal Distribution

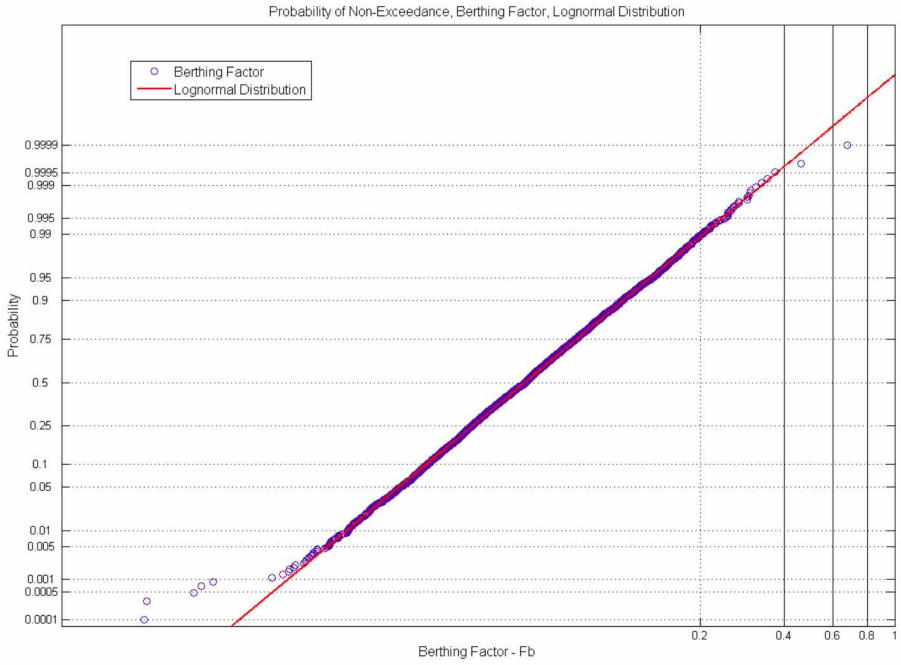

Figure 4.25: Probability of Non-Exceedance: Berthing Factor

Table 4.11: Berthing Factor Probability of Non-Exceedance

Berthing Factor, Fb			
One Event	Complete Set	North Wingwall	South Wingwall
Probability of Non-Exceedance, %	ft^2/sec^2	ft^2/sec^2	ft^2/sec^2
95	0.1319	0.1352	0.1282
98	0.1711	0.1750	0.1664
99	0.2035	0.2079	0.1981
99.9	0.3307	0.3370	0.3225
99.99	0.4933	0.5014	0.4819
99.999	0.6980	0.7079	0.6827
99.9999	0.9522	0.9640	0.9326
99.99995	1.0397	1.0520	1.0186
99.99999	1.2643	1.2779	1.2397
99.999999	1.6436	1.6586	1.6134
99.9999999	2.1006	2.1167	2.0640

4.7 Reliability Design Charts

Reliability design charts present the relationship between a given number of berthing events and a parameter (such as approach velocity or energy) at varying levels of reliability. Figures 4.26 through 4.30 are design charts for five different design parameters presented with reliability levels of 90%, 95%, 98%, 99%, 99.9% and 99.99%. The horizontal axis of the design charts corresponds to a design life of a berthing structure. The design life of a Washington State Ferry Terminal ranges from 200,000 to approximately 730,000 berths at current scheduling levels. Using the plots is accomplished by selecting a design number of berths and a given reliability level, the projection onto the vertical axis is defined as a value of the parameter of interest that will not be met or exceeded at the given reliability level and the given number of berthing events.

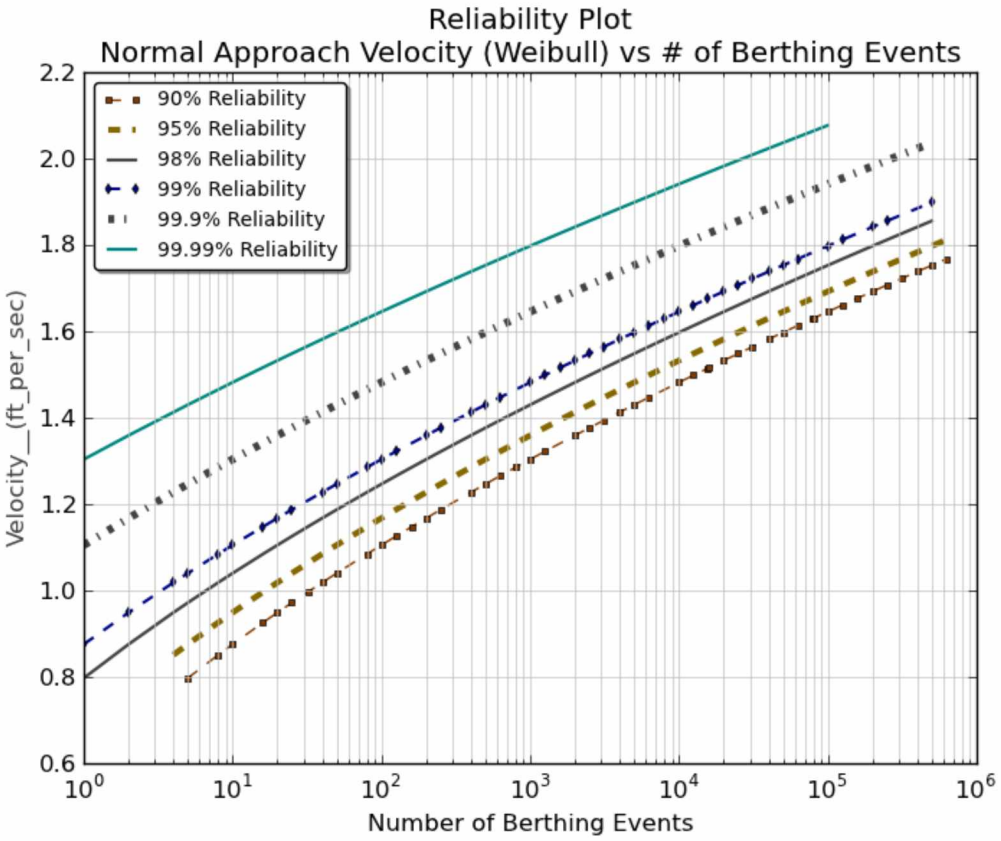

Figure 4.26: Berthing Event Reliability Plot, Approach Velocity (Weibull)

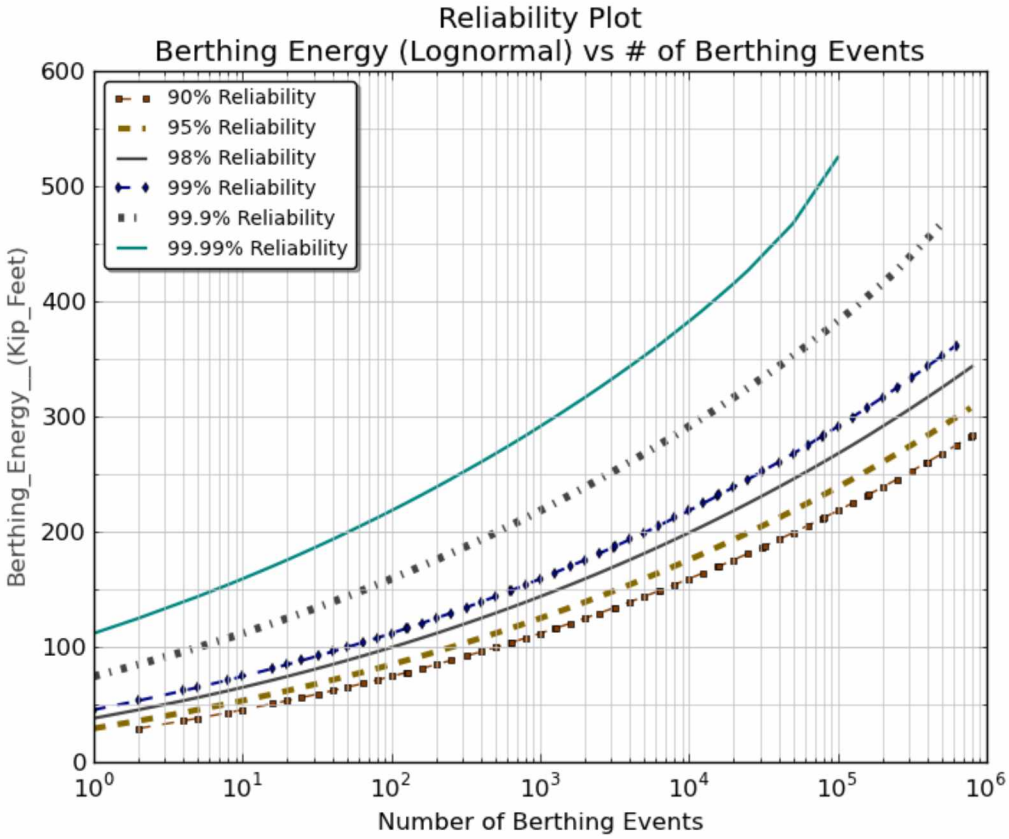

Figure 4.27: Berthing Event Reliability Plot, Kinetic Energy (lognormal)

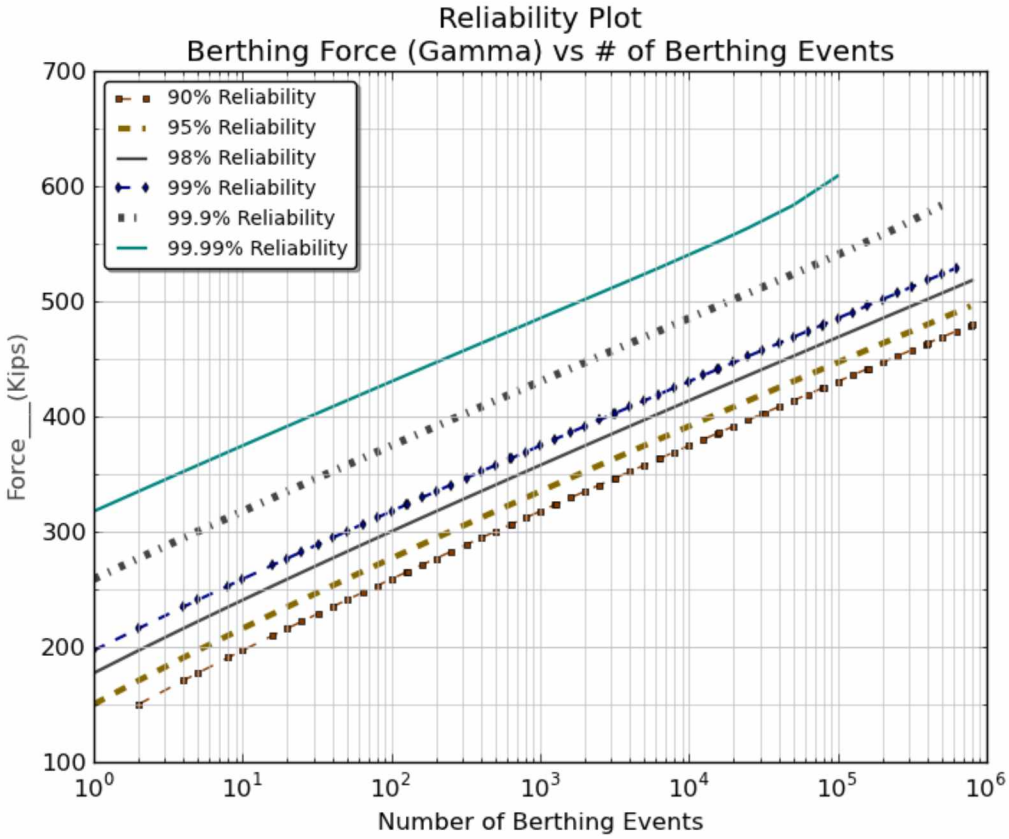

Figure 4.28: Berthing Event Reliability Plot, Berthing Force (Gamma)

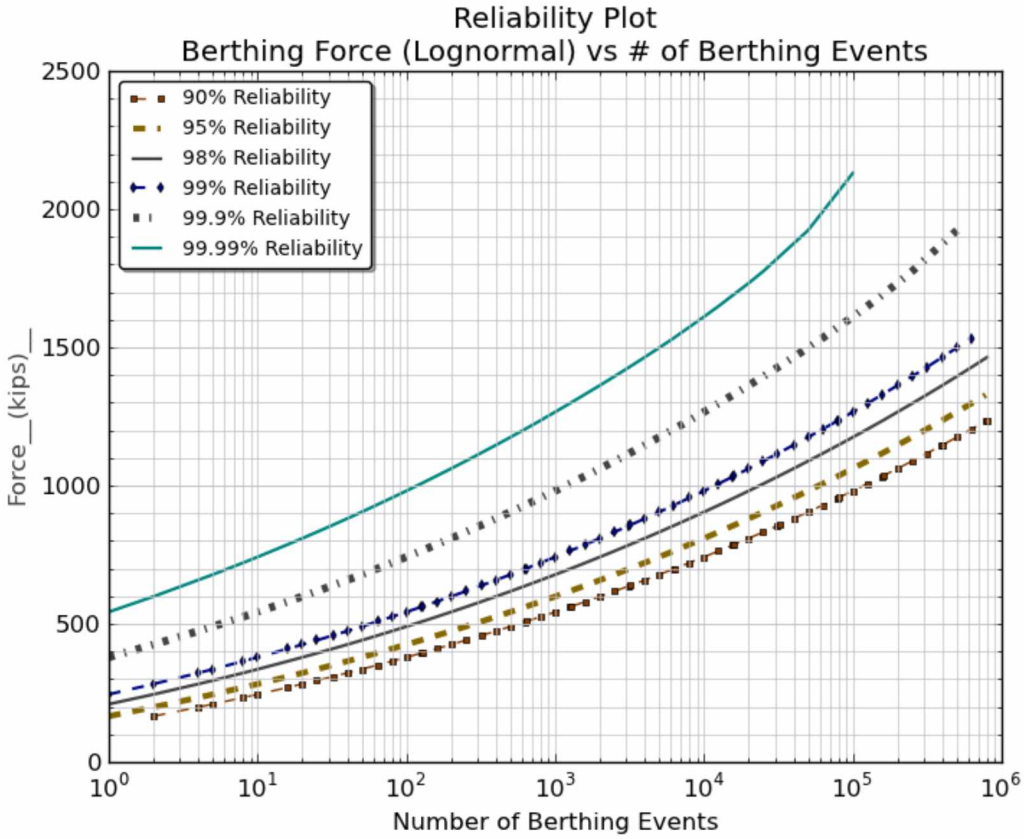

Figure 4.29: Berthing Event Reliability Plot, Berthing Force (lognormal)

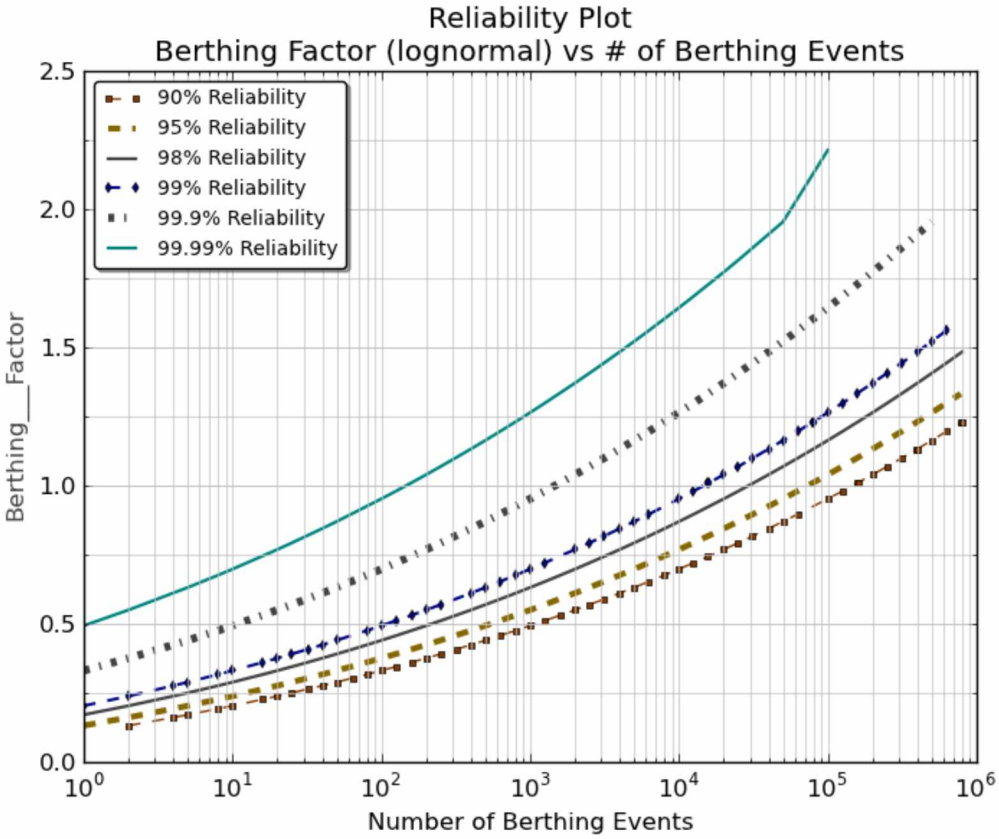

Figure 4.30: Berthing Event Reliability Plot, Berthing Factor (lognormal)

4.8 Point of Impact Results

The instrumentation of all wingwall fenders allows for a fairly precise determination of where the vessel is contacting the impact face. Utilizing the deflection characteristics of each fender in a given event allows estimation of the vessel contact point with the impact face for each event using Equations 4.8 and 4.9. Fender deflection is non-linear; therefore the force absorbed by each fender is utilized in order to determine the point of contact.

$$\bar{x} = \frac{\sum_1^6 F_i * x_i}{\sum_1^6 F_i} \qquad \text{Equation 4.8}$$

$$\bar{y} = \frac{\sum_1^6 F_i * y_i}{\sum_1^6 F_i} \qquad \text{Equation 4.9}$$

Where:

$\bar{x}$ = Horizontal location of vessel impact with respect to impact face

$\bar{y}$ = Vertical location (elevation) of vessel impact with respect to impact face

F_i = Force absorbed by fender *i*

x_i = Horizontal distance to fender *i*

y_i = Vertical distance to fender *i*

Point-of-impact results are displayed in the Figure 4.31 in the form of scatter plots and histograms presented at scale overlaid on the wingwalls. The results are segregated into North and South Wingwalls because the landing procedures differ at each wall. The North wingwall has a large floating dolphin on the north side of the landing slip that necessitates berthing maneuvers of a different character than the south side, which has no such obstructions to its south. The graphic is a

representation of the wingwalls as viewed from the water looking towards the shore. A point of impact summary is given in Table 4.12.

Table 4.12: Point of Impact Summary

Mean Point of Impact Summary		
	North	**South**
Lateral Distance from "Throat" of Wingwall (feet)	5.84	8.61
Elevation with respect to bottom edge of wingwall (feet)	16.18	14.54

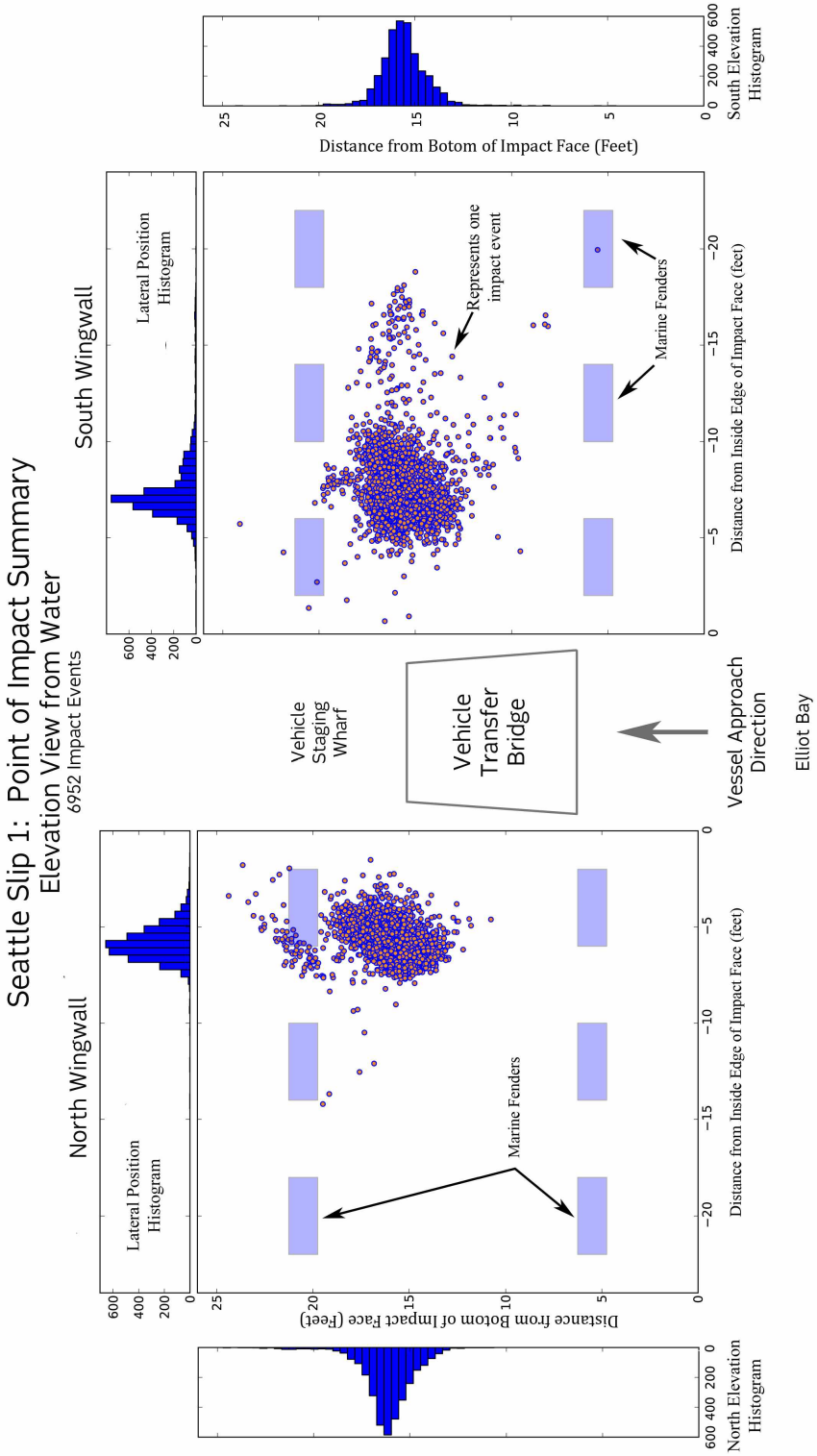

Figure 4.31: Point of Impact Summary Graphic

Chapter 5: Discussions and Recommendations

5.1 Overview

The instrumentation and monitoring program at the Bremerton Slip was operational between August 2011 and July 2012, during which approximately 4875 vessel-berthing events occurred. Each vessel berthing can be characterized by an impact event at both the north and south wingwalls. Out of a possible 9750 impact events, greater than 6950 wingwall impact events were recorded, characterized, and analyzed in this study. The sample collected at the site is assumed to be representative of Issaquah and Super Class vessels landing at the Bremerton slip. This chapter discusses recommendations with regard to the results generated by this study and further details procedures used to obtain results and research products.

5.2 Reliability Design Charts

The application of reliability engineering methods to the berthing load environment is a major component of the research performed at the Bremerton Terminal. Estimation of extreme values is the primary objective of fitting probability distributions to the empirical data. The percentile plots and associated tables presented in Chapter 4 utilize probability density functions (*pdfs*) to predict the magnitude and occurrence of design parameters, and allow for determination of 'service' and 'ultimate' values. Designers may apply the plots by first establishing reliability levels at which the 'service' and 'ultimate' loads are defined, and then matching the desired reliability level with the design parameter of interest. These empirically and statistically determined values provide a rational foundation upon which the designer may begin the process of designing an efficient structure that is both reliable and economical.

The design charts and tables presented in Section 4.7 are to be used for selecting design loads corresponding to both design life and reliability level. Selection of design values is dependent on the number of vessel-berthing occurrences a structure is expected to experience over a given life cycle. For example, if a wingwall design is to have a 50-year service life (design life), the appropriate design parameter value is determined by selection of a target reliability level that satisfies the number of berthing-events a structure will experience over its design life. Figures 4.27 through 4.31 illustrate the relationship of design parameter, number of berthing-events, and reliability level. Design values corresponding to a structural life cycle of berthing-occurrences at a high reliability level are to be considered as 'ultimate' – akin to values representing the 'demand' condition in the LRFD methodology.

5.3 Determination of Exceedance and Reliability Probability Levels

After establishing a dataset of empirically determined parameters and overlaying a *pdf* that appears to fit the data reasonably well, a probability associated with a given parameter value occurring or not occurring can be established. Knowledge of this determined reliability level also defines the probability of the value being exceeded. Equation 5.1 illustrates the relationship between reliability, (also known as 'probability of non-exceedance' - the probability of a parameter value not being exceeded in any one impact event), and the probability of exceedance (the probability that a parameter value will be exceeded in any one impact event). Extending these concepts to probability levels for a specific number of events is easily accomplished using probability theory in Equations 5.2 and 5.3.

$$R = 1 - p_{exceedance} \qquad \text{Equation 5.1}$$

$$R_n = R^n = (1 - p_{exceedance})^n \qquad \text{Equation 5.2}$$

$$R = R_n^{(1/n)} \qquad \text{Equation 5.3}$$

Where:

$R =$ Reliability level or non-exceedance level; the probability that a parameter value will be at or below a specified magnitude in *one* berthing event

$p_{exceedance} =$ Probabilty of exceedance; probability that a parameter of specified magnitude will be exceeded in one berthing event

$n =$ Number of berthing events

$R_n =$ Reliability level, probability of non-exceedance in '*n*' events; the probability that a parameter value will be at or below a specified magnitude in '*n*' impact events

The parameter values presented in Chapter 4 are provided for a range of reliability levels (probability of non-exceedance levels) that a designer can employ. Table 5.1 further illustrates the relationship between reliability levels, number of berthing-events, and design parameter exceedance probabilities.

The determination of reliability levels requires a multifaceted approach that is dependent on the goals of the designer and supporting organization. Considerations that need to be addressed may include: what effects will exceeding a design parameter have on the system; what is the amount redundancy built into the system to handle exceedance of a berthing parameter; and what are the life-cycle cost considerations associated with achieving reliability levels.

The design tables presented in Chapter 4 contain a large variety of reliabilities, (probability of non-exceedance) for the designer to work with. Table 4.12 is a summary of parameter design values that correspond to reliability levels over a range of berthing event numbers. This table provides a range of options to better inform the structural design. If the engineer desires a design value that has not been illustrated in the charts, parameter values for any reliability may be accomplished by; (1) utilizing a design number of berthing-events (n), and the corresponding reliability at that number of events, (R_n) in Equations 5.2 and 5.3 to calculate the desired reliability in any one impact event. (R), and (2) refer to the percentile for the desired parameter in Chapter 4, and utilize the calculated reliability (R) to determine the parameter value.

Table 5.1: Design parameter exceedance chart, as a function of reliability and number of berthing-events

Reliability percentile, (Probability of Non-Exceedance of a selected berthing parameter for oneimpact event), %	90	95	99	99.99	99.9999	99.9999999
Number of Berthings, *n*	**Probability of design parameter being exceeded in *n* berths (1- Reliability), %**					
1	10.00	5.00	1.00	0.01	0.0001	0.000001
15	79.411	53.67	13.99416	0.1499	0.0015	0.000015
450	100	100	98.91398	4.4005	0.0450	0.000450
5475	100	100	100	42.1622	0.5460	0.005475
27375	100	100	100	93.5277	2.7004	0.027371
54750	100	100	100	99.5811	5.3278	0.054735
109500	100	100	100	99.9982	10.3718	0.109440
164250	100	100	100	100	15.1470	0.164115
273750	100	100	100	100	23.9478	0.273376
410625	100	100	100	100	33.6765	0.409783
547500	100	100	100	100	42.1606	0.546004
821250	100	100	100	100	56.0119	0.817887

5.4 Parameter Recommendations

Berthing design parameters are presented below concerning service loads and ultimate loads based upon the results of the research accomplished at the Bremerton slip of the Seattle Ferry Terminal. The recommendations discussed in this section are specific to the site conditions and vessel classes landing at the Bremerton slip.

Service loads/parameters (also referred to as nominal loads/parameters) will refer to the upper bound concerning typical loading conditions that the wingwall structure will need to endure on a regular basis. In this report, the *service demand* will be defined as a parameter that has a 10% probability of occurring or being exceeded in 450 berthing events per wingwall (this represents a month of berthing-events at the Bremerton terminal). This corresponds to a reliability level of 99.977% for one berthing event, a 90% reliability level in a month of berthing

events, and a 72.25% probability of occurrence in one year at the Bremerton slip (5475 berthing events per wingwall).

Ultimate loads/parameters in this report will represent theoretical maximum parameters that could be expected during the design life of the berthing structure, at a particular reliability level. Ultimate loads represent events that may require the berthing structure to be taken out of service due to partial or total structural failure if exceeded. Two levels of ultimate parameter values are presented to provide a range that is dependent on the expected service life of a facility. The 'lower' values for *ultimate demand* are defined in this report as a 2% probability the berthing parameter will be exceeded in 273,750 berthing events, (representing a 50 year life-cycle at the Bremerton terminal), this corresponds to a 99.999993% reliability that the parameter will not be exceeded in any one berthing event, and a reliability level of 98% over 50 years at the Bremerton terminal. The 'lower' ultimate values are greater than any parameter recorded in this study. The 'higher' values for ultimate demand are defined in this report as a 2% probability the berthing parameter will be exceeded in 750,000 berthing events (representing a 50 year life-cycle at the highest frequency terminals in the WSF inventory), this corresponds to a 99.9999973% reliability the parameter will not be exceeded in any one berthing event, and a 98% reliability level over a 750,000 event service life.

Table 5.2: Empirically Determined Service and Ultimate Values

Loads	Service 10% 450 events	Ultimate 2% 273,750 events	Ultimate 2% 750,000 events
Energy - (kip feet)	97	302	340
Force -Gamma (kips)	296	492	516
Force - Lognormal (kips)	479	1307	1451
Parameters			
Velocity (feet/second)	1.24	1.82	1.88
Berthing Factor (feet^2/second^2)	0.43	1.31	1.47

5.5 Load Factors

The Load Resistance Factor Design (LRFD) methodology is a standard design approach used by both the building and bridge industries in the United States and Internationally. Structural design that utilizes the LRFD approach is a combination of applying resistance factors to the structural capacity, and multiplying loading conditions by a load factor. A design is considered safe and reliable when the factored capacity is greater than the factored demand. Resistance factors applied to the structural capacity have values that are less than 1.0, and loading conditions multiplied by 'load factors' employ values that are typically greater than 1.0. Both the resistance and load factors are based on probability distributions that describe the limit states of the structural component, and the likelihood of extreme loading condition occurring, see equation 5.4 (Ellingwood, Galambos et al. 1980).

$$\phi R_n \geq \sum_{i=1}^{n} \gamma_i Q_i \qquad \text{Equation 5.4}$$

Where:

ϕ = Resistance factor, less than 1.0, accounts for uncertainty in determining component resistance

R_n = Nominal Resistance corresponding to a limit state of a component being designed

γ_i = Load factor, typically greater than 1.0, though in load combinations can be less than 1.0 at times, accounts for uncertainty in determination of forces

Q_i =Nominal 'load effect', such as force or energy

The combination of scaling down the capacity and scaling up the load is intended to compensate for uncertainty and variability of materials, and the loading conditions they must endure in order to remain functional. The commonly employed load factor criteria that controls the design load is typically a combination of two or more loading conditions, such as dead, live, seismic, etc., multiplied by their corresponding load factors. Since the maximums of two loading conditions occurring simultaneously is highly unlikely, the greatest combination of loads (multiplied by their load factors) is considered the design load. This report details the load environment associated with vessel berthing structures, which may be a starting point for incorporating the LRFD methodology into the marine infrastructure industry. Further research is required to define and quantify the additional pertinent loads that a wingwall (or other) structure is required to resist such as wind and wave loading.

The load factors developed here are the result of dividing the ultimate load quantities by the corresponding service loads as developed in Section 5.4. These load factors correspond to a 2% probability that the particular parameter will be exceeded in 273,750 or 750,00 berthing events, which is the approximate service life range of structures in the WSF inventory (98% reliability over 50 years).

Table 5.3: Load Factor Development for Berthing Parameters

Load Factor Development for Berthing Parameters					
Load Parameter:	Service/ Nominal Load (*Q*)	Ultimate Load (Qγ)	Load Factor (γ)	Ultimate Load (Qγ)	Load Factor (γ)
	10% exceedance	2% exceedance		2% exceedance	
	450 events	**273,750 events**		**750,000 events**	
Berthing Energy (kip feet)	97	302	3.11	340	3.51
Berthing Force - Gamma (kips)	296	492	1.66	516	1.74
Berthing Force - Lognormal (kips)	479	1307	2.73	1451	3.03
Velocity (feet/second)	1.24	1.82	1.47	1.88	1.52
Berthing Factor ($feet^2/second^2$)	0.43	1.31	3.05	1.47	3.42

5.6 Normal Approach Velocity

Traditionally, approach velocity is the starting point for determining the impact energy associated with a berthing vessel when employing the kinetic energy method. A suitable approach velocity is typically selected by either referring to previously published information, or by direct determination. The velocity term is squared when determining the vessels' kinetic energy and therefore has significant influence on the calculated kinetic energy amount. The application of various berthing coefficients then attempts to refine the calculated kinetic energy value of the vessel to better reflect the uniqueness of the berthing situation.

Approach velocity is one of the foremost concerns using traditional design methodologies. Characterizing the ferry berthing maneuvers is the starting point in designing the wingwall structures; several observations are presented here with the intent of assisting the design engineer in making appropriate use of the empirical dataset. The current state of practice utilized by the WSF personnel is to assume that the vessel either contacts both wingwalls simultaneously, or impacts one wall and continues to slide forward toward the centerline of the slip, loading both walls relatively equally. Each wingwall is designed for one half of the total calculated design berthing energy (WSF 2012).

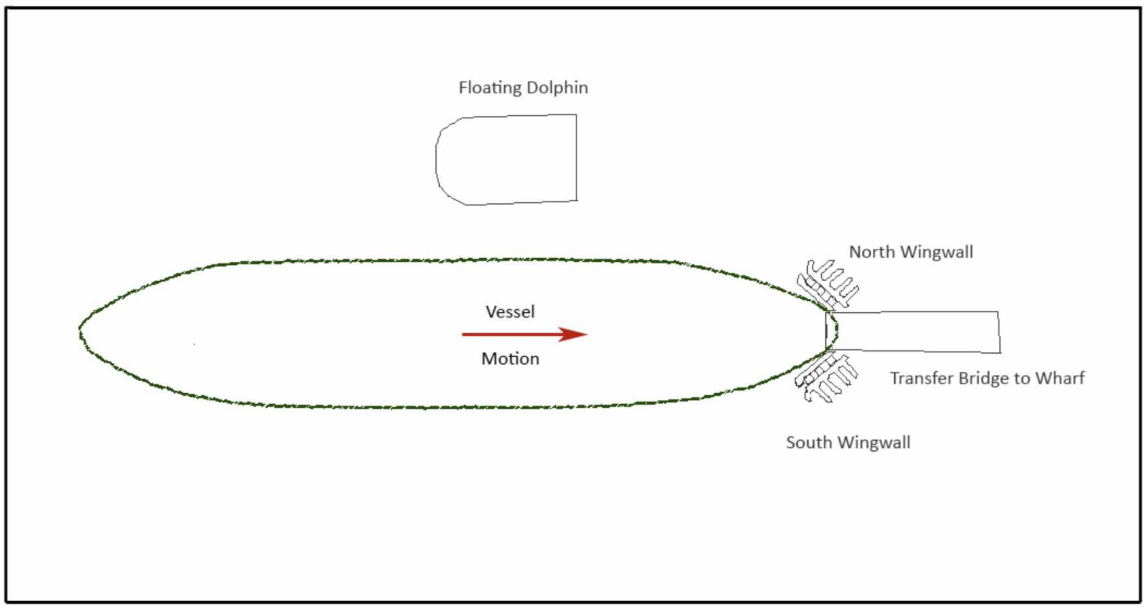

Figure 5.1: Idealized Berthing Overview, Plan view

This approach has resulted in robust wingwall designs that have functioned well, with the backing structures even surviving two 'runaway' vessel impacts over the past 19 years, (Fauntleroy and Seattle Slip 3). However, the review of thousands of berthing events allows for further characterization of the actual manner in which the vessel interacts with the berthing structures. Primarily, the idea that the vessel contacts both wingwalls simultaneously and loads both wingwalls with approximately the same energy could benefit from some refinement. After visually observing hundreds of landings at the Bremerton slip, and analyzing thousands more through the recorded data, it was determined that very few events involved the simultaneous impact of both wingwalls. The prominent condition involves ferry impacts at each wingwall that are independent, and the initial impact may, or may not, be the most significant impact of the event. The events analyzed at the Bremerton slip most frequently exhibit behavior that resembles a slow-motion 'pinball' – the vessel tends to alternate impacts with each wingwall before coming to

rest in the pocket shaped berth. Each wingwall is subject to multiple significant impacts in this typical vessel approach scenario; see Figure 5.2 for an annotated plot that displays this behavior. With regards to approach velocity, this observation is significant as it differs from the methodology currently in use. The kinetic energy method assumes a 'dead-float' into the structure. The 'dead-float' berthing scenario results in approach velocity measurements that would be nearly equal at either end of the wingwall structure see Figure 5.3. Vessel berthing events observed and analyzed in this report depict a contrasting scenario. In reality, thrust and maneuvering influences the vessel motion up to, during, and following the initial vessel impact. The implementation of this approach velocity dataset may require adjustments to the design procedures in order to achieve desired wingwall capacity.

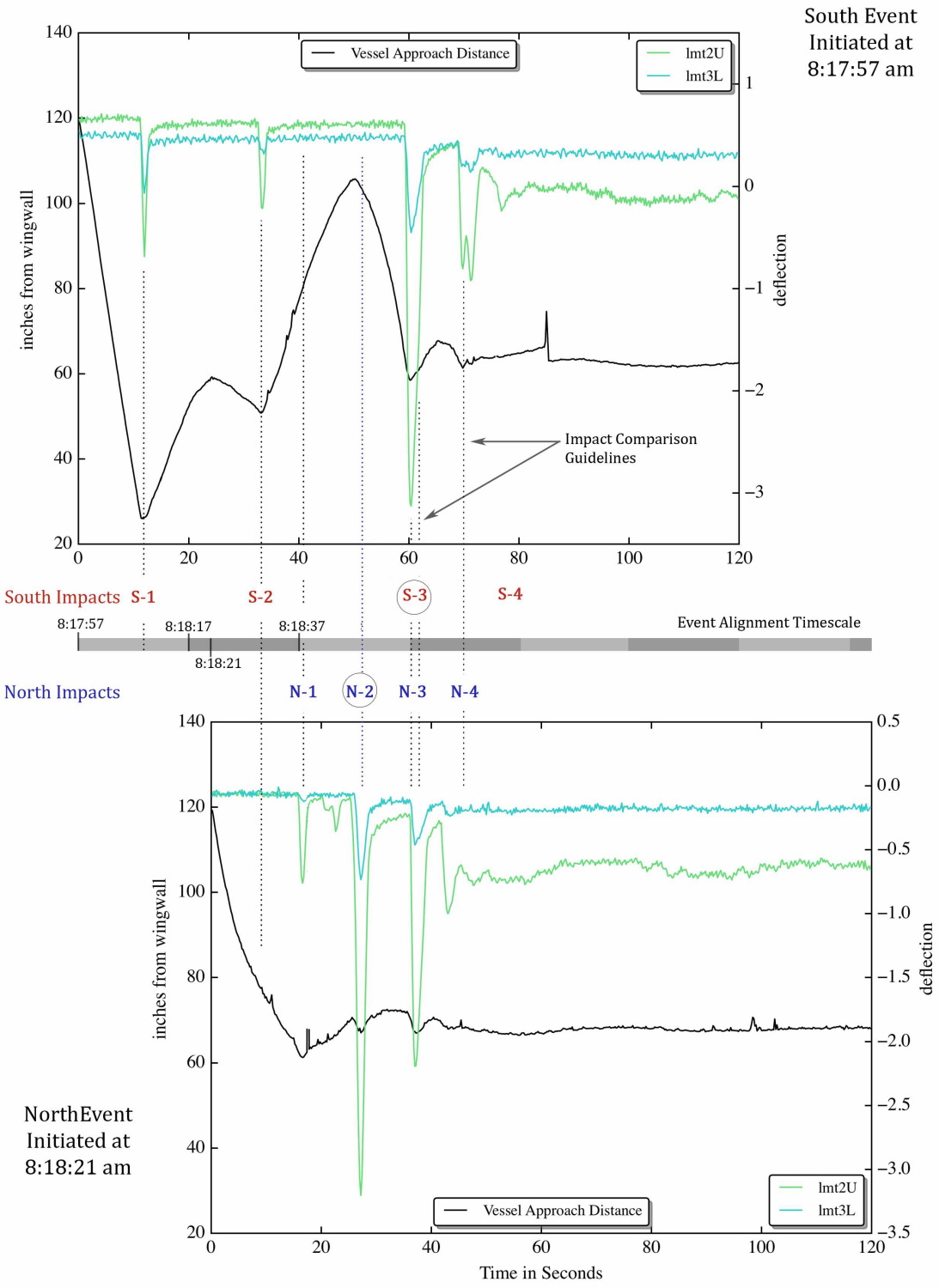

Figure 5.2: Illustration of complete berthing event with asynchronous impacts

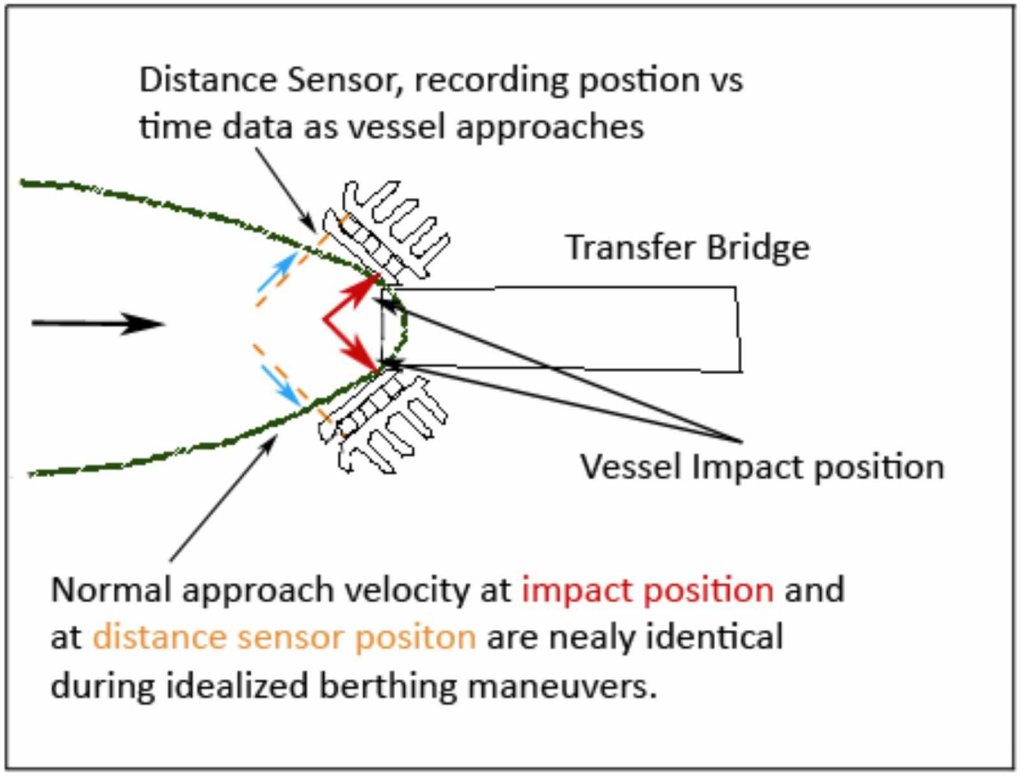

Figure 5.3: Close up of Idealized Berthing

However, small (less than 0.1 feet/second) or negative approach velocities were frequently recorded just prior to the deflection of the impact face. A common scenario observed at the site that may explain these measurements involves the vessel approaching the slip at a slight angle. Immediately prior to, or upon contact with the wingwalls, motion in the yaw direction (likely do to steerage and/ or environmental factors) was observed. Laying the vessel against the breasting dolphin was a frequently utilized maneuver that requires motion in the yaw direction. This was likely done to provide stability for offloading/ on-loading procedures. The result of these maneuvers is that the vessel has both a surge and yaw component to its motion when berthing. This condition has significance for the amount of energy imparted to the berthing structure, and is not easily quantified by velocity measurements taken during the field campaign.

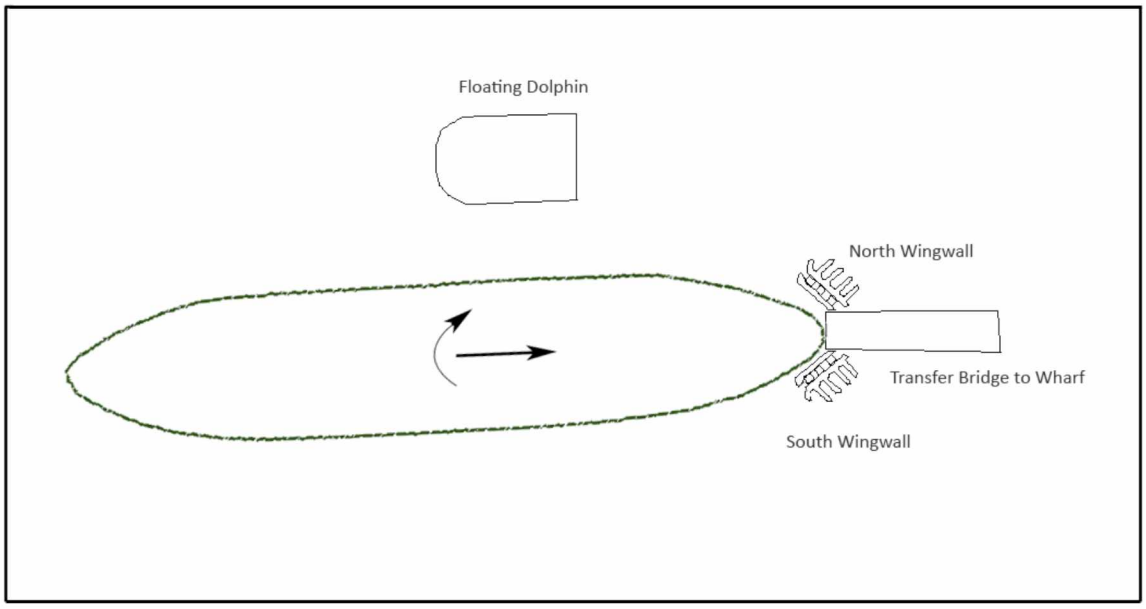

Figure 5.4: Berthing maneuver with rotational velocity component

The concept of a rotational velocity component also demonstrates that the initial velocity figure of interest is most meaningful at the point of impact, which varies for each event, thus making an accurate estimate of initial velocity elusive. Any amount of rotation about the vessel's vertical axis diminishes the applicability of the empirically recorded normal approach velocity at the edge of the wingwall, and also contributes to the impact energy of the vessels bow; see Figure 5.5.

For example, the normal approach velocity determined from the vessel position information may be determined to be 0.02 feet per second (0.25 inches per second), however the amount of energy absorbed by the wingwall can suggest that the impact velocity at the point of impact was likely greater than the recorded velocity at the outside edge of the structure. Figure 5.6 illustrates this concept using plots of two different events.

The velocity data presented in Chapter 4 is accurate at the outside edge of the wingwall, and should be used with some discretion when applied to the kinetic energy method for reasons discussed above. Energy associated with the berthing event often surpassed the amount of kinetic energy (based on the recorded approach velocity) associated with the vessel, and therefore designers should use caution when attempting to design berthing structures based on normal approach velocity distributions and berthing coefficients.

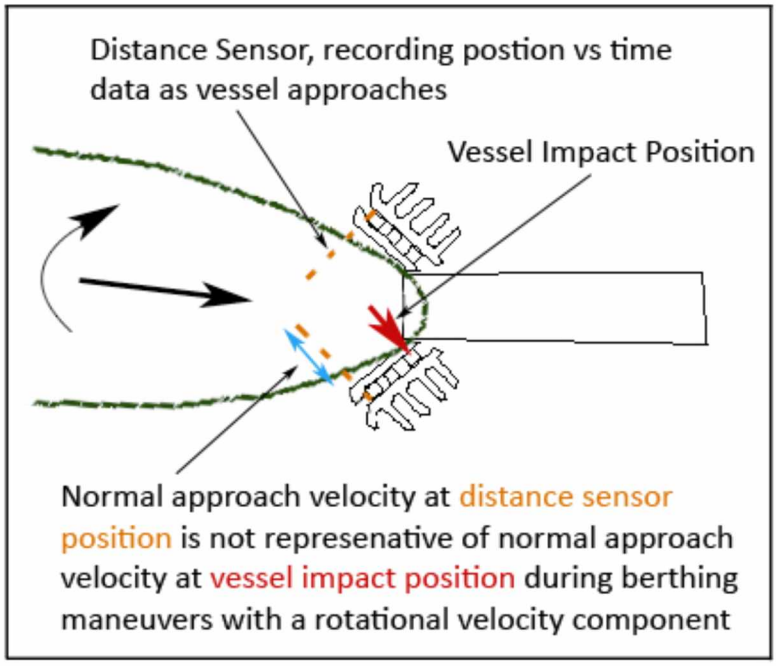

Figure 5.5: Close up of Berthing Maneuver with yaw component

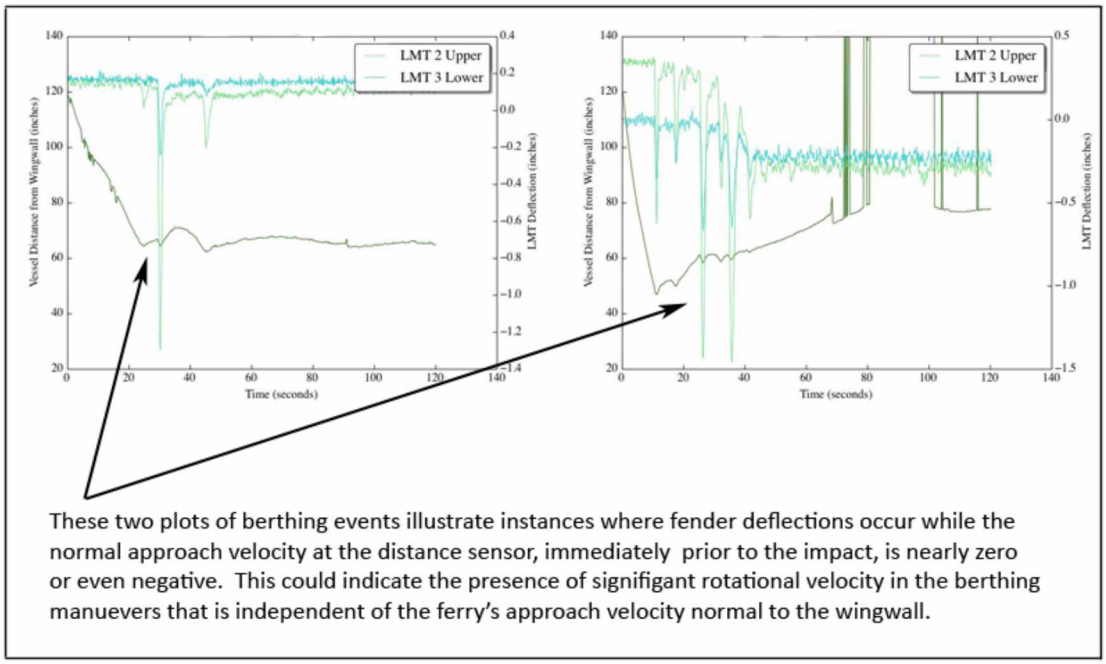

Figure 5.6: Evidence of rotational velocity component during vessel berthing impact

5.7 Berthing Energy

Empirically determined berthing energy information is a more direct and less ambiguous approach to designing berthing structures than employing the kinetic energy method and empirically determined approach velocities. All factors affecting the berthing structure are included in the experimental sample of berthing energy, and the designer can employ the energy information with far less challenges.

The berthing energy results displayed in Section 4.3 represent the total energy absorbed by the impact face and fender. Challenges of operating instrumentation in the intertidal zone resulted in seven LMT failures over the course of this study. Logistical challenges associated with replacement of the devices resulted in intervals of up to three weeks where a LMT would not be

recording information. The data obtained during these periods was adjusted to counteract the effects of the failed sensor. This was accomplished by first calculating the ratio of deflection experienced by each fender pair (upper and lower fender at the same piling) of the wingwall when all sensors were operational over the period of the study. Next, the deflection ratio was applied to the fender pairing in an effort to approximate the amount of deflection that would likely be experienced by the out of service fender. For example; if the north side lower LMT, closest to the transfer bridge was out of service for 2 weeks before being replaced, all data from that time period would under-represent the total energy absorbed by the wingwall, since one of the six instruments was not functioning. The ratio of upper to lower deflection at that position is approximately 1.59 to 1.0. During a berthing event the upper fender deflection was measured to be 3.0 inches, and the corresponding measurement at the out-of-service LMT is 0.0 inches. Utilizing the deflection ratio, the lower fender displacement can be approximated to be 1.887 inches, allowing for a more accurate estimation of vessel berthing energy.

The capacity of each marine fender at maximum displacement is approximately 283 kip feet, which is greater than any event estimated over the duration of the study (147.6 kip feet was the maximum estimated energy absorbed by the wingwall). This suggests that the wingwalls employed at the Bremerton slip are designed with significant excess capacity. The north wingwall has a slightly higher mean energy absorption value than the south wingwall, and also recorded a maximum berthing event that was 1.8 times the maximum event that occurred on the south wingwall.

Quantifying the amount of energy to be absorbed by the wingwalls for typical landings by WSF personnel is considered to be a Type I berthing event, a landing that causes no damage. A typical starting point for WSF wingwall design is the 'standard wingwall design energy' spread sheet that incorporates berthing coefficients and variables for all vessels in order to establish a baseline design number. The Type I design energies to be absorbed by the wing wall are 343 kip

feet for the Kitsap, and 379 kip feet for the Kaleetan. These design values correlate to a 99.7% reliability level for a 50-year design life. Design of wingwalls by WSF is complicated by the desire to protect shore side infrastructure, such as the towers and transfer bridge, in the event of an extreme, Type III, berthing event. Type III berthing events include the failure of some part of the wingwall, and are meant to account for a condition in which the vessel loses control of the propulsion system. The newest generation of wingwalls is softer and undergoes a partial analysis of a Type III berthing event in order to understand the amount the wingwalls will deflect during a Type III event that occurs directly at the throat of the structure. The purpose of this analysis is to quantify approximately how far the vessel can progress towards the shore, and to design the structure to fail in a controlled manner. The Type III design energy amounts for the Kitsap and Kaleetan are 3160 and 3486 kip feet.

5.8 Berthing Force

The force recommendations are specific to the Bremerton Wingwalls, as berthing force is dependent on system stiffness. The berthing force discussed in Section 4.4 represents the sum of the reaction forces at all six marine fenders and the force associated with displacing the impact face of the wingwall. The forces applied to various components of the wingwall can be determined from the berthing force data and structural analysis.

The maximum amount of force applied to the wingwall was approximately 408.5 kips, and each marine fender has a maximum rated reaction force of 150 kips. The stiffness of the wingwall system is directly related to the reaction force exerted by the wingwall, this makes it difficult to employ berthing force data to systems with different stiffness characteristics.

Berthing force results have been provided for both the Gamma and Lognormal probability distributions. Both distributions have qualities that may be of interest to the designer and are presented to provide additional context for the designer.

5.9 Berthing Coefficient

The berthing coefficient results of Section 4.5 display high variability and exceed ranges suggested in the literature (Costa 1964) and (Gaythwaite 2004). The challenges of measuring the approach velocity as discussed in Section 5.6 help to illuminate this discrepancy between berthing coefficients that are empirically determined and recommended in the literature.

The results associated with the berthing coefficient values suggest caution when applying the traditional kinetic energy approach that utilizes a berthing coefficient and approach velocity to determining the vessels impact energy. Most

notably, approach velocity data that corresponds to very low approach speeds tends to have high berthing coefficients; high enough that when filtered out the mean berthing coefficient drops significantly into a range more in line with the literature, see Figures 5.7 through 5.10 for filtered berthing coefficient histograms. However, the velocity dataset has previously been filtered and is considered representative of vessel behavior at the point of measurement; and therefore the justification required to manipulate the velocity dataset is absent. Further examination of the results reveals that as the calculated berthing coefficient (C_b) increases above 1.1 (the upper bound of published values), the mean velocity ($v_{approach}$) associated with the kinetic energy of the vessel prior to impact decreases.

The experimentally determined berthing coefficient results suggest that there is energy being added to the berthing event that is not accounted for in a simple vessel kinetic energy calculation. Also, as discussed above, the presence of a yaw component to the vessel motion influences the approach velocity at the point of impact. The kinetic energy method attempts to account for rotational velocity with the eccentricity coefficient. However the application of values found in the literature (0.5 to 0.8) may not be representative of the berthing scenario at the Bremerton slip. Sources of additional energy not associated with a 'dead-drift' approach velocity could be the use of the vessel's propulsion system, or environmental conditions affecting the berthing procedures. Neither of these aforementioned factors are accounted for when developing a berthing coefficient, and given the high values associated with the empirically determined berthing coefficient there are clearly some components that cannot be overlooked. As discussed in Section 5.6, the rotational or 'yaw' component of the incoming ferry motion provides insight into why vessel approaches with 'slow' recorded approach velocities may apply larger than anticipated amounts of energy to the berthing structure.

The berthing coefficient results were further investigated to ascertain the influence of the approach velocity. Table 5.4 displays berthing coefficient

information after filtering the lower bound of the approach velocity to illustrate its effect on the berthing coefficient estimates. By filtering out the lowest approach velocity measurements, the mean berthing coefficient drops significantly and does not converge to a value. This illustrates a challenge associated with utilizing the berthing coefficient approach; the berthing coefficient exhibits variation with respect to normal approach velocity.

Table 5.4: Berthing Coefficient Results with lower-bound approach velocity filtered

Berthing Coefficient, C_b				
Approach Velocity Lower-Bound ft/sec	**Mean**	**Standard Deviation**	**Max**	**# of events**
0.04	3.299	9.457	199.842	5065
0.32	0.683	0.436	5.76	2224
0.50	0.477	0.28	2.42	769
0.75	0.2896	0.202	1.03	186
1.00	0.1567	0.155	0.789	54

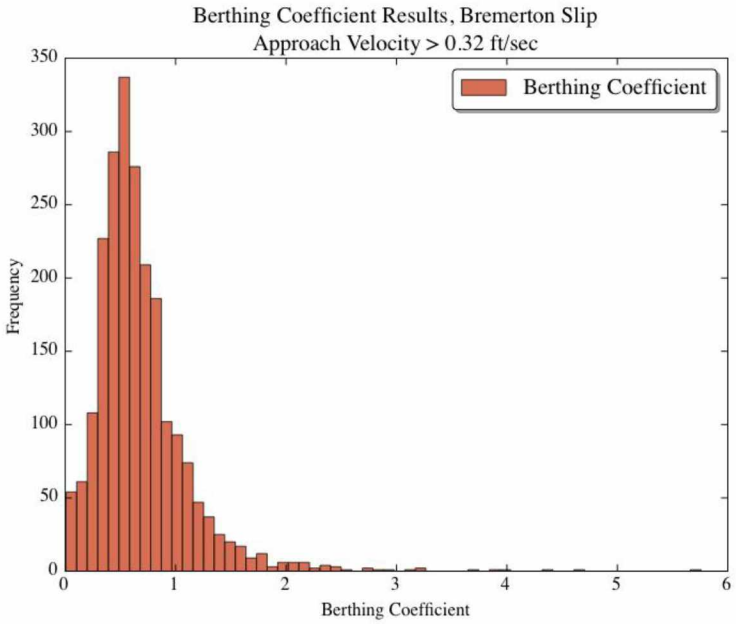

Figure 5.7: Berthing Coefficient Results, Approach Velocity > 0.32 ft/sec

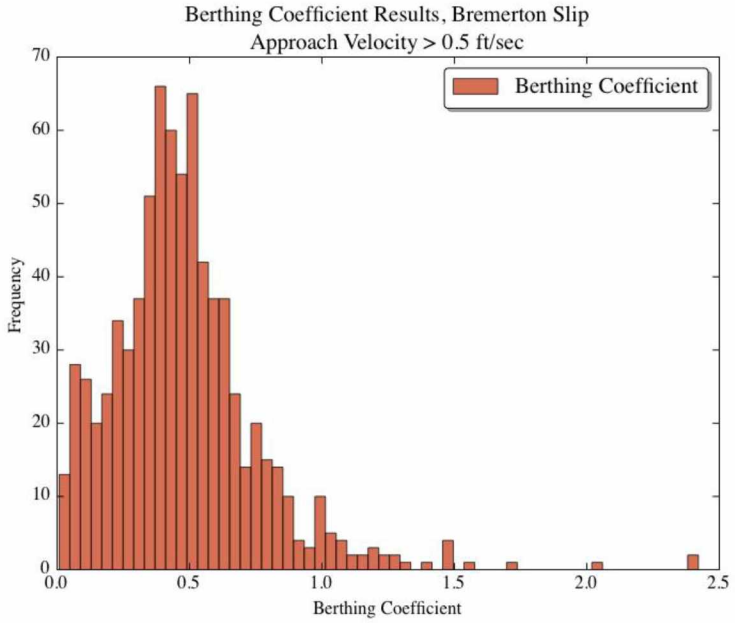

Figure 5.8: Berthing Coefficient Results, Approach Velocity > 0.5 ft/sec

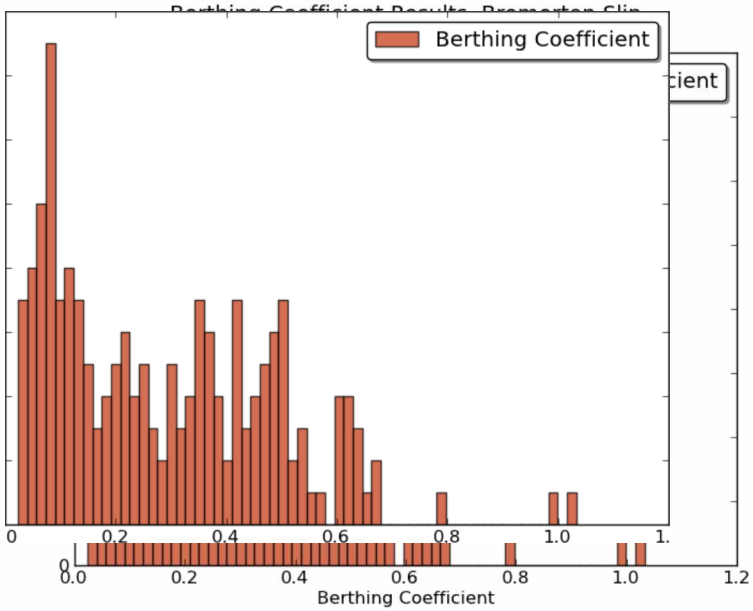

Figure 5.9: Berthing Coefficient Results, Approach Velocity > 0.75 ft/sec

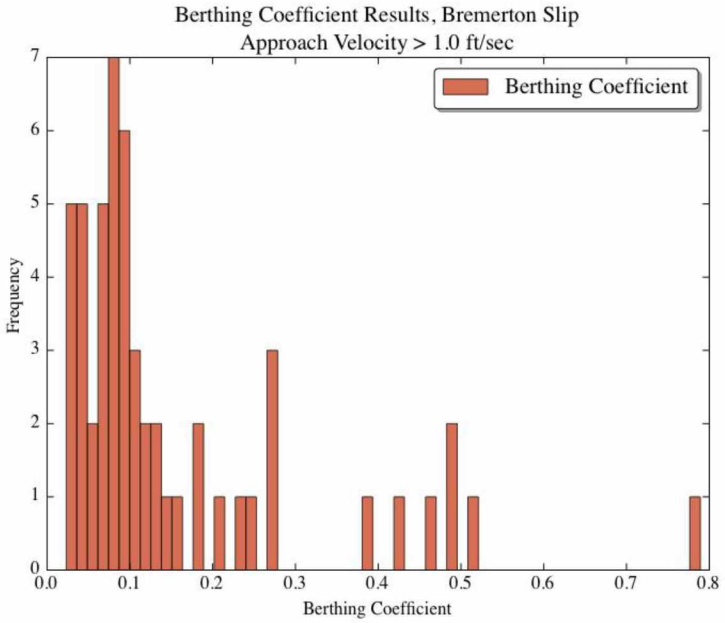

Figure 5.10:Berthing Coefficient Results, Approach Velocity > 1.0 ft/sec

Despite the challenges associated with the experimental justification of a berthing coefficient, the kinetic energy approach is still considered the standard method for solving the berthing energy problem. The Alaska and Washington State Departments of Transportation have successfully utilized this method by applying decades of experience in working with the berthing coefficients and approach velocities unique to their sites. The proper application of the kinetic energy method is dependent on proper selection and *balance* of approach velocity and berthing coefficients. For example; there are multiple combinations of berthing coefficients that could provide accurate berthing energy estimates based on erroneous approach velocity estimates. The challenge facing designers is how to proceed using berthing coefficients that have been refined over time when presented with empirical velocity data that conflict with historically employed standards.

Attempting to derive a reasonable estimate for a design energy using the estimated berthing coefficients (Section 4.5) and approach velocities (Section 4.2) is not possible. Another method is proposed here to provide designers with a procedure that bridges the traditional kinetic energy methodology with the empirically determined estimates of berthing energy. Utilizing the empirically determined approach velocities, the estimated berthing energies and their associated distributions, a reasonable estimate for berthing coefficients at varying reliability levels can be obtained. The kinetic energy equation for a berthing vessel is reprinted here, Equation 5.5.

$$E_w = \frac{W}{2g} v^2 C_b \qquad \text{Equation 5.5}$$

Where:

E_w = Berthing Energy to be absorbed by wingwall
W = Vessel mass
v = Approach velocity
C_b = Berthing Coefficient

Utilizing Equation 5.6, the probability based estimates of berthing energy and approach velocity (Sections 4.2 and 4.5), and solving for C_b, a range of berthing coefficient values can be obtained correspond to the empirically parameters, see Table 5.5.

$$E_{R\,\%} = \frac{W}{2g} v_{R\%}^2 C_{b-R\%} \qquad \text{Equation 5.6}$$

Where:

$E_{R\,\%}$ = Berthing Energy at a given reliability level
W = Vessel mass
$v_{R\,\%}$ = Approach velocity at a given reliability level
$C_{b-R\%}$ = Berthing Coefficient at a given reliability level

Table 5.5: Berthing Coefficient Estimates

Berthing Coefficient Estimates		
Probability of Non-Exceedance, %	Velocity, feet/second	Cb, estimated
98	0.797	0.555
99	0.876	0.549
99.9	1.105	0.565
99.99	1.304	0.609
99.999	1.482	0.672
99.9995	1.533	0.693
99.9999	1.646	0.747
99.99995	1.692	0.772
99.99999	1.798	0.835
99.999999	1.941	0.936
99.9999999	2.077	1.049

By utilizing the berthing coefficient estimations and velocity figures presented in Table 5.5, the design berthing energies can be calculated that are calibrated at the given reliability levels. The use of the data in this way is presented for illustration purposes; the use of the design berthing energy information represents a more direct application of the study.

5.10 Berthing Factor

The berthing factor results provide a methodology for scaling the empirically determined design berthing energy to vessel classes not represented in this study (vessels with different displacement values). After adjusting for proper units, the berthing factor may be multiplied by the vessel mass of interest to obtain a design berthing energy that is founded upon the empirical data obtained in this study. Please refer to the example in Section 6.3 for details regarding this procedure.

The mean berthing factor observed in the study period at the Bremerton slip was 0.057, and the maximum-recorded berthing factor was 0.684. The service value for berthing factors obtained in this study by methods detailed in Section 5.5 is 0.435; this corresponds to a service energy level between 89.3 and 98.3 kip feet when applied to the vessel displacements that service the Bremerton slip and compares favorably with the service level berthing energy recommendation for the slip of 97.8 kip feet. The *ultimate* berthing factor value recommended by this study is 1.33, corresponding to a 98% reliability over the course of 50 years. For the ferries landing at the Bremerton slip, this corresponds to *ultimate* values for the 'Issaquah' class vessels of 272.9 kip feet, and ultimate values for the 'Super' class vessels of 301.0 kip feet. These ultimate values correspond favorably with the ultimate berthing energy recommendations suggested for the Bremerton slip of 304.7 kip feet.

Applying the berthing factor to vessel displacements, the design energy for service and ultimate loads can be extrapolated for a range of vessels; this is exhibited in Figure 5.11. It should be noted that scaling parameters has limitations that may not be anticipated from the outset of design using scaled values. Design errors attributable to the effects of scaling up successful designs have been persistent throughout history (Petroski 2000), and every effort must be made to comprehend the potentially unique failure mechanisms and operational differences associated with larger (or smaller) systems.

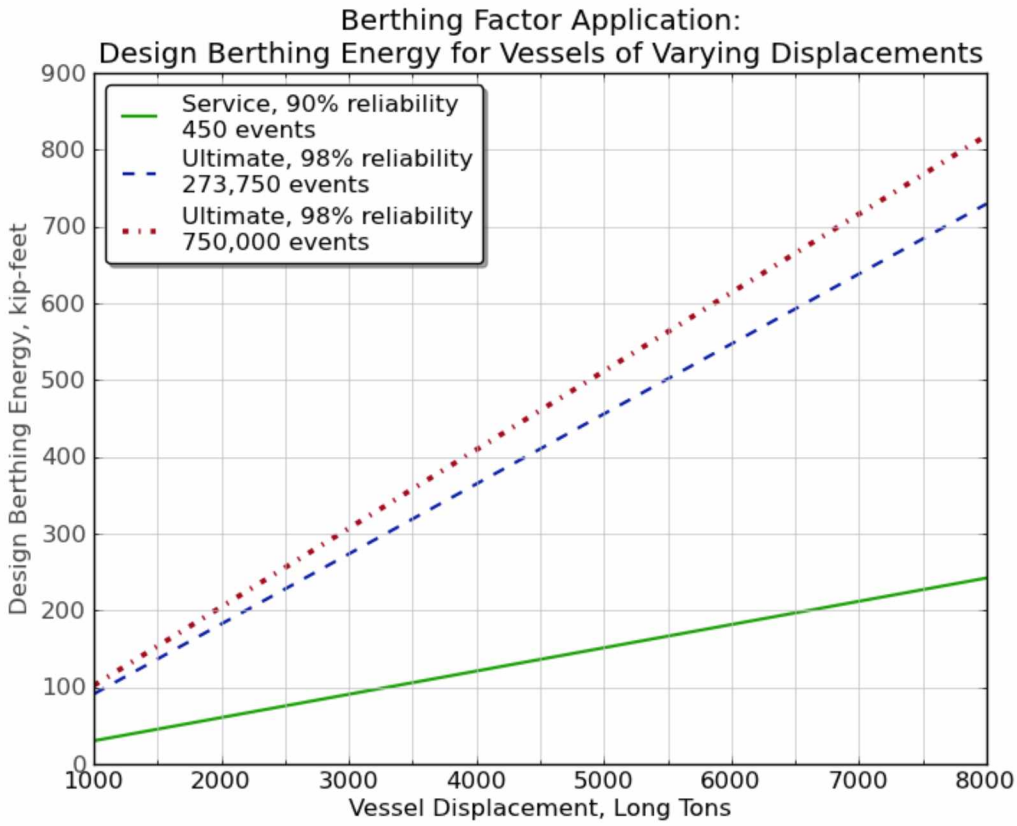

Figure 5.11: Application of berthing factor to a range of vessel displacements

5.11: Vessel Point of Impact Results

The point of impact results are intended to provide insight into where and with what frequency the vessel is contacting the impact face. The visual representation provided by the figures of Section 4.8, and the fender impact synopsis of Table 5.6 attempt to quantify the vessel landing location.

This analysis provides some interesting observations that may be useful to designers:

- The lower marine fender furthest from the 'throat' typically goes into tension.
- The vessel impact locations on the north wingwall result in a more precise distribution than the vessel impact locations on the south wingwall. This may be attributed to the presence of the breasting dolphin along the north side of the approach. The mean impact elevation is located closer to the upper fender than the lower fender and generally occurs between pile lines 2 and 3.

Table 5.6: Fender Impact Synopsis

	Average deflection (in)	Average Force (kips)	Average Energy (kip-feet)	Avg. Energy Absorbed per fender, %
North				
LMT2 Lower	1.01	19.25	2.70	22.97
LMT2 Upper	1.69	31.61	5.00	42.51
LMT 3 Lower	0.40	7.74	0.95	8.10
LMT 3 Upper	0.87	16.52	2.22	18.86
LMT 4 Lower	-0.26	-5.05	0.55	4.66
LMT 4 Upper	0.14	2.74	0.34	2.91
South				
LMT2 Lower	0.90	17.07	2.35	21.37
LMT2 Upper	1.51	28.32	4.36	39.70
LMT 3 Lower	0.47	9.01	1.14	10.40
LMT 3 Upper	0.83	15.85	2.12	19.30
LMT 4 Lower	-0.07	-1.30	0.34	3.12
LMT 4 Upper	0.28	5.29	0.67	6.11

Chapter 6: Implementation and Design Considerations

6.1: Overview

The berthing structures at the Bremerton slip at the Seattle Ferry Terminal were originally designed for a larger vessel class than they currently serve, and have performed adequately since installation in 1993. There is no evidence that the design capacity of the wingwalls has been exceeded at the Bremerton slip since their installation. The results of this study are intended to further the understanding of the vessel structure interaction, characterize the loading environment of the Bremerton slip, and provide design tools to WSF personnel.

The structures at Washington State Ferry terminals are subject to large numbers of berthing events daily, and are designed for relatively long service lives. There exists considerable variation of berthing energy demands between service and ultimate events, which adds to the challenges of designing an efficient structure. The use of a reliability based design approach is a rational way to characterize uncertainty associated with demands placed on a structure. Although a structure cannot be efficiently designed to resist every possible loading condition, the use of reliability-based criteria allows for a design based on the likelihood of loads occurring over the service life of the project.

The transition to a reliability based design approach requires an adaptation of the traditional design methodologies used when establishing design-berthing energy. When employing a reliability based approach, subjectively determined safety factors are replaced by rationally determined load factors; and the engineer is empowered with information that assigns a probability to demands being exceeded or not. Before selection of a desired reliability level can proceed, the consequence of the associated 'failure' must be clearly understood. The working definition of 'failure' in this document is that the design parameter value is exceeded. All discussion of 'reliability' levels relates to this idea that a design parameter is not being exceeded, and the probabilities of exceedance relate to design values being

surpassed. It is important to note that if a design parameter is exceeded, structural failure is not implied by this definition. Another factor that must be defined in order to properly employ reliability techniques is the interval of concern. For a wingwall, the interval of concern is most easily described as the estimated number of berthing events the wingwall is expected to endure during its service life.

When selecting a desired reliability level, potential failure mechanisms that could result if the design parameter is exceeded must be explored and analyzed with regards to repair/replacement costs, maintenance costs, and lifecycle costs. Reliability levels of different structural elements may vary depending on the function of the element and amount of redundancy. The cost/benefit analysis of the various reliability levels may be based on historical performance of structures and the associated maintenance costs.

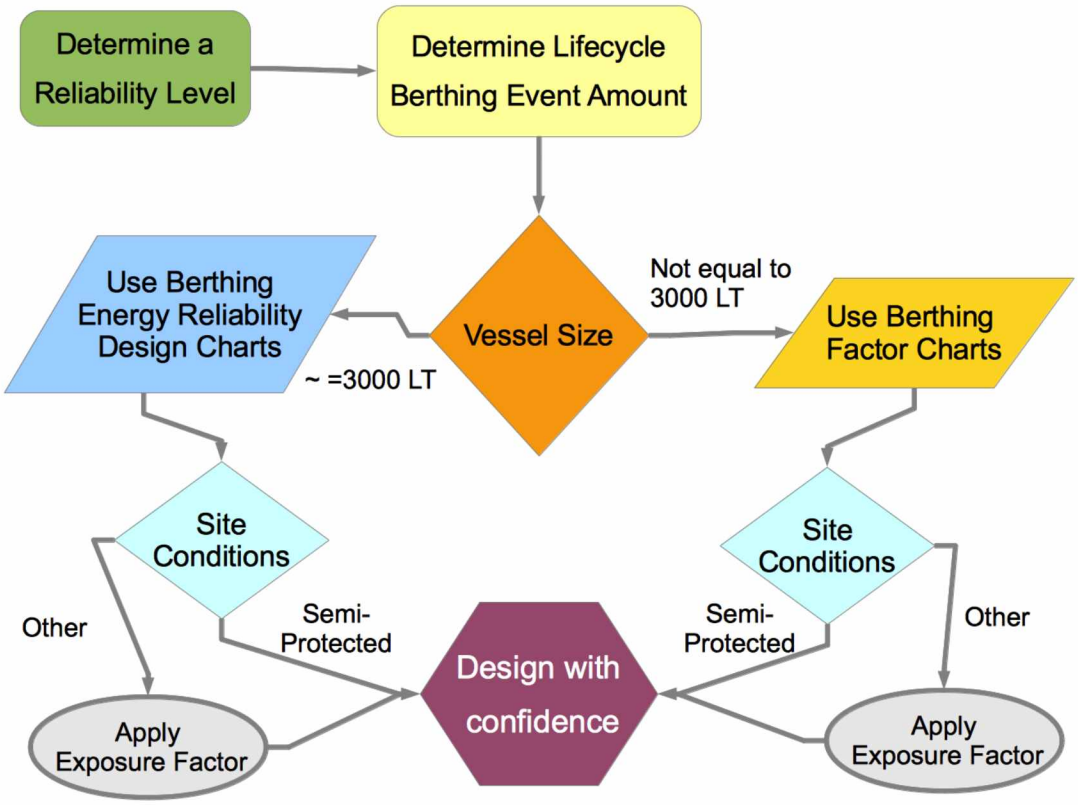

Figure 6.1: Implementation Graphic

6.2 Elastic Energy Approach, Design Option 1

The use of the berthing energy recommendations of Section 4.3 and 4.7 is the most direct application of this research. For locations that have analogous site conditions and receive vessels of similar size, the procedure is elementary. Following the selection of a desired reliability level, and number of berthing events the structure is intended to receive; a design berthing energy may then be selected from the reliability plots of Section 4.7, as presented in Example 6.3.1(a). If the designer desires to utilize a reliability level not represented in the plots of Section 4.7, the procedure is outlined in Section 5.3, and further expanded in Example 6.3.1(b).

Application of the berthing energy recommendations to sites with conditions that vary from the Seattle Terminal may be accounted for using an exposure factor, *k*, developed by (Toppler and Weersma 1973) for tanker vessels with displacements between 300,000 and 500,000 long tons. The selection of exposure factors specific to conditions of the greater Puget Sound region may benefit from refinement by WSF personnel.

$$E_{exposure-design} = k * E_{design} \qquad \text{Equation 6.1}$$

Where:

k = Exposure factor for location

= 1.10 for very exposed locations

= 1.0 for locations of normal exposure, Seattle Terminal

= 0.85 for very sheltered locations

$E_{exposure-design}$ = Design berthing energy, adjusted for exposure

E_{design} = Design berthing energy

Example 6.2.1:

Determine a 'Type 1' design berthing energy for a wingwall located in Elliott Bay that will need to handle approximately 750,000 berthing events over the course of its design life. Site conditions are similar to the Bremerton Slip. The ferries are 'Issaquah' and 'Super' class vessels that are identical to those utilizing the Bremerton Slip of the Seattle terminal.

(a) For a desired Reliability level of 98% and a 500,000 event design life
Utilizing Figure 4.27: the design berthing energy at the intersection of the 98% reliability curve and 500,000 berthing events is approximately 320 kip feet.

$$E_{design} = 320 \text{ kip feet}$$

(b) For a desired reliability level of 98% and a 900,000 event design life:

The 900,000 berthing event design life is not represented on Figure 4.27, therefore an alternate method is required. (1) Determine the reliability level for one berthing event that corresponds to a 98% reliability level at 900,000 events by utilizing equation 5.3.

$$R = R_n^{(1/n)} \qquad \text{->} R = 0.98_{900,000}^{(1/900,000)} = 0.999999975 \approx 0.99999999$$

Look up the appropriate value of R in Table 4.4, remembering to convert to a percentage, and associate with the corresponding design berthing energy level.

$$E_{design} = 380.5 \text{ kip feet}$$

6.3 Berthing Factor Approach, Design Option 2

The berthing factor approach extends the use of the empirical data to a range of vessel displacements. There are several methods of using the berthing factor results; they are covered in the following examples. Figure 5.7 offers the most efficient use of the berthing factor results, allowing the design berthing energy to be defined as a function of vessel displacement and ultimate limit state. Section 4.6 provides berthing factor results that may be used to obtain design berthing energy values with a more precision

Example 6.3.1:

Determine the 'Type I' Ultimate Design Berthing Energy of a vessel with an operational displacement of 5000 long tons at a 98% reliability level for a design life of 274,000 berthing events.

Solution: The use of Figure 5.7 offers a direct result to the problem; simply line up the reliability level with the vessel displacement.

$$E_{design} = 460 \text{ kip-feet}$$

Example 6.3.2:

Determine the 'Type I' Ultimate Design Berthing Energy of a vessel with an operational displacement of 6600 long tons at a 96% reliability level for a design life of 700,000 berthing events.

Solution: Figure 5.7 does not provide information for the desired reliability level; therefore it is necessary employ another method. (1) Determine the reliability level for one berthing event that corresponds to a 96% reliability level at 700,000 events by utilizing equation 5.3.

$$R = R_n^{(1/n)} \qquad \text{->} R = 0.96_{700,000}^{(1/700,000)} = 0.99999994 \approx 0.9999999$$

Look up the appropriate value of *R* in Table 4.11, remembering to convert to a percentage, 99.99999%, and find the corresponding berthing factor in the table.

At *R* = 99.99999; f_b= 1.2643 feet²/seconds²

Apply the berthing factor to the vessel displacement to obtain the design berthing energy.

$$E_{design} = f_b * \frac{W}{g} \qquad \text{Equation 6.2}$$

Where

W = Vessel displacement, 6600 long tons * 2240 lbs/ ton

g = Gravity acceleration = 32.174 feet/second

f_b = Berthing factor = 1.28

Solving for E_{design}, and converting to kips; E_{design} = 588 kip-feet

For landings with different site conditions, the exposure factors provided in Section 6.3 could be used to modify the design energy accordingly.

6.4 Kinetic Energy Approach, Design Option 3:

The use of the Kinetic Energy Approach is the standard method to solve the berthing energy problem. A design option is presented based on the estimated berthing coefficients presented in Table 5.5. This method allows the berthing coefficients to be applied over a range of vessel sizes.

Example 6.4.1:

Using the kinetic energy equation, and approach velocity information and adapted berthing coefficient values from the Bremerton Load Environment Study, determine a 'Type 1' design berthing energy for a wingwall located in Elliott Bay that will need to handle approximately 550,000 berthing events over the course of its design life. Site conditions are similar to the Bremerton Slip. The ferry is an 'Evergreen State' class vessel and a reliability level of 98% over the structure design life is required.

Solution: First, determine the reliability level for one berthing event that corresponds to a 98% reliability level at 550,000 events by utilizing Equation 5.3.

$$R = R_n^{(1/n)}$$

$$R = 0.98_{550,000}^{(1/550,000)} = 0.999999963 \; rounds\ up\ to\ 0.99999999$$

Look up the appropriate value of R in Table 5.5, convert to a percentage, 99.999999%, and find the corresponding velocity and berthing coefficient values.

At R = 99.999999%, v = 1.941 feet/second, and C_b = 0.936. Utilizing the kinetic energy equation (Equation 5.6), the design berthing energy can be calculated.

W = 2276 long tons = 5,098,240 pounds

$$E_w = \frac{5{,}098{,}240}{2*32.174} 1.941^2 * 0.936 = 279.4\ kip\ feet$$

6.5 Impact Face, Fender, and Backing Structure Considerations

Design of the wingwall system is accomplished by balancing the requirements of energy dissipation, hull reaction forces, structural redundancy, and shore-side infrastructure protection. The wingwall design at the Bremerton terminal has proved to be capable of handling the demands of its loading environment for the past 20 years without any issues. After characterizing the berthing energy loads at the Bremerton slip, it would appear that there is significant excess capacity built into the wingwall system.

The fender system and support structure are may designed to resist up to double the maximum service load. However, the common practice is to design fender systems to meet service energy requirements based on a 98-99% design approach velocity without additional safety factors applied. High frequency ferries are recommended to be designed with approach velocities that are four times the nominal approach speed (Gaythwaite 2004).The modular fenders of the impact resisting wingwall system are typically designed to be easily replaceable, and therefore require a lower factor of safety than other components of the berthing structure, such as pilings.

The recommendations of this report are based upon a reliability-based approach that recommends design-berthing energy at ~3 times the nominal service load (Section 5.5). This recommendation is slightly lower than the literature recommendations, but is based on measurements of structural response.

Minimizing the energy-to-reaction ratio (*E/R*) is also an important consideration when designing a marine fender system for ferry vessels (Gaythwaite 2004). The selection of a fender system with a high *E/R* ratio reduces the reaction forces placed on the vessel hull and provide for more safety and comfort for passengers on the vessel.

The reaction frame support structure for the impact face was instrumented with strain gauges in this study in an effort to measure strain in the pilings during

vessel impact. During vessel impacts the strain gauge readings rarely registered above the signal 'noise', indicating that in most berthing procedures the support structure was not subjected to significant axial strain. The support structure consists of 24" and 30" concrete filled steel piles framed together with steel wide flange and pipe sections, and creates a reaction frame that has very little axial displacement. The backing structure deflection mechanism is primarily the result of bending, and therefore the strain gauges were unable to measure the flexural component of the structural reaction. The support structure serves a dual purpose, it provides shore-side protection and as reaction frame for the fenders and impact face. The Bremerton wingwalls were originally designed for the largest class of vessels in the WSF fleet, and that can explain its robust design. Current WSF designs have shifted to a simpler reaction frame that allows for a considerable amount of energy to be absorbed by deflection of the vertical pile structures. This new design also has the advantage of vastly simplified installation and fabrication procedures when compared to the design utilized at the Bremerton terminal. A design challenge of the new reaction frame structure is ensuring that a runaway vessel does not deflect the wingwalls to the extent that the transfer bridge is damaged.

Point of impact information presented in Chapters 4 and 5 may be used to assist in refining the geometry and placement of the impact face relative to sea level, and the transfer bridge. The information can be utilized to 'fine-tune' the kinematic balance of the impact face, and potentially provide a more efficient structural design. An evolution of the wingwall design has the potential to reduce structural components considerably if redesigned to accommodate the point of impact data. Any alteration to the geometry of the wingwall may warrant other forms of structural protection for shore-side infrastructure. Potential areas for improvement could be the reduction in size of the impact face, elimination of the seaward fender line and a rebalancing of the two fender lines nearest the throat of the slip. Any design alterations should consider effects that different vessel classes would have corresponding to these changes. The consequences associated with a more flexible

wingwall system should also be considered with respect to vessel berthing maneuvers.

Chapter 7: Conclusion

7.1 General

Selection of an appropriate design berthing energy is reliant on subjective decisions made by engineers with years of experience in marine structural design. Structures that prove to be resilient over their lifespan provide little information regarding the actual amount of energy they are absorbing. Without evidence regarding the loading conditions experienced by the structure, design is based on trial-and-adjustment. Uncertainties regarding loading conditions and vessel-structure interaction are applied as berthing coefficients based upon assumptions. Providing engineers with information regarding the actual demands placed on the structure allows for less reliance on subjectivity and can result in more reliable and efficient designs.

There is substantial research available to assist facility designers in the shipping industry. This information corresponds to vessels with displacements of approximately 20 to 100 times the vessel displacements of the Washington State Ferry Fleet; and tugboats typically assist vessel-berthing maneuvers. Although these studies may expand analytical techniques and provide for increased understanding of the berthing process, they are of limited applicability to the high frequency ferry-landing engineer.

Advanced mathematical techniques, and the use of software to analyze vessel-fluid-structure interactions allows for a range of options to be considered for unique berthing situations. However the use of these techniques requires highly trained individuals, is expensive, and has practical limitations for design professionals. The berthing maneuver of a ship represents a very complicated system that is dependent on many difficult to model systems such as vessel piloting, the environment, and hydrodynamic effects.

Measurements of the berthing process capture all aspects of the berthing ship and provide the designer with a representation of the actual energy absorbed by the structure; which, ultimately, is the metric of concern to the design engineer. Compiling information for a sample of statistical relevance then allows for a more complete picture of the berthing demand placed upon the structure. In the presence of a statistically significantly sample of berthing events, the traditionally employed kinetic energy method is obsolete. Empirical and statistical techniques provide a comprehensive understanding of the load environment, and provide a rational basis for which an engineer can implement a reliable and efficient design.

7.2 Findings

This study investigated and characterized thousands of ferry berthing events at the Bremerton slip of the Seattle Ferry Terminal. The findings of this research further the understanding of vessel-structure interaction and the load environment at the Bremerton slip of the Seattle Ferry Terminal. Due to the challenges of obtaining pertinent berthing demand data for ferries, this information will serve to bridge the gap between design assumptions and operational realities. Another component of the analysis is to present design utilities based upon statistical techniques and reliability engineering principles. Application of probability distributions to a large empirical sample allows for extreme event parameters to be quantified by a probability of occurrence. The development of reliability-based tools is intended to quantify the likelihood of extreme events and provide designers a methodology to rationally determine service and ultimate berthing load parameters.

The wingwall structures at the Bremerton slip have handled the berthing demands without issue over the past 20 years, and have significant excess capacity. The maximum berthing energy recorded was less than 40% of the current design criteria.

This report focuses on the development of probability-based occurrences of berthing load demand, and facilitates a transition to a LRFD based design methodology. The major assumptions associated with this approach are: (1) that the extreme values are, in fact, approximated reasonably well by the selected probability density function; and (2) that the empirical data represents a stationary random process, i.e. the year the facility was monitored is considered a typical year, and the associated statistical properties do not vary over time. Service and ultimate loads are presented, and based on probabilities associated with design values occurring or being exceeded. Service loads represent the maximum loads that the wingwalls experience on a regular basis. Ultimate loads represent the maximum loads the wingwalls are expected to experience over their service life. Both service and ultimate loads represented in this study are based upon reliability levels arbitrarily chosen by the author, and may not reflect the desired reliability level of the WSF.

Dissipation of kinetic energy associated with a berthing vessel is a complex process in which there is significant uncertainty associated with the load environment. Quantifying this load environment with the characterization of nearly 7000 impact events provides for information that can be confidently used by a design engineer to refine future structural designs.

7.3 Summary

The following is a compilation of findings, comments and recommendations from the project:

- The arrangement of WSF ferry terminals is often characterized as 'end berthing' facilities as opposed to 'side' berthing. WSF terminals are shaped more similarly to a 'pocket' shaped berth, with the wingwalls oriented at 40 degrees to the berthing vessel. This arrangement may allow for vessel landings that share characteristics of side berthing and end berthing maneuvers – or something completely different from either.
- The current WSF design assumption is based upon the premise that the vessel contacts both wingwalls simultaneously, and loads both wingwalls with approximately the same energy. After characterizing events over the course of the past year, it is has been observed that each wingwall is subject to independent impacts, and the impact energy associated with the north and south wingwalls are rarely equal.
- Analysis of berthing events reveals that a vessel impacts each wingwall multiple times per berthing event, and the initial impact may, or may not, be the most significant.
- Approach velocity is a challenging quantity to measure accurately. It is most relevant at the point of impact, and may be misleading when measured at even small distances from the impact location. Rotational velocity effects are present, and may have significant effects on the kinetic energy of the berthing vessel. Eccentricity coefficients from the literature may not be appropriate for the berthing scenario common at the Bremerton Slip.
- Kinetic energy estimates based on small approach velocities tend to underestimate the amount of kinetic energy the structure absorbs by a substantial amount. This suggests that the combination of ship propulsion,

environmental, and rotational velocity components may contribute significant amounts of energy to the berthing process.

- The wingwall system installed at the Bremerton slip contains substantial excess capacity based on the observation of this study.
- Each berthing event has a unique transfer of energy to the wingwalls due to the use of the propeller, rudder, effects of weather, etc.
- The empirically determined kinetic energy data used in conjunction with the reliability based approach represents a logical paradigm for developing design energies.
- Reliability Design Charts and tables offer a concise method of approximating design berthing energy demands over a given service life.
- Berthing factor results allow for the use of the empirical energy data to be utilized for vessels of different classes (displacements) than were recorded at the Bremerton slip.
- The berthing coefficient recommendations are general in nature because the maximum energy absorbed by the berthing structure often includes additional effects unrelated to the initial kinetic energy of the vessel. In this study, a few examples that have effects that are impossible to isolate would be the use of the ship's controls (rudder(s)), propulsion system, wind, wave, and tidal effects. Therefore it is recommended that the berthing coefficient results be used for preliminary inquiries only.
- Point-of-impact results provide information that could be utilized to refine the geometry and placement of the wingwall impact face.
- The existence of a statistically significant sample of energy absorbed by the structure renders the Kinetic Energy Method obsolete

7.4 Areas for further study

Future research concerning the load environment of ferry terminals could be focused on similar instrumentation schemes for the current generation of reaction frame wingwall systems utilized by the WSF. Another area of study could focus on instrumentation of a terminal that services a 'Super Jumbo' class vessel. By focusing on a terminal that handles the largest vessels, the berthing factor approach could be validated, and provide for a design berthing energy chart that would reduce uncertainties associated with larger vessel berthing events. Continuation of this research could liberate terminal design engineers from subjective evaluation of berthing parameters, and future ferry landing design could be more efficient and have a quantifiable degree of reliability. If the kinetic energy method is still a priority for designers in the WSF staff, more study could also be done that investigates the rotational velocity (and associated rotational kinetic energy) component associated with berthing maneuvers.

References

ANSYS (2012). "ANSYS Aqwa." from http://www.ansys.com/Products/Other+Products/ANSYS+Aqwa.

Beckett-Rankine (2010). Berthing Velocities and Brolsma's Curves. London, Beckett Rankine Marine Consulting Engineers.

Brolsma, J. U. (1977). On Fender Design and Berthing Velocities. PIANC 24th International Naval Congress, Leningrad, U.S.S.R.

BSI (1994). British Standard: Maritime Structures. Part 4: Code of practice for design of fendering and mooring systems. England, British Standard Institute.

Costa, F. V. (1964). "The Berthing Ship: The Effect of Impact on the Design of Fenders and Other Structures." The Dock & Harbour Authority **45**.

Cummins, W. E. (1962). The Impulse Response Function and Ship Motions, Department of the Navy.

Dickenson, S. E. (2007). Instrumentation and Monitoring of Port Facilities: Planning, Funding, Field Applications, and Long Term Benefits. ASCE Ports 2007: 30 Years of Sharing Ideas...1977-2007. San Diego, California, ASCE -TCLEE Ports Lifelines Committee.

DOD, U. (2005). Unified Facilities Criteria. Design: Piers and Wharves, U.S. Department of Defense.

Ebeling, C. E. (1997). An Introduction to Reliability and Maintainability Engineering. United States, McGraw-Hill Companies, Inc.

Ellingwood, B., T. V. Galambos, et al. (1980). Development of Probability Based Load Criteria for American National Standard A58. Washington, D.C., U.S. Department of Commerce, National Bureau of Standards.

Fontijn, H. L. (1980). "The Berthing of a Ship to a Jetty." Journal of the Waterway, Port, Coastal, and Ocean Division **WW2**(15407): 239- 259.

Fontijn, H. L. (1988). On the prediction of fender forces at berthing structures Part II: Ship berthing related to fender structure. NATO Advanced Study Institute of Advances in Berthing and Mooring of Ships and Offshore Structures, Trondheim, Norway, Kluwer Academic Publishers.

Gaylord, E. H., C. N. Gaylord, et al. (1992). Design of Steel Structures. United States, McGraw Hill, Inc.

Gaythwaite, J. W. (2004). Design of Marine Facilities for the Berthing, Mooring and Repair of Vessels. Reston, Virginia, ASCE.

Girgrah, M. (1977). Practical Aspects of Dock Fender Design. PIANC 24th International Navigation Congress, Leningrad, PIANC.

Jahren, C. T. and R. Jones (1993). Ferry Landing Design. Phase 1, Washington State Transportation Center
Washington State Department of Transportation
U.S. Department of Transportation, Federal Highway Administration.

Jahren, C. T. and R. Jones (1996). "Design Criteria for Ferry Landings." Journal of the Waterway, Port, Coastal, and Ocean Engineering(July/August 1996): 187-195.

Jahren, C. T. and S. J. Margaroni (1993). Vessel Tracking Methods for Ferry Landing Design. Seattle, Washington, Washington State Transportation Center(TRAC) Washington State Department of Transportation.

MARIN, M. R. I. N. (2012). "MARIN website." from http://www.marin.nl/web/Facilities-Tools/Software/Offshore-Multibody-Software.htm.

Petroski, H. (2000). Design paradigms; Case Histories of Error and Judgement in Engineering. United States, Cambridge University Press.

PIANC (2002). Guidelines for the Design of Fender Systems:2002. Brussels, Belgium.

Playter, D. (1994). The End Berthing Simulation Model. Civil Engineering. Seattle, Washington, University of Washington. **M.S.:** 136.

Rizos, D. C. and E. H. Stehmeyer, Jr. (2004). Software Development for Berthing Analysis and Structural Loading on Waterfront Facilities. Ports 2004: Port Development in the Changing World, ASCE, American Society of Civil Engineers**:** 1-10.

Seelig, W. N. and G. Lang (2010). Dynamic Modeling of Ferry Berthing. Technical Memorandum. Port Hueneme, California, Naval Facilities Engineering Command.

Toppler, J. F. and J. Weersma (1973). "Planning and Design of Fixed Berth Structures for 300,000 to 500,00 DWT Tankers." Journal of Petroleum Technology(July 1973): 764-774.

Transportation, W. S. D. o. (2012). from http://www.wsdot.wa.gov/ferries/.

Tsinker, G. (2004). Port Engineering; Planning, Construction, Maintenance, and Security. Hoboken, New Jersey, John Wiley & Sons, Inc.

Ueda, S., T. Hirano, et al. (2002). Reliability Design Method of Fender for Berthing Ship. PIANC 2002, 30th International Navigation Congress, Sydney, Australia.

Ueda, S., R. Umemura, et al. (2001). Statistical Design of Fenders for Berthing Ship. 11th International Offshore and Polar Engineering Conference, Norway, International Society of Offshore and Polar Engineers.

WSF (2012). Terminal Design Manual, Washington State Department of Transportation. **1**.

Appendix A Velocity

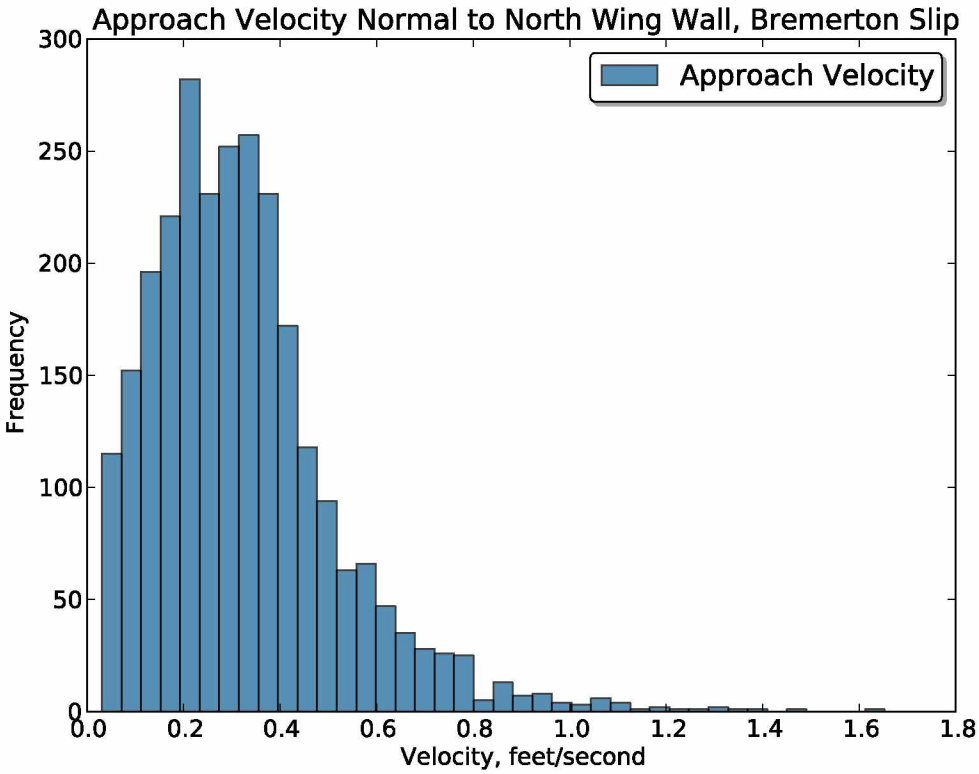

Figure A-1: Normal Approach Velocity, North Wingwall

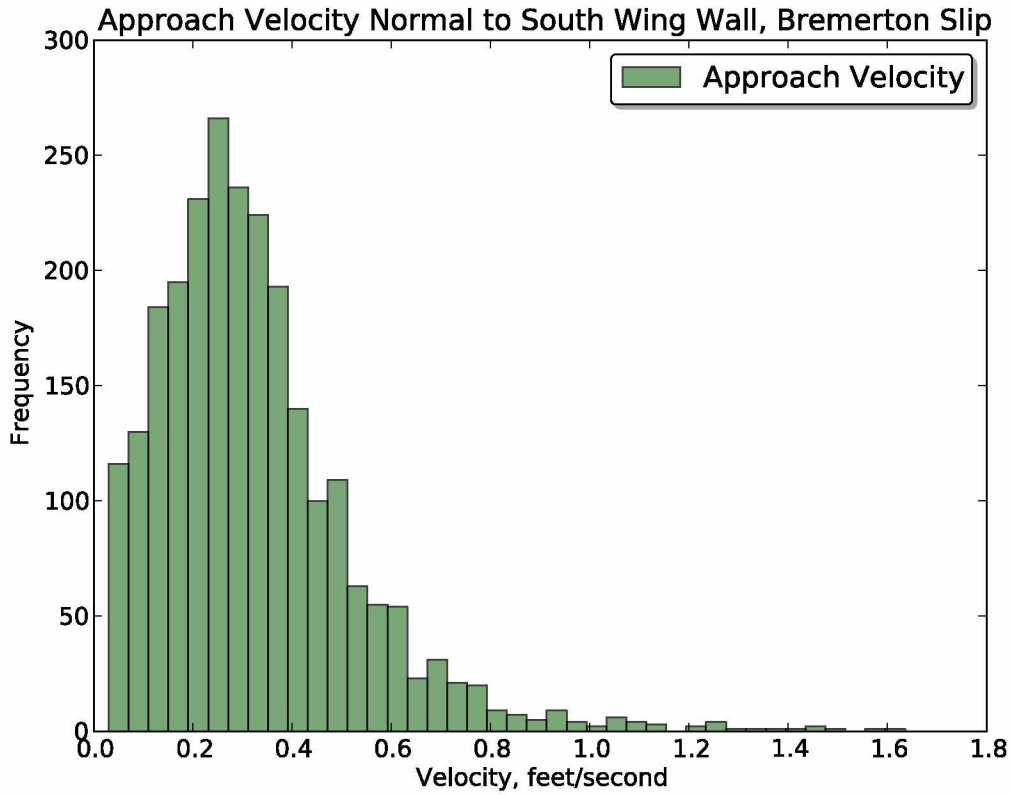

Figure A-2: Normal Approach Velocity, South Wingwall

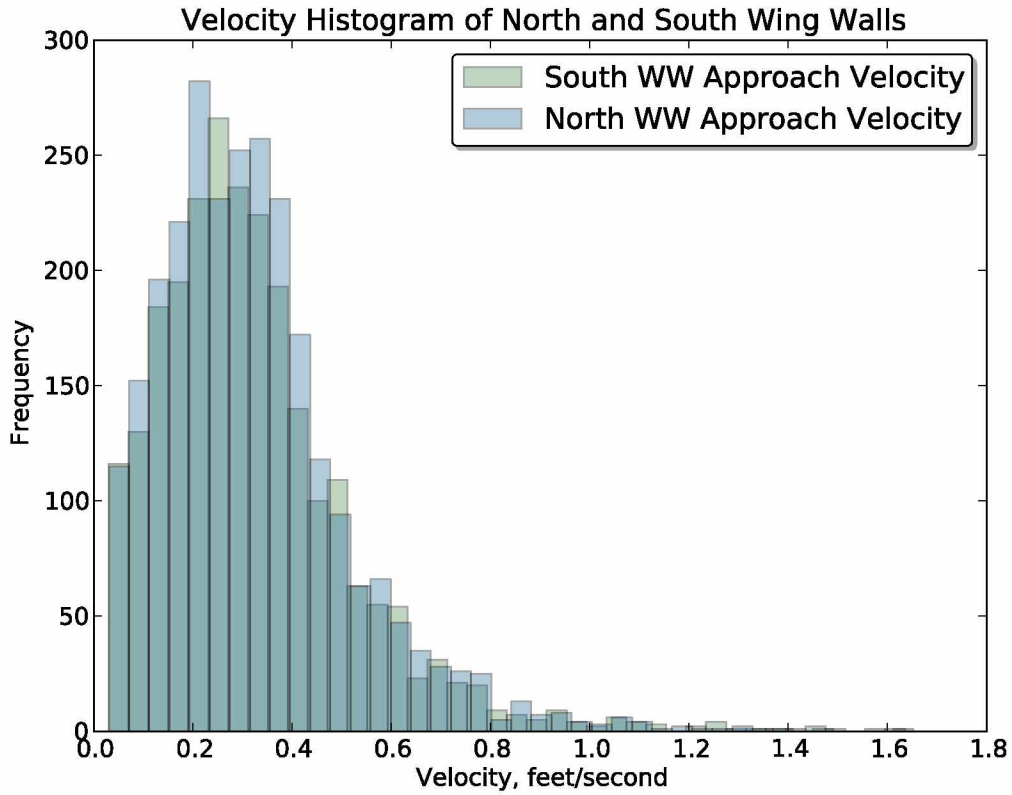

Figure A-3: Normal Approach Velocity Histogram, North and South Overlay

Appendix B Energy

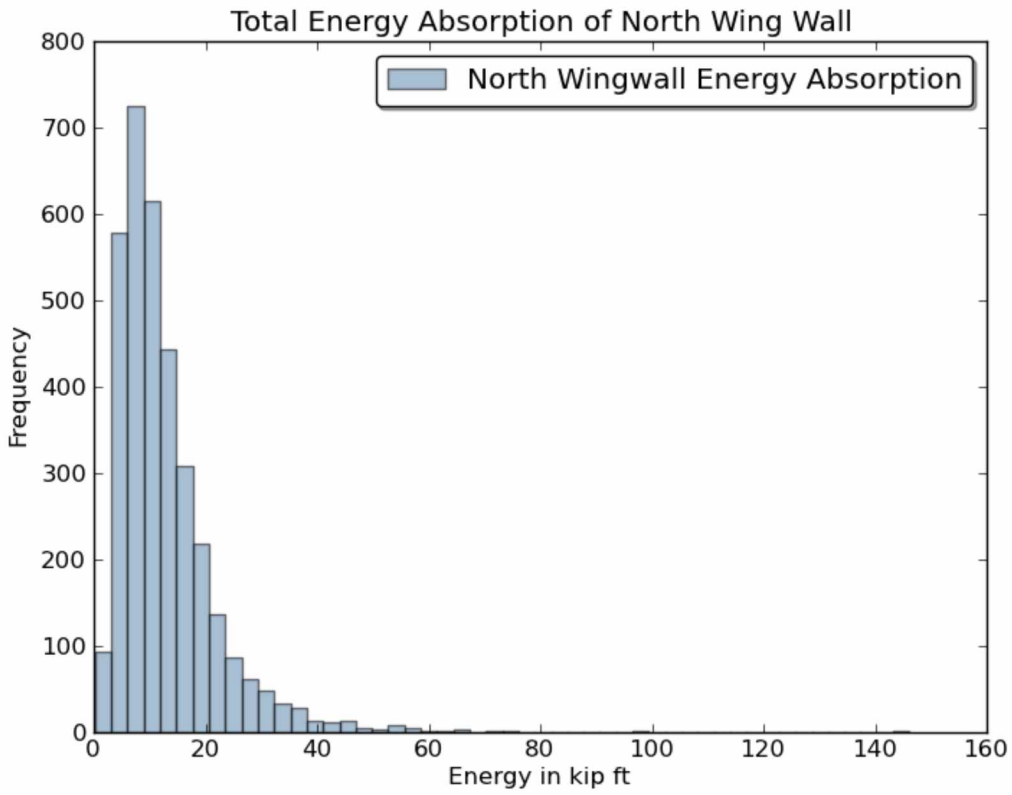

Figure B-1: Berthing Energy at North Wingwall

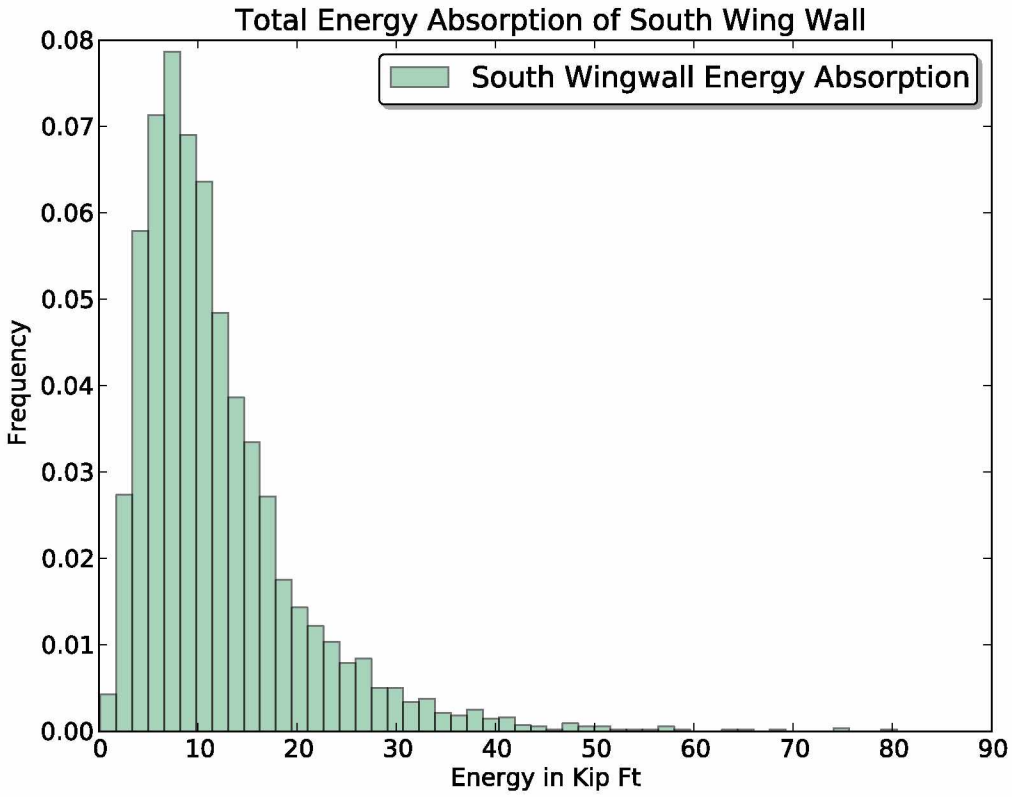

Figure B-2: Berthing Energy at South Wingwall

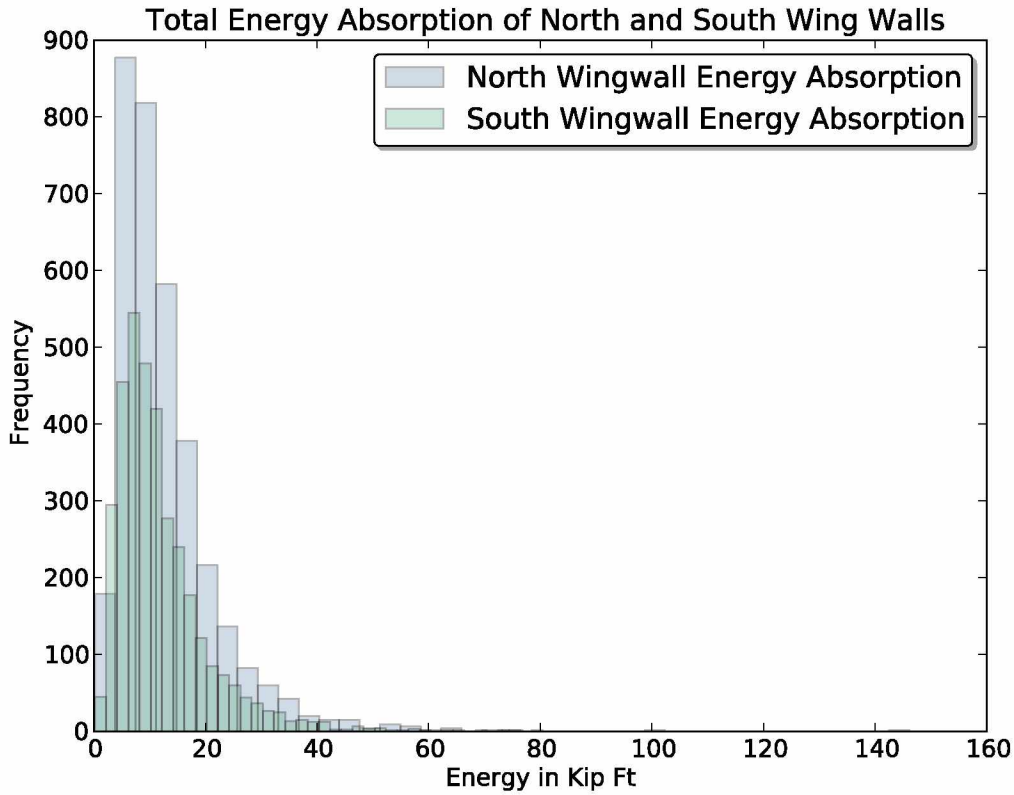

Figure B-3: Berthing Energy North and South Overlay

Appendix C Force

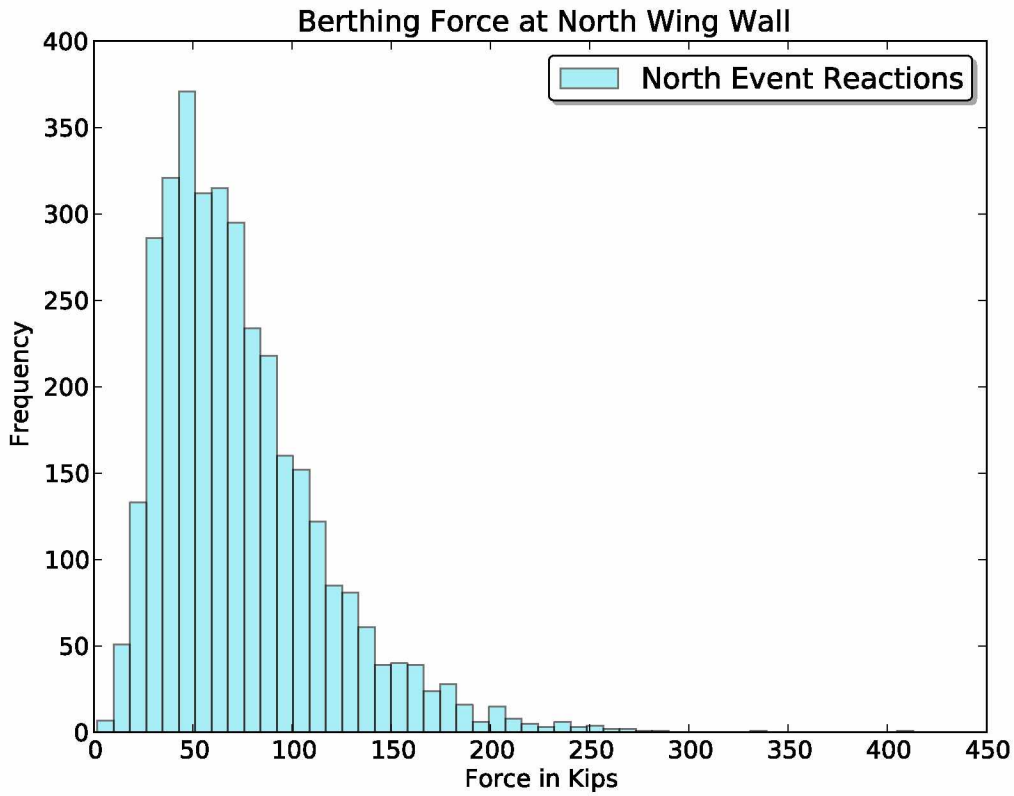

Figure C-1: Berthing Force Applied at North Wingwall

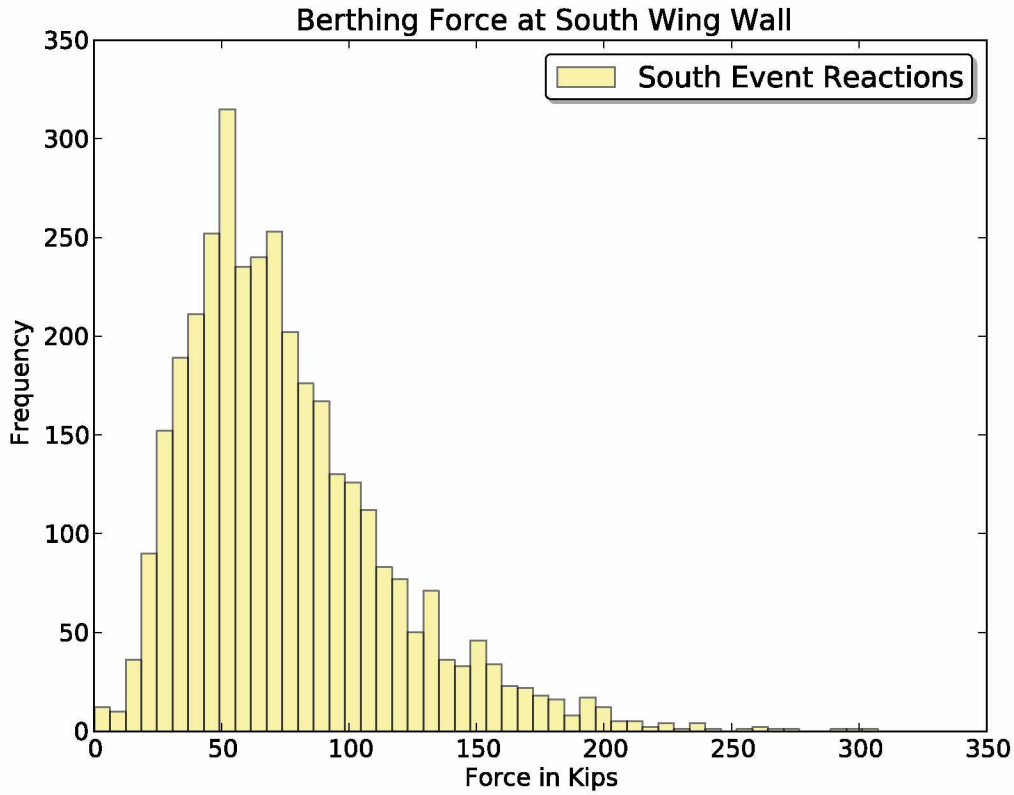

Figure C-2: Berthing Force Applied at South Wingwall

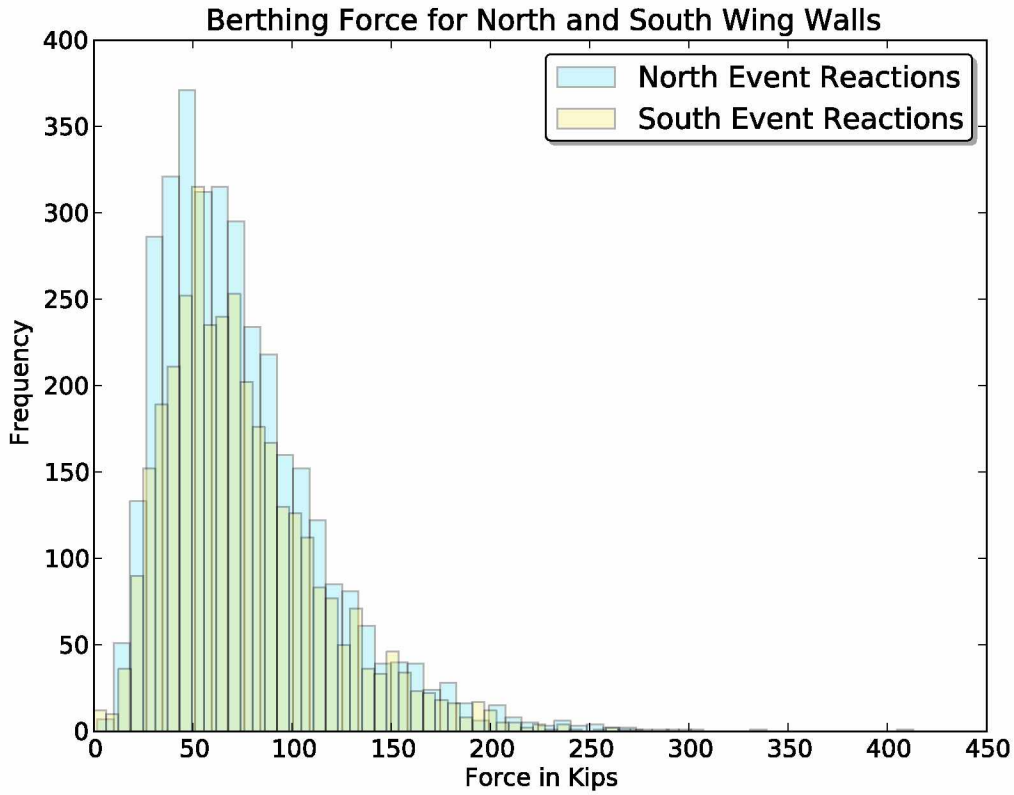

Figure C-3: Berthing Force Applied at North and South Wingwalls

Appendix D Berthing Factor

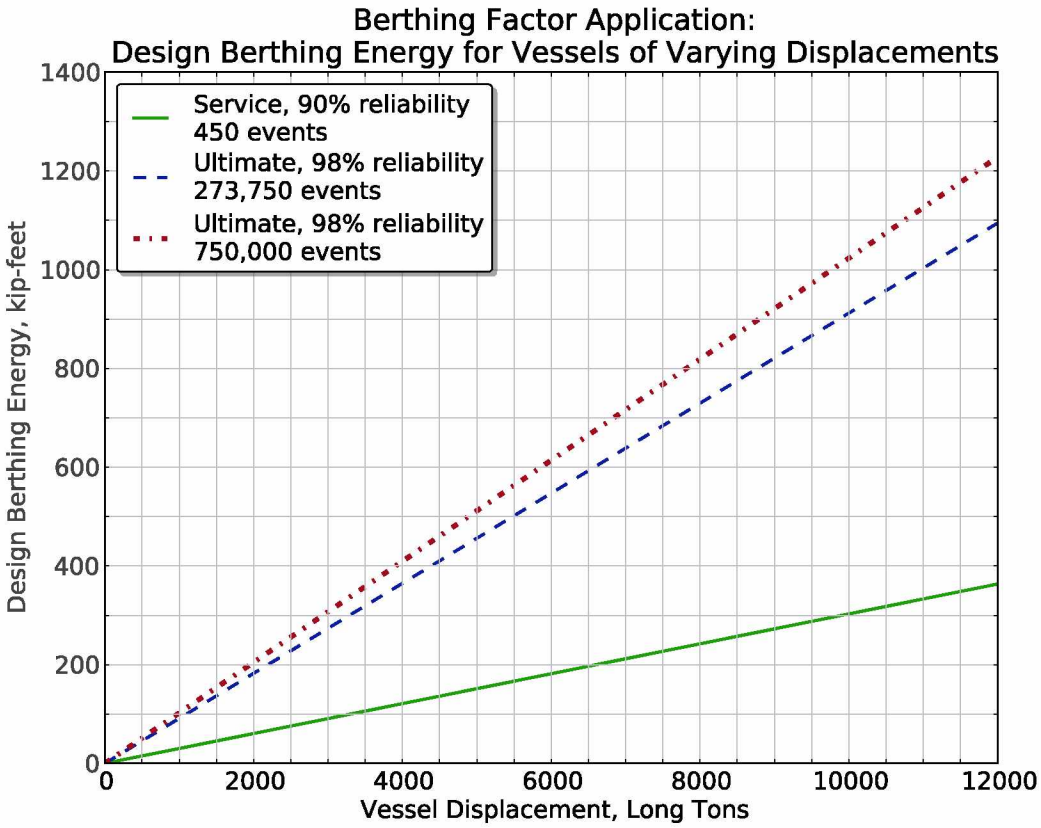

Figure D-1: Expanded Berthing Factor Application, 0-12,000 long tons

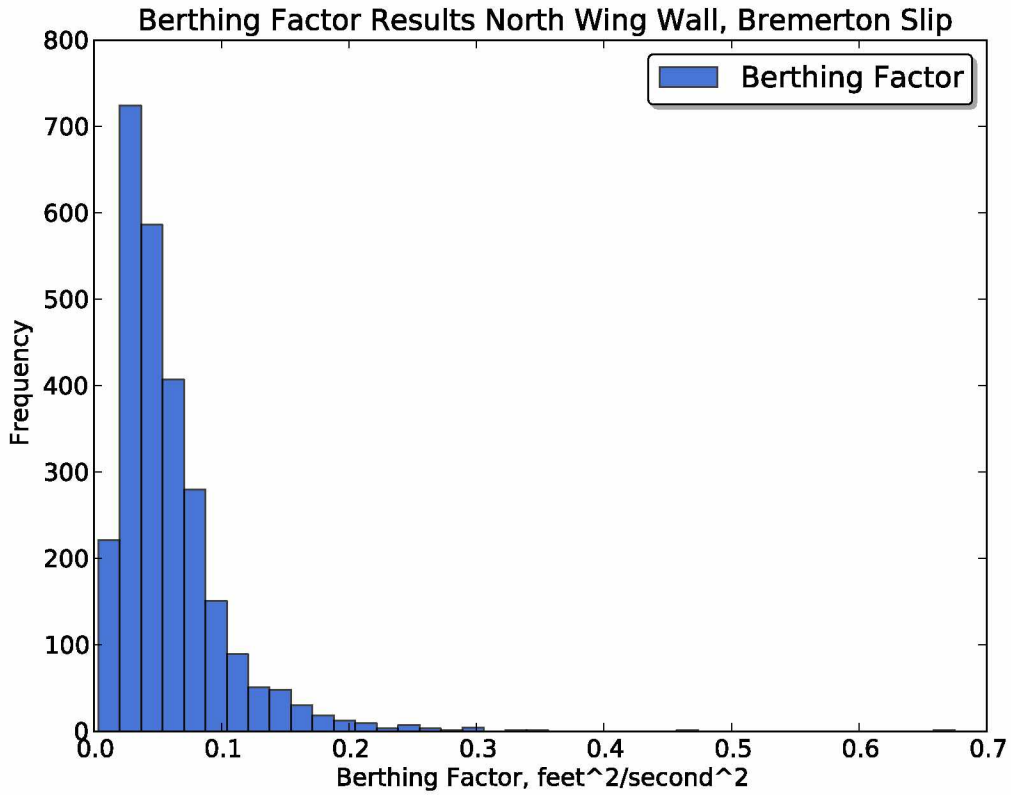

Figure D-2: Berthing Factor Results; North Wingwall

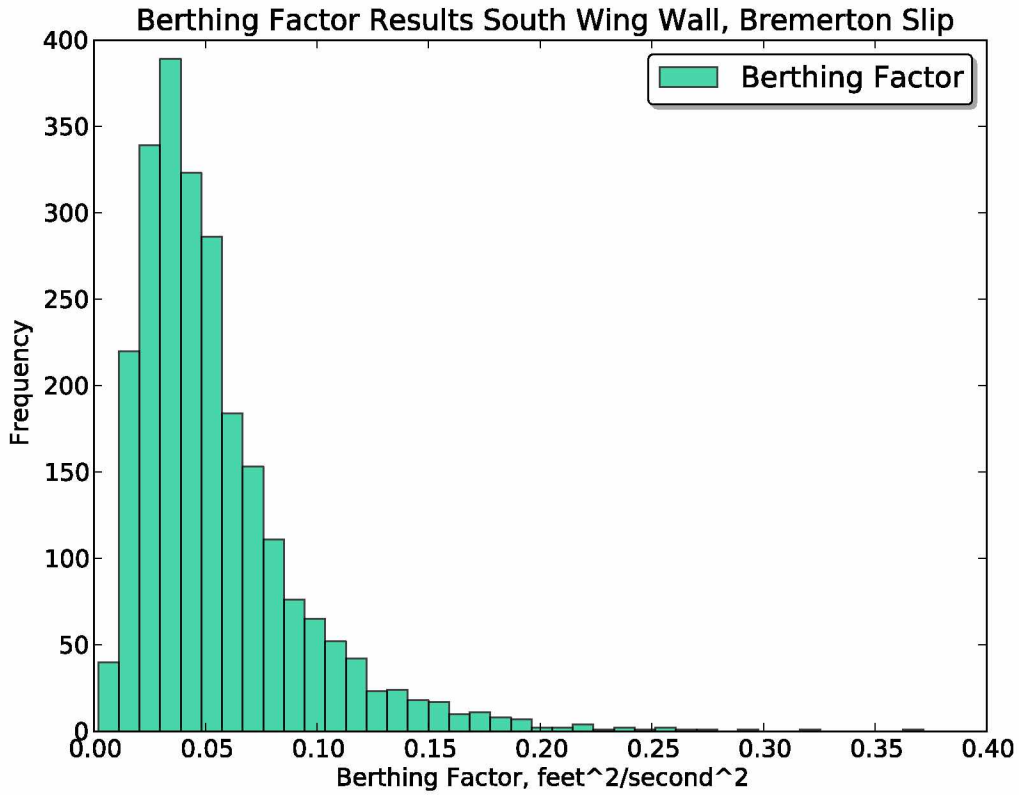

Figure D-3: Berthing Factor Results, South Wingwall